



universität
wien

DIPLOMARBEIT / DIPLOMA THESIS

Titel der Diplomarbeit / Title of the Diploma Thesis

„Immunohistochemical evaluation of NK cells in tumor
tissue “

verfasst von / submitted by

Katharina Schilcher

angestrebter akademischer Grad / in partial fulfilment of the requirements for the degree of
Magistra der Pharmazie (Mag.pharm.)

Wien, 2019 / Vienna, 2019

Studienkennzahl lt. Studienblatt /
degree programme code as it appears on
the student record sheet:

A 449

Studienrichtung lt. Studienblatt /
degree programme as it appears on
the student record sheet:

Diplomstudium Pharmazie

Betreut von / Supervisor:

Univ. Prof. Dipl. Ing. Dr. Manfred Ogris

Mitbetreut von / Co-Supervisor:

Dr. Haider Sami

Danksagung

An dieser Stelle möchte ich mich bei allen bedanken, die mich bei meiner Diplomarbeit unterstützt haben.

Einen besonderen Dank an Univ. Prof. Dipl. Ing. Dr. Manfred Ogris, der mir diese Diplomarbeit ermöglicht hat und an MSc. Magdalena Billerhart, die meine Arbeit betreut hat.

Ein großes Dankeschön gilt meiner Familie, die mir dieses Studium ermöglicht haben.

Table of contents

1. Abbreviations.....	5
2. Aim of the thesis	7
3. Abstract.....	8
4. Zusammenfassung.....	9
5. Introduction.....	11
5.1. Histology.....	11
5.2. Haematoxylin and Eosin staining.....	11
5.3. Immunohistochemistry.....	12
5.4. Antibodies	16
5.5. Breast cancer	17
5.6. Human tumor xenografts.....	18
5.7. CD47	18
5.7.1. Cancer immunotherapy targeting CD47	19
5.8. NK cells.....	20
5.8.1. NCR1	21
5.8.2. Activation of NK cells via CD16 (Fc γ RIIIa).....	22
5.8.3. Role of NK cells in immunotherapy	22
5.9. Macrophages	23
5.9.1. SIRP α	24
5.9.2. Activation of macrophages via CD16.....	24
5.9.3. Role of macrophages in tumor microenvironment	25
5.10. Luciferase	25
5.11. Overview of former in vivo experiments for this project.....	26
6. Materials and Methods.....	28
6.1. Buffers and solutions.....	28
6.2. Embedding	29

6.3.	Sectioning.....	30
6.4.	Haematoxylin and Eosin staining (H&E staining).....	31
6.5.	Immunohistochemistry (IHC) staining - standard protocol	31
6.6.	NCR1 staining.....	33
6.7.	CD47 staining.....	34
6.8.	Firefly Luciferase staining	34
6.9.	SIRP α staining.....	35
6.10.	CD 16 staining.....	35
6.11.	Immunocytochemistry (ICC).....	36
6.12.	Analysis of results	36
6.13.	Materials, Reagents, Devices.....	37
7.	Results.....	42
7.1.	Haematoxylin & Eosin staining	42
7.2.	Optimization of NCR1 staining.....	44
7.3.	Optimization of SIRP α staining	53
7.4.	Optimization of CD16 staining	54
7.5.	Optimization of ICC.....	55
7.6.	In vivo experiments.....	59
8.	Discussion.....	93
References.....	Fehler! Textmarke nicht definiert.	

1. Abbreviations

AB	Antibody
ABC	Avidin-Biotin-complex
ADCC	Antibody dependent-cell-mediated cytotoxicity
BMDMs	Bone marrow-derived macrophages
BSA	Bovine serum albumin
CD47	Cluster of differentiation 47
CDC	Complement-dependent cytotoxicity
DAB	Diaminobenzidine
ECM	Extracellular matrix
ER	Estrogen receptor
EtOH	Ethanol
FFPE	Formalin fixed - paraffin embedded
H&E	Haematoxylin & Eosin
HBS	HEPES buffered saline
HER 2	Human epidermal growth factor receptor 2
HIER	Heat induced epitope retrieval
HRP	Horse radish peroxidase
IAP	Integrin associated protein
ICC	Immunocytochemistry
ICH	Immunohistochemistry
Ig	immunoglobulin
Luc	Luciferase
mAB	Monoclonal antibody

MDSC	Myeloid derived suppressor cells
MMS-domain	Multiple membrane-spanning domain
NK cells	Natural killer cells
pAB	Primary antibody
PBS	Phosphate Buffered Saline
PR	Progesterone receptor
RT	Room temperature
RTU	Ready to use
sAB, sek	Secondary antibody
SCID	Severe combined immunodeficiency
SIRP α	Signal regulatory protein alpha
TAMs	Tumor-associated macrophages
TNBC	Triple-negative breast cancer
TU LE	Tumor left
TU RI	Tumor right
WEK	Demineralized water

2. Aim of the thesis

The aim of this thesis was to establish new staining protocols for Natural Killer cells and macrophages in tumor tissue. Several different protocols were evaluated.

The second aim was to investigate immune cell infiltration in tissue samples from an in vivo experiment. In this in vivo experiment tumors were treated with polyplexes containing a plasmid, which encoded for the fusion protein SIRP α -Fc. This fusion protein should block CD47 and promote the infiltration of immune cells.

3. Abstract

CD47 is a surface protein frequently overexpressed on tumor cells. It sends a “don’t eat me” signal to macrophages when interacting with the surface receptor SIRP α expressed in macrophages. This signal leads to an inactivation of the macrophages and protects the CD47-expressing tumor cells from phagocytosis. Blocking this interaction could be a promising tool in cancer therapy. In previous work, a gene therapy approach was developed, which enables the tumor-restricted expression of a fusion protein consisting of a CD47 blocking domain and a functional Fc domain derived from IgG. After binding of the fusion protein to CD47, the Fc part can also lead to antibody dependent-cell-mediated cytotoxicity (ADCC) via an interaction with Fc receptors, mostly expressed on the surface of Natural Killer cells, macrophages and dendritic cells.

This thesis focuses on the immunohistological evaluation of an in vivo experiment, in which triple negative breast cancer xenografts in SCID mice were treated with gene transfer particles containing the plasmid encoding for this fusion protein. The expressed transgene product should block CD47 and inhibit the interaction with SIRP α in macrophages. Furthermore, the Fc part on that protein should lead to the apoptosis of the tumor cells via ADCC.

First, a staining protocol for NK cells using two different antibodies was established to evaluate the infiltration of NK cells in the tumors. In the second step it was tried to establish a staining protocol for macrophages, which was not used in the evaluation of the in vivo experiment since no specific staining could be achieved.

The in vivo experiment was evaluated for CD47, Luciferase and NK marker expression. Albeit cellular staining was achieved, the intensity on unspecific staining was too high to draw conclusions about the expression of the antigens. Potential reasons for this are discussed. Nevertheless, in tumors samples stained with Haematoxylin and Eosin, a clear immune cell infiltration would be observed in samples treated with polyplexes.

4. Zusammenfassung

CD47 ist ein Oberflächenprotein, welches häufig auf Tumorzellen überexprimiert ist. Es sendet ein „Friss mich nicht“-Signal an Makrophagen über eine Interaktion mit dem SIRP α Rezeptor an Makrophagen. Dies bewirkt deren Inaktivierung und verhindert die Phagozytose der Tumorzellen. Die Blockade dieser Interaktion stellt eine vielversprechende neue Behandlungsmethode für Tumore dar. In bisherigen Arbeiten wurde ein gentherapeutischer Ansatz entwickelt, in Zuge dessen ein Fusionsprotein bestehend aus einer CD47-blockierenden Domäne und dem funktionellen Fc Teil von Immunglobulin G gezielt in Tumorzellen exprimiert wird. Nach Bindung des Fusionsproteins an die Zelloberfläche kann der Fc Teil auch zu antikörperabhängiger zellvermittelter Zytotoxizität (ADCC) durch Natural Killer (NK) Zellen führen, da der Fc Rezeptor auf NK Zellen exprimiert wird.

Diese Diplomarbeit fokussiert sich auf die histologische Auswertung eines in vivo Experiments, in dem triple negative Brustkrebs Xenotransplantate in der SCID Maus mit Gentransferpartikeln behandelt wurden, die ein für das Fusionsprotein codierende Plasmid beinhalten. Das exprimierte Transgenprodukt sollte somit CD47 blockieren, die Interaktion mit SIRP α auf Makrophagen inhibieren und über den Fc-Teil auch zum Abtöten der Tumorzellen durch ADCC führen.

Zuerst wurde ein Protokoll für ein NK Zell Färbung mit zwei verschiedenen Antikörpern erstellt. Die Färbung dient zur Evaluierung der Einwanderung von NK Zellen in die Tumore. Des Weiteren wurde ein Protokoll für die Färbung von Makrophagen entwickelt, welches nicht weiterverwendet wurde, da keine eindeutige Färbung erzielt werden konnte. Die Tumore des in vivo Experiments wurden auf CD47, NK Zellen und Luciferase untersucht. Es konnte jedoch keine spezifische Färbung erreicht werden. Die möglichen Ursachen dafür werden in der vorliegenden Arbeit diskutiert. In mit Hämatoxylin und Eosin gefärbten Präparaten konnten jedoch die Immunzellinfiltration in Polyplex behandelten Tumoren klar gezeigt werden.

5. Introduction

5.1. Histology

Histology, the microscopic study of body tissues, is an important tool in clinical diagnostics and cancer research. Histology has its focus on how the function of each organ is optimized by its cells' structure and arrangement. The orderly combination of several tissues allows the function of each organ. There are two interacting components for tissue: cells and the extracellular matrix, which consists of macromolecules, such as collagen and basement membranes.

To preserve tissue structure and avoid degradation by bacteria or enzymes, tissue has to be fixed and embedded as soon as possible after obtaining it. No ideal fixation has been found to date, which would be a fixative that preserves cellular morphology and does not change the reactivity of proteins or affects their detection. The ideal fixative should also harden the tissue and prevent autolysis and decomposition. A widely used fixative is formaldehyde, its aqueous solution is termed formalin. It is an aldehyde that acts by cross linking proteins in the tissue. Formalin penetrates the tissue by diffusing into the specimen to reach every layer of cells and reacts with functional groups forming cross links. The initial stage of those is completed after 48 hours after penetration, but it can take up to 30 days to form stable covalent cross links. (Thavarajah et al., 2012) The tissue is then dehydrated and infiltrated with melted paraffin, after which it is embedded. For light microscopy, paraffin is widely used as embedding material. The solidified paraffin block can then be sectioned using a microtome. Sections are between 1-10 μm thick, while for example for electron microscopy, where other embedding materials and an ultramicrotome is used, sections of less than 1 μm thickness are used. (Mescher & Junqueira, 2013)

5.2. Haematoxylin and Eosin staining

Since most cells are completely colourless, tissue must be stained to be studied microscopically. Haematoxylin and Eosin are the most commonly used stains for routine histology.

Haematoxylin behaves like a basic dye and stains basophilic components in the tissue, like DNA in the nuclei and other acidic structures like RNA-rich portions of the cytoplasm, which appear dark purple or blue. Eosin stains cytoplasmic components pink. This simple staining method allows a general histologic examination of tissue. (Mescher & Junqueira, 2013)

5.3. Immunohistochemistry

In Immunohistochemistry antibodies are used to detect proteins and provide information about expression, localization and distribution of distinct antigens. This staining method can be used on FFPE (formalin fixed, paraffin embedded) tissue or on frozen tissue, which must be sectioned in very thin slices prior to the staining. (Dako, 2013; Novus Biologicals) If Formalin is used as a fixative, an antigen unmasking procedure has to be performed. There are several methods for this, for example treating the sections with enzymes or non-enzymatic methods. Heat-Induced Epitope Retrieval (HIER) is the most commonly used one, for this the sections are heated in a buffer solution. (Cattoretti et al., 1993; Shi et al., 1997) Formalin is a superior fixative in preserving morphology, but it impacts IHC (immunohistochemical) staining by crosslinking amino acids within the target protein and masking the antigen. This results in weak signal, sometimes undistinguishable from the background. The pH during the HIER has a high impact on the staining, the right pH can improve the affinity for an antigen.

In general, there are two detection methods. The direct method uses only antibodies specific for the antigen, which are directly conjugated to a reporter enzyme. This direct method is faster and requires fewer working steps but is also less sensitive.

The indirect method uses a primary antibody directed against the protein of interest and a secondary antibody directed against the constant region of the primary antibody. In this case, the secondary antibody is labelled with the reporter enzyme, which leads to a higher sensitivity through signal amplification. Several secondary antibodies can bind to one primary antibody.

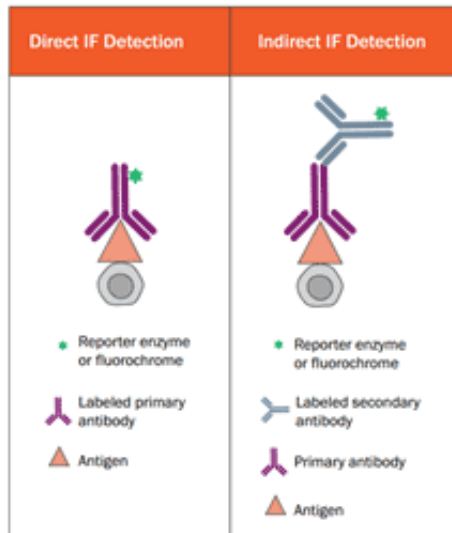


Figure 1 direct and indirect detection in IHC. On the left side direct detection can be seen. This uses a labelled primary antibody, on the right side indirect detection can be seen. This uses a labelled secondary antibody directed against the primary antibody. (Novus Biologicals, 2019)

The sensitivity can be further improved by using ABC or Polymer-based detection systems (Dako, 2013; Novus Biologicals): One possibility for signal amplification is the Avidin-Biotin Complex (ABC) method. Biotin conjugated secondary antibodies link tissue bound primary antibodies to a complex of avidin, biotin and peroxidase. Avidin contains four binding sites for biotin and is linked together by the enzyme. Because of this complex the enzyme-to-antibody ratio is high, which leads to an increase in sensitivity. This detection system has some limitation, mostly due to the presence of endogenous biotin in the tissue. The FFPE fixation procedure reduces the amount of endogenous biotin, but it can lead to increased background staining.

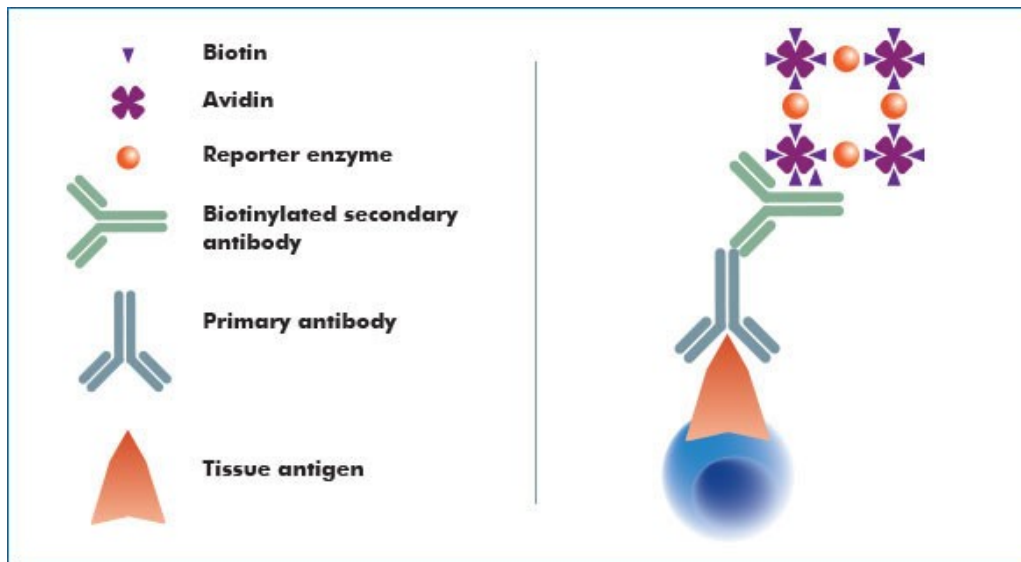


Figure 2 ABC detection method, this method uses a biotinylated secondary antibody, to which a complex of avidin, biotin and the reporter enzyme binds. (Novusbio.com, 2019)

Prior to incubation with biotin-conjugated reagents, the tissue should be treated with avidin followed by biotin to block additional biotin binding sites on the avidin used. This procedure then reduces background staining. This is especially important when staining liver, kidney, spleen, lung and brain, or frozen tissue in general. To examine if the blocking is effective, a background control can be performed, in which the staining procedure is carried out on the tissue but omitting the antibodies. (Dako, 2013; Novus Biologicals)

Another possibility is a Polymer-based detection system. In this case secondary antibodies and enzymes are conjugated to a polymer. Because of the large number of enzymes this method is more sensitive than the ABC detection method. This system also decreases the number of steps necessary for IHC staining, as no blocking of endogenous biotin and no incubation with the ABC reagent is necessary, in which the complex would bind to the biotinylated secondary antibody. (Novusbio.com, 2019a)

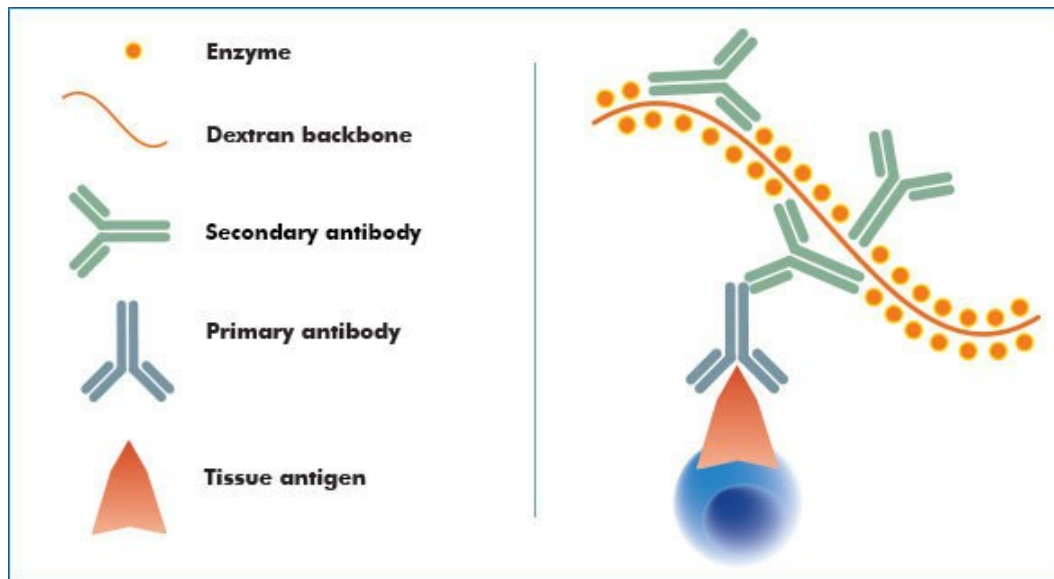


Figure 3 Polymer-based detection method. The secondary antibody is linked to a polymer which also contains the reporter enzyme. (Novusbio.com, 2019)

For accurate staining results, the antibody binding has to be specific for the antigen. Nevertheless, also be unspecific binding can occur, e.g. due to hydrophobic or ionic interactions and by hydrogen bonding. To prevent this, a blocking step can be performed, usually using normal serum or BSA (bovine serum albumin). If the blocking is performed with normal serum, the species of the serum should be the same as the host for the secondary antibody. There are several kinds of unspecific staining, one of them occurs because of endogenous peroxidase activity, which can lead to unspecific results if HRP (horseradish peroxidase) is used for a chromogenic detection. HRP is conjugated to the antibody and converts DAB (Diaminobenzidine) to a brown stain, hence this conversion can also be catalysed by endogenous peroxidase. To prevent this effect, the tissue is treated with hydrogen peroxide prior to incubation with the secondary antibody. This is especially important in kidney, liver and areas with red blood cells, as such tissues have a high of endogenous peroxidase activity. (Abcam, 2019a; Novus Biologicals) Another possibility for unspecific antibody binding is thought to occur because of the binding of the primary and secondary antibodies to endogenous Fc receptors. Preincubation of the tissue with normal serum from the same species as the secondary antibody is derived from prevents this interaction. Goat serum and antibodies derived from goat are widely used in immunohistochemistry, but goat serum has been reported not to block the Fc receptors on human cells. Buchwalow et. al. evaluated different blocking methods using BSA and normal goat serum on FFPE tissue, frozen tissue

and cell smears. Interestingly, the results showed no differences in background staining. However, it is still recommended by manufacturers to use a blocking step, and a blocking serum is usually included in the staining kits. (Buchwalow et al., 2011)

Due to the complex staining procedure and the various effects of sample preparation and fixation, control antibodies help to confirm the presence of the antigen. An isotype control can confirm the specificity of the primary antibody. For this, the primary antibody is replaced with an immunoglobulin of the same isotype and the same concentration as the primary antibody, but without known binding specificity to any antigen on the tissue it is exposed to. A secondary control can show the contribution of the secondary antibody and the reagents to the (background) staining. This control is performed by omitting an incubation step with primary antibody. A buffer control can show the effect of endogenous factors and reagents. These controls can play an important role in the correct interpretation of the staining results. (Abcam, 2019b; Novus Biologicals)

5.4. Antibodies

Antibodies belong to the group of immunoglobulins and can be found in the blood of immunized individuals. Immunoglobulins bear variable and constant domains. Several hyper-variable domains are in the variable region and those recognize the epitope of the antigen. Polyclonal antibodies are a mixture of different antibodies directed against the same antigen, but various epitopes thereof. Polyclonal antibodies are expressed by a heterogeneous B-cell population and are produced by immunizing a host animal with multiple doses of antigen followed by purification of the antibodies from the serum. The antibodies can be produced in various species, but rabbits are most frequently used to generate polyclonal antibodies.

Polyclonal Antibodies can lead to a higher signal intensity, as they can react with multiple epitopes of the antigen, but this can also increase the probability of cross-reaction with other proteins, unspecific staining and higher background levels.

Monoclonal antibodies are defined as being identical molecules with high specificity for one distinct epitope of the antigen. This reduces unspecific binding but can also lead to a less robust staining. They are generated by a single B-cell clone, which is isolated from the spleen of an immunized animal and then fused with a myeloma cell line. While the cell

line is immortalized and exhibits indefinite growth, the B lymphocytes enable the production of the antibody. This fused cell line, called a hybridoma, is further cultured and a stable clone with high antibody production is selected and isolated. For large scale growth, Bioreactors can be used. (Dako, 2013)

5.5. Breast cancer

Breast cancer has the second highest incident of all cancers and is the most diagnosed cancer in females, with 2.1 million newly diagnosed cases in 2018. Incidence rates are especially high in developed countries like Europe, Australia and Northern America. Known risks for breast cancer are late age at first birth, fewer children, exogenous hormone intake like oral contraceptives or hormone replacement therapy, alcohol intake and obesity, whereas protective factors are breastfeeding and physical activity. (Bray et al., 2018)

Triple negative breast cancer (TNBC) tests negative for estrogen and progesterone receptors and excess HER2 protein, which leads to a poorer prognosis because of fewer targets for treatment. Only about 10-20% of breast cancers are triple negative, and it appears more often in younger people and patients with a BRCA1 mutation, 70% of those cases are triple negative.

Because hormone receptors are not expressed, the cancer will not react to a hormone treatment, which only leaves neoadjuvant chemotherapy, PARP inhibitors or checkpoint inhibitors as possible treatments. TNBC is also more aggressive, it is more likely to spread and metastasise and also more likely to recur after treatment. In addition, it tends to be of higher grade, which means that the cells have a high degree of malignancy and are of the mesenchymal type. Because of all these facts there is intense interest in finding new treatment options. (Breastcancer.org)

In preclinical research, cell lines are often used to model the disease. Those cell lines also represent part of the heterogeneity of the disease and therefore it is important to choose the right cell line for research. There have been questions raised how well such immortalised cell lines represent the features of breast cancer, but they still remain a powerful tool when used the right way.

For the in vivo part of this thesis, performed by Magdalena Billerhart, MDA-MB-231 LM2-4 EGFP-Luc cells were used.

The MDA-MB-231 cells are generally regarded as invasive in vitro but remain poorly metastatic in vivo. Metastasis of this cell line can be studied through intravenous injection, for example intracarotid artery injection for the study of brain metastasis or left ventricle injection for metastasis in the bone. Through rounds of selections, the LM2-4 cell line also shows metastasis in vivo. (Holliday & Speirs, 2011; Kang et al., 2003)

5.6. Human tumor xenografts

For cancer research xenograft models are widely used. For this purpose, human cancer cells from cell lines are transplanted into severely immunodeficient (SCID) mice. SCID mice do not have functional B or T-cells, but macrophages and NK cells function normally. Because of this, innate immune reaction against tumors can be seen after treatment, but the human cells are not rejected. The tumor cells can be transplanted into the correlating organ in mice or subcutaneously or also applied intravenously and the tumor will develop over the following weeks.

These models can be used to analyse the tumor response to the therapeutic regime but on the downside the mice are immunocompromised, so the tumor microenvironment is not the same as in humans. (Morton & Houghton, 2007; Richmond & Su, 2008)

5.7. CD47

Cluster of differentiation 47 (CD47), also known as integrin-associated protein, is a membrane protein and belongs to the immunoglobulin superfamily. It consists of a single IgV-like domain at the N-terminus, a hydrophobic part with five membrane-spanning segments and an alternatively spliced C-terminus, which ranges from a length of 3 to 36 amino acids. Human and mouse CD47 molecules show about 70% amino acid identity and genomics studies suggest that homologous genes are also present in other vertebrate species. The C-terminal domain is heavily glycosylated and CD47 is ubiquitously expressed on all cells and tissues. (Brown, 2001)

It was first recognized after being co-purified with integrin, and as a 50 kDa protein which could regulate integrin function. It was later shown that it is identical to the CD47 protein

on erythrocyte cell surface and is therefore referred to as CD47 and no longer as integrin associated protein, because erythrocytes do not express any integrins. (Oldenborg, 2013) Human CD47 has a calculated molecular weight of 31871-35213 Da, depending on the splicing of the C-terminal domain the degree of glycosylation of the Ig domain. CD47 is expressed ubiquitously in all cells and tissues. (Brown, 2001; The Human Protein Atlas, 2019)

The most important ligand of CD47 is SIRP α (signal-regulatory protein alpha), the interaction can mediate cell-cell adhesion and it acts as a “don’t eat me”-signal to macrophages. Cells that express CD47 on their surface can interact with SIRP α on macrophages and prevent their own phagocytosis. CD47-deficient cells are cleared by macrophages, especially CD47-deficient erythrocytes are rapidly cleared by splenic macrophages. (Brown, 2001) CD47 also plays an important role in tumor biology, as it is frequently overexpressed in human cancers. The CD47 expression correlates with metastasis and tumor invasion and could be used as a prognostic factor for disease progression and metastasis. By the overexpression of CD47 tumor cells are able to evade the immunorecognition, since they give the signal to macrophages and trick those into believing they are healthy cells. (Zhao et al., 2016)

As well as a checkpoint for immune reaction, CD47 also has other cellular functions like cell migration, axon extension and cytokine production. This also means that metastasis can be influenced by blocking CD47. It also plays a role in the relapse of cancer, since studies have shown that cancer stem cells overexpress CD47 and can protect themselves from immune reaction during conventional anti tumor therapy and repopulate a new tumor lesion at a later timepoint. (Liu et al., 2017)

5.7.1. Cancer immunotherapy targeting CD47

Anti-CD47 antibodies can decrease the tumor size in haematological and epithelial tumor models and show a decrease in the number and size of metastasis in leiomyosarcoma. This effect can be explained by the interference of these antibodies with the protection from phagocytosis provided by the interaction between CD47 and SIRP α on macrophages. (Edris et al., 2012)

If the therapeutic effects are due to the specific intrinsic functions of CD47 or the non-specific ADCC is controversially discussed. Studies have shown the presence of both of these mechanisms. CD47 blockage leads to increased phagocytosis by macrophages, even

without a Fc-part, but this Fc part can also trigger unspecific ADCC through neutrophils, macrophages and Natural Killer cells. All these effects could be shown in xenograft models, if the therapy would bring the same benefits in human is still unclear. In 2017 there were already three CD47 antagonists in phase I clinical trials. The antagonists TTI-621, CC-90002 and Hu5F9-G4 are applied against both solid and haematological malignancies and the current focus lies on comparing the side effects and efficacies of these reagents. The detailed mechanisms of the therapies are still unclear and it is not known if the clinical efficacy will be as efficient as the findings in preclinical trials. (Huang et al., 2017)

5.8. NK cells

Natural killer cells are a specialized population of lymphocytes that are part of the first line of defence against infections and cancer. They can eliminate tumor cells without prior sensitization. Their status is controlled by the balance between activating and inhibitory receptors. Examples for activating receptors are NKp46 and CD16. (Li & Sun, 2018)

The major homing site for NK cells is the spleen, which has a dual role as secondary lymphoid organ and for filtration of exhausted erythrocytes. Most lymphocytes can be found within the white pulp, while the red pulp is a specialized area for the elimination of erythrocytes by macrophages. Reports have shown that NK cells are mostly located in the red pulp, but they can migrate to the white pulp in case of inflammation, where they interact with T-cells and dendritic cells and enhance the immune reaction. Conversely, it was also shown that NK cells could also kill immature dendritic cells and thus induce immunopathologies. (Grégoire et al., 2008)

NK cells can eliminate target cells by two different cytotoxic mechanisms. The first is the death receptor pathway, which is activated either by the interaction of the tumor necrosis factor-related apoptosis inducing ligand family (TRAIL) with the TRAIL receptors or by the interaction of FAS Ligand with FAS. Both interactions allow the formation of a death inducing signalling complex consisting of Fas-associated death domain (FADD), caspase-8 and caspase-10. This leads to further activation of caspases and ultimately results in apoptosis. The second possible pathway is the granule dependent pathway, which is activated after NK cells adhere to target cells after which cytotoxic granules are delivered toward the

target cells. These granules contain different types of granzymes, which can activate different pathways leading to cell death. (Martín-Antonio et al., 2017)

NK cells play a critical role in tumor surveillance: both, in clinical research and in animal models a correlation between NK cell malfunction and increased tumor incidence has been found. As mentioned above, no exposure to tumor cells is necessary for the activation of NK cells, as they are activated by the decreased expression of MHC class I on the surface of tumor cells and the resulting lack of inhibitory signals, also known as the “missing-self” theory. Besides this mechanism, tumor cells can also trigger stress induced expression of NK cell activating receptors, such as Nkp46. In addition, NK cells can be activated by specific therapeutic antibodies via CD16 mediated ADCC. Several studies have demonstrated that the function of intratumoral NK cells is impaired, whereas they remain active in the tumor periphery. This tumor immune-escape occurs via two main mechanisms, i.e. the reduction of activation signals and the increase of inhibitory signals. Suppressive molecules and negative regulatory immune cells can further promote suppression of NK cells in tumors, mainly by regulatory T-cells and tumor-associated macrophages. Furthermore, NK cells are rarely found inside the tumor tissue, which could be due to the tissue barriers around tumors protecting the tumor and preventing immune cells infiltration, for example the fibrotic shield surrounding pancreatic cancer. (Li & Sun, 2018)

5.8.1. NCR1

For many years it was thought that NK cells are only controlled by inhibiting mechanisms. This “missing-self” theory states that NK cells are modulated by MHC I, which after being recognized by NK cells inhibits their activity. In case this signal is missing, the cell is killed. Years later the existence of activating NK cell receptors was proven, two of those are Nkp46 and CD16. (Watzl, 2014)

NCR1, also known as Nkp46, is one of three NK cell activating receptors, also referred as natural cytotoxicity receptors. They belong to the immunoglobulin superfamily, although with each other they do not share any homology, and also only low identity with other human or murine surface proteins. The ligands for NCRs are mostly unknown, but a functional interaction between Nkp46 and hemagglutinin of influenza virus was described. (Arnon et al., 2004)

5.8.2. Activation of NK cells via CD16 (FcγRIIIa)

For the activation of NK cells Nkp46 alone is not sufficient, it is necessary to engage at least two activation receptors. The only receptor, which can activate NK cells by itself is CD16, a Fc receptor mediating ADCC. The activation via CD16 is therefore dependent on antibodies produced by B cells. (Watzl, 2014)

5.8.3. Role of NK cells in immunotherapy

The antitumoral function of NK cells is usually impaired in cancer patients and restoring this function can be a therapeutic objective in cancer therapy. Currently, there are several strategies under development to use NK cells in immunotherapy.

One possible strategy is the NK cell based adoptive cellular immunotherapy. Large amounts of activated NK cells are infused to revive the innate immune surveillance. There are several different possibilities for this treatment. It is possible to use autologous NK cells, which are induced by IL-2 in vivo. Because of the systemic application of IL-2 and its toxicity this approach is no longer followed, also due to the limited antitumoral effects. Instead ex vivo expanded autologous NK cells are now in use. Another approach is the adoptive, allogeneic NK cell transfer or the use of NK cell lines. Advantages of NK cell lines are their stability and the quantity of cells obtained. In 2017 the therapy with activated NK cells was qualified by the FDA as orphan drug for Merkel cell carcinoma. (Li & Sun, 2018)

Another approach is the use of CAR-NK cells. These cells are genetically modified to express CAR, a chimeric antibody receptor composed of three regions: the extracellular domain which redirects the activity toward a specific antigen on the tumor, a transmembrane domain and an intracellular domain which induces signalling pathways in NK cells. This treatment ultimately results in the death of the target cell. (Martín-Antonio et al., 2017)

A third promising approach for cancer therapy is the immune checkpoint blockade. In case of NK cells, the receptors for inhibiting signals are blocked by antibodies, like Anti-KIR or Anti-NKG2A. This should in theory lead to a sustained activation. But since NK cell activation depends on the balance of inhibiting and activating signals, the blockade of inhibitory signals is apparently not sufficient to restore NK cell activity, it has to be combined with an activating signal. More investigations have to be performed, since the prolonged blockade of NK cell inhibiting receptors may also result in hyperresponsiveness.

Therapeutic antibodies can also have an effect on NK cells. The Fc-fragment can lead to

ADCC. Since NK cells are the key effectors of ADCC, the efficacy of some of these therapeutic antibodies depends on the immune reaction of NK cells. The reaction of NK cells can be enhanced by engineering antibodies to optimize their binding to the Fc receptor CD16. However, chronic stimulation of NK cells can also lead to negative effects. The continual engagement by the ligands can result in a downregulation of the NK cell receptors and it can lead for example to hyporesponsiveness. It could be the reason for resistance towards this treatment which develops in patients over time. (Li & Sun, 2018)

Unfortunately, the activation of NK cells also correlates with the production of pro-inflammatory mediators and a prolonged inflammation can even lead to tumor cell proliferation. An acute inflammation is needed for the elimination of tumor cells by the immune system, but prolonged inflammation can have a negative effect on the outcome of the anti tumor therapy. High levels of inflammatory molecules correlate with risk of death in patients. NK cells used for immunotherapy produce especially high levels of inflammatory proteins and this could lead to severe problems, but further clinical studies are necessary to gather more information. (Martín-Antonio et al., 2017)

5.9. Macrophages

Macrophages are a central component of the innate immune system. They are usually the first cells to respond to disturbances like infections and tissue damage. Macrophages can sense their environment via various receptors and can kill pathogens or necrotic or apoptotic cells by phagocytosis. They also play an important role in wound healing and present antigens to T-cells. There are several subsets of macrophages and their origin and function varies between tissues. (Ley et al., 2016)

Different subsets of macrophages have vastly different functions. Classically activated (M1) macrophages have important functions in immune surveillance and have antiviral, antibacterial and antitumoral activities. Alternatively activated (M2) macrophages play a role in wound healing and have anti-inflammatory function. In tumor development, TAMs (tumor associated macrophages) play an important role since they suppress antitumor activity and can therefore even promote tumor growth. (Murray & Wynn, 2011)

In general, macrophages can be derived from various sources: macrophages in the skin and microglia in the brain are yolk-sac derived and are maintained by continuous self-renewal

for the entire lifespan of an organism. Other tissue like the intestine contain mostly bone-marrow derived macrophages. (Okabe & Medzhitov, 2016) Those circulate in the blood system as monocytes after being derived from hematopoietic stem cells in the bone marrow and they migrate into tissue within a few days. During this migration they differentiate into either macrophages or dendritic cells.

Macrophages have distinct functions according to their anatomical location. Kupffer cells in the liver, for example, have a role in clearing pathogens and toxins from the circulatory system, while alveolar macrophages remove allergens from the lung. (Murray & Wynn, 2011) Within the red pulp of the spleen, macrophages kill senescent red blood cells and process hem and iron, but in other tissue macrophages can also have other functions like the bone resorption in osteoclasts or have a role in the function and development of the central nervous system like microglia in the brain. (Okabe & Medzhitov, 2016)

5.9.1. SIRP α

Signal regulatory protein α is expressed on macrophages, dendritic cells, neutrophils and neurons and belongs to the immunoglobulin (Ig) superfamily. Its most important ligand is CD47, which is ubiquitously expressed and sends a “don’t eat me signal” to macrophages. This prevents phagocytosis. SIRP α is a promising target in tumor immunotherapy since the disruption of the SIRP α -CD47 signalling could lead to phagocytosis of tumor cells. (Lin et al., 2018)

5.9.2. Activation of macrophages via CD16

CD16 can also mediate macrophage activity, besides mediating ADCC via NK cells. Although NK cells are considered the main mediators of ADCC, CD16 is also expressed by a subset of monocytes. These monocytes can also kill tumor cells and virus infected cells via ADCC.

ADCC begins with the recognition of the antigen, which is expressed on target cells, by specific antibodies. Fc receptors on immune cells, such as CD16, recognize the Fc part of the antibody. This leads to the release of cytotoxic granules or the expression of death receptors on the target cell ultimately leading to cell death.

Not all monocytes in humans express CD16, only CD16⁺ can exert ADCC activity, they are as efficient in the ADCC as NK cells. (Yeap et al., 2016)

5.9.3. Role of macrophages in tumor microenvironment

Macrophages can mediate both, antitumor response and tumor progression, because different subsets can have vastly different functions. M1 macrophages, for example, are responsible for phagocytosis and activate tumor killing mechanisms. Further, they also suppress the activity of other macrophage subsets, such as M2, TAMs (tumor associated macrophages), MDSCs (Myeloid derived suppressor cells) and regulatory macrophages, which all suppress the immune response. In contrast, M1 macrophages amplify the immune response by activation of T-cells.

Tumor associated macrophages (TAMs) can contribute to tumor progression by suppressing the antitumoral response. The amount of TAMs and other immune suppressive subsets of macrophages in the tumor correlates with poor outcome in cancer patients. (Murray & Wynn, 2011) TAMs resemble M2 polarized macrophages and they are associated with tumor progression, metastasis and invasion and can also stimulate angiogenesis in the tumor and inhibit the antitumoral T-cell response to the tumor. Like for other macrophages, monocytes are the precursors of TAMs. They are recruited into the tumor and differentiate due to chemokines produced by the tumor microenvironment, like regulatory T-cells or B cells and factors produced by the tumor cells. TAMs also play an important role in cancer initiation since they connect inflammatory processes and cancer. This inflammation has been shown to promote genetic instability. Some studies suggest that TAMs do not only have an effect on the local tumor but could also have an effect on tumor metastasis. TAMs can influence macrophages in several other organs and contribute through a complicated signalling pathway to tumor metastasis and therefore disease progression. Furthermore, TAMs can promote angiogenesis and several studies have shown that there is a higher number of blood vessels in tumors with higher levels of TAMs. These higher levels are generally associated with worse clinical prognosis, both in tumor models and in human cancer. Therefore, TAMs would be an interesting prognostic biomarker of cancer, next to being a possible therapeutic target. (Yang & Zhang, 2017)

5.10. Luciferase

Firefly luciferase is an enzyme which can produce yellow-green light through the reaction with its substrate luciferin. It is widely used in the field of bioimaging. The reaction was

first discovered in *Photinus pyralis*, the North American Firefly, through scientific research on bioluminescence. Firefly luciferase consists of two domains, a large N-terminal and a smaller C-terminal domain, which are joined by a flexible linker peptide. The substrate luciferin is clustered between them during the reaction, while the two domains come together which requires a change in conformation. Luciferase has its typical emission spectrum in the yellow-green region with the peak at 562 nm. The reaction requires the substrate luciferin next to ATP, oxygen and a Mg^{2+} . There are two main fields of application for Luciferase: one is the luc gene as a reporter in gene expression- and bioimaging studies, and the other possible application is the quantification of analytes connected to ATP. In tumor research, it is mostly used as a reporter gene to investigate gene expression, the activity of cellular receptors, signal transduction pathways, RNA processing and protein-protein interactions. For in vivo imaging the reporter gene luc can be introduced into the organism via a plasmid and the expression can be followed by bioimaging, in which the light production in vivo within the whole organism can be investigated. In tumor research it can be introduced to tumor cells, after which the growth of these tumor cells can then be followed in vivo in an animal model. (Marques & Esteves da Silva, 2009)

5.11. Overview of former in vivo experiments for this project

Several in vivo experiments were performed to test the effect of CD47 blockade in triple negative breast cancer. For this purpose, the MDA-MB-231 LM2-4 cell line was transfected with the fusion protein IL2-P-Fc, where P encodes for SIRP α . The SIRP α part of the fusion protein should block CD47 on the surface of the tumor cells. (Kassem, 2017) The variant CV1 was used since it binds to CD47 with higher affinity. (Weiskopf et al., 2013) The Fc part used (derived from human IgG1) can efficiently trigger ADCC and complement-dependent cytotoxicity (CDC) because of a single point mutation (substitution of residue E333 with alanine; (Shields et al., 2001)). The IL2 part is necessary to secrete the protein outside the cell, it is needed since CD47 is a surface protein and has to be blocked extracellularly. (Kassem, 2017)

In the first in vivo experiment there were three groups of animals: a treated group with expression of IL2-P-Fc, a transfection control group with expression of bb-mCherry and a control group with untransfected breast cancer cells. (Pichler, 2019)

The breast cancer cells were transfected with either pCpG-hCMV-SCEP-IL2-P-Fc (treated group) or pCpG-hCMV-SCEP-bb-mCherry (transfection control group). The latter plasmid contains the same backbone, but instead of the fusion protein, bb-mCherry is expressed. (Kassem, 2017) The cells were implanted into the 4th pair of inguinal nipples of SCID mice 48 hours after transfection. In the control group, untransfected cells were implanted. Via 2D bioluminescence imaging (BLI) the tumor growth was followed for 34 days, after which the mice were euthanized and the tumors were histologically evaluated. The experiment was performed with three mice per group.

In the second in vivo experiment the influence of the Fc part on treatment efficacy should be evaluated. The experiment was performed similarly to the first experiment, with one additional treatment group. The cells were transfected with a pCpG-hCMV-SCEP-IL2-P plasmid (encoding for secreted SIRP α only). The endpoint was 25 days after implantation, where the tumors were dissected, fixed and later on stained.

The third experiment was different from the first two. Untransfected cancer cells were implanted and after 13 days of tumor growth the mice were treated with polyplexes containing the IL2-P-Fc- or the bb-mCherry plasmid via intratumoral injection. As negative control only buffer was injected. After 24, 48 and 72 hours the tumors were obtained to see when and if infiltration of immune cells occurs. The experiment was performed with one mouse (with two tumors each) per group. (Pichler, 2019)

In the fourth in vivo experiment, the same procedure as in the third was performed, but with different time points. It was presumed that 24 hours after in vivo transfection no macrophage infiltration and CD47 blockade might be observed due to the possibility that the immune reaction occurred much faster than first thought. Tumors were explanted 12, 17 and 24 hours after transfection and embedded. The experiment was performed with two to three mice per group (two tumors each).

6. Materials and Methods

6.1. Buffers and solutions

4% buffered formaldehyde solution:

paraformaldehyde (4% w/v) was dispersed in HEPES buffered saline (20 mM HEPES, 150 mM NaCl, pH 7.4), heated under stirring to 60°C until the paraformaldehyde was dissolved. Evaporated water was replaced by distilled water and the solution filtered (0.22 µm pore size). Aliquots of the solution were stored frozen at -20°C. (R&D Systems, 2019)

Haematoxylin solution:

Harris Haematoxylin diluted 3:1 in Aqua dest., it has to be filtered before use to eliminate crystals

Ammonium-water:

a mixture of 10 drops Ammonium solution 32% in 250 mL Aqua dest.

Eosin solution:

25 mL Eosin Y solution, 200 mL Aqua dest. and 0,125 mL glacial acetic acid

PBS:

1370 mM NaCl, 27 mM KCl, 54 mM Na₂HPO₄ and 18 mM KH₂PO₄

Dilution buffer:

2 % Bovine serum albumin (BSA) w/v in PBS (0.45 µm filtered with Steriflip)

DAB (Diaminobenzidine) solution:

1 tablet 3,3'- Diaminobenzidine tetrahydrochloride (10 mg), 15 mL PBS, 75 µL Triton X and 10.3 µL freshly added 35% H₂O₂ shortly before use

HCl solution:

175 ml EtOH 100%, 2.5 ml hydrochloric acid (30%) and 72.5 mL Aqua dest.

Sodium Citrate buffer

10 mM Tri-sodium citrate in MiliQ-water and 0.05 % Tween 20, adjusted to pH 6 with HCl. (IHC World, 2015b)

Tris-EDTA Buffer:

10 mM Tris Base and 1 mM EDTA in MiliQ-water, adjusted to pH 9 with NaOH, add 0.05 % Tween 20 (IHC World, 2015e)

EDTA buffer:

1mM EDTA in Aqua dest., adjust to pH 8 using NaOH, add 0.05% Tween 20. (IHC World, 2015c)

RBC lysis buffer:

9 g NH₄Cl, 1 g KHCO₃, and 36 mg Disodium EDTA in 1 L MilliQ water

Triton X solution for permeabilization:

0.025% Triton X in PBS (62.5 µl Triton X and 249.93 mL PBS)

6.2. Embedding

Organs were explanted, split into smaller pieces where necessary (i.e. liver and lung) and fixed for 22h in 4% buffered formaldehyde solution. Fixed tissue was placed in cassettes. The cassettes were submersed in 70% EtOH to avoid drying out the organs. The SLEE MTP embedding carousel was used for the further procedure, with increasing concentrations of Ethanol (70%, 96%, 100%) for dehydration and Xylene. As a final step the cassettes were put into paraffin to infiltrate the tissue. This process takes 13 hours.

For embedding the organs, the SLEE MPS/P1 embedding system was used. A metal mould was partly filled with paraffin and the organ was put inside and pushed down using forceps, then the bottom of the mould was put on and it was filled up with melted paraffin. After this the mould was transferred to the cooling plate and the paraffin block was taken out

after it solidified. If there were bubbles in the block it had to be melted again and the organ had to be re-embedded.

6.3. Sectioning

For sectioning, a semi-automatic precision microtome (SLEE CUT 5062) was used to obtain sections of 2 μm thickness. The best results were achieved by cooling the paraffin block before sectioning, for this the Para cooler model A was used at a setting of $-21\text{ }^{\circ}\text{C}$. After sectioning slices were floated on distilled water in a water bath heated to $40\text{ }^{\circ}\text{C}$, to let them unfold. Afterwards they were picked up carefully with a labelled microscope slide. For H&E staining Superfrost slides were used, for IHC Superfrost plus adhesion microscope slides.

6.4. Haematoxylin and Eosin staining (H&E staining)

Sections were placed in a slide holder and pre-warmed in a drying chamber at 55°C for 2 hours. Afterwards they were passed through 3 containers containing Xylene for deparaffinisation for 5 minutes each, followed by 3 containers with 100% EtOH, 3 containers with 96% EtOH and 3 containers with 70% EtOH for 30 seconds each for rehydration. Before staining the slides were incubated in distilled water for one minute.

This was followed by the first staining step with Haematoxylin for 3 minutes, rinsing in tap water for 20 seconds to get rid of excess dye, followed by incubation in Ammonium-water and then by rinsing in tap water again for 1 minute. After this the second staining step followed by incubating the slides in Eosin solution for 2 minutes and rinsing in tap water for 10 seconds.

The next step was to dehydrate the sections. Sections were put successively in 3 containers with 70% EtOH, 3 containers with 96% EtOH and 3 containers with 100% EtOH for 1 second each. In the end they were incubated in Xylene, 1 minute in the 1st container and 2 minutes each in two more containers.

Sections were mounted with Entellan new to preserve them for staining and covered with a coverslip.

6.5. Immunohistochemistry (IHC) staining - standard protocol

For each organ, one section was stained with primary and secondary antibody, one with an isotype control and secondary antibody, one section with secondary antibody only and one with buffer only.

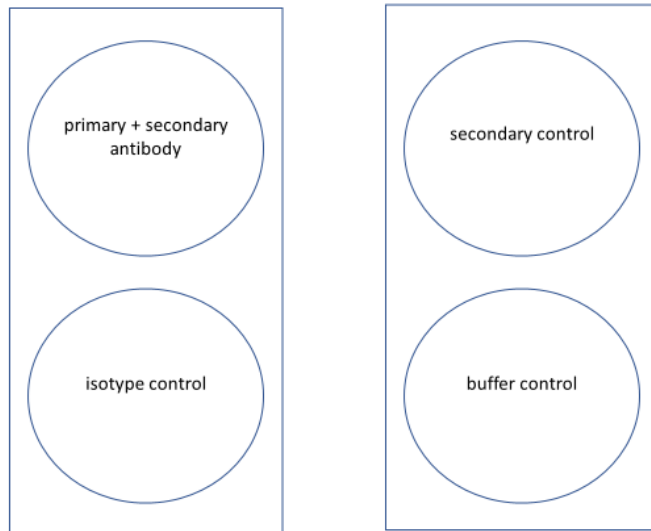


Figure 4 Arrangement of sections for IHC

Sections were labelled, placed in a slide holder and pre-warmed in the drying chamber for 2 hours at 55°C. Afterwards they were passed through 3 containers holding Xylene for deparaffinisation for 5 minutes each, followed by 3 containers with 100% EtOH, 3 containers with 96% EtOH and 3 containers with 70% EtOH for 30 seconds each for rehydration. Before staining the slides were incubated in distilled water for 30 seconds.

Because the sections were fixed with paraformaldehyde, which can lead to crosslinking of proteins, sections had to undergo HIER (heat induced epitope retrieval) to recover masked antigens (Novus Biologicals). For this purpose, slides were submersed in buffer and heated for 30 minutes using a silicone oil bath set to a temperature between 121°C and 130°C. Different buffers were used, depending on the primary antibody, for example Tris EDTA buffer for CD47 staining or Sodium citrate buffer for NCR1 staining.

After this, sections were left to cool down to room temperature for 30 minutes, followed by permeabilization with Triton X100 in case intracellular antigens were stained, and a washing step with PBS. The sections were encircled with a hydrophobic PAP pen to prevent reagents from leaking out, then incubated with blocking serum (provided by the staining kit, the host has to be the same as the host of the secondary antibody, which is also provided by the staining kit), to block any unspecific binding of the primary antibody, followed by another washing step with PBS and an avidin-biotin blocking step, which includes incubation for 15 minutes for each, avidin and biotin solution. After another washing step with PBS the sections are incubated with the primary antibody diluted in dilution buffer (2 % Bovine serum albumin (BSA) w/v in PBS (0.45 µm filtered with Steriflip) or buffer only

for the controls overnight in the fridge at 4°C.

On the second day the staining starts with incubating the slides in 0.3% H₂O₂ for 15 minutes after a washing step with PBS to block endogenous peroxidase. The sections are then washed again and incubated with the secondary antibody for 30 minutes, followed by a washing step and incubation with ABC Reagent (5 ml BSA/PBS, 1 drop of Reagent A and 1 drop of reagent B provided by the staining kit used) for 30 minutes. This step is not necessary if a polymer-based detection system is used. After another washing step the slides are incubated with a DAB (Diaminobenzidine) solution until the sections turns brown, because of a reaction of horse radish peroxidase with DAB. The staining can be checked under the microscope after the slides are washed in PBS and DAB can be applied again if necessary. If the staining is intense enough, the reaction is stopped by placing the slides in distilled water.

The sections are counterstained with haematoxylin for 3 minutes, rinsed in tap water for 10 seconds, put in HCl solution for 1 second and again rinsed in tap water for one minute.

The sections are dehydrated and mounted with Entellan according to the H&E staining protocol.

This standard protocol must be adapted to the Antibodies and detection kits used.

6.6. NCR1 staining

In this thesis we wanted to see, if the blocking of CD47 led to an increased number of Natural Killer cells in the tumor tissue. For this purpose, Vectastain ABC kit was used and two different primary antibodies. HIER was performed with Sodium Citrate buffer.

The antibody ab199128 binds to the intracellular NCR1 domain near the C-terminus (Abcam, 2019d), while the antibody ab214468 binds to the extracellular side. (Abcam, 2019c)

Primary antibodies	Product No.	Lot No.	concentration
Rabbit anti NCR1 (polyclonal)	ab199128	GR256711-45	1:500
Rabbit anti NCR1 (polyclonal)	ab214468	GR3224201-4	1:300

Table 1 Primary Antibodies for NCR1 staining

Isotype	Product No.	Lot No.
Rabbit IgG Isotype monoclonal [EPR25A] control	ab172730	GR3179509-19

Table 2 Isotype for NCR1 staining

For this staining an Avidin-Biotin based detection system was used, which was described in the Introduction, using the Vectastain ABC kit.

The staining was performed according to the standard staining protocol.

6.7. CD47 staining

This staining was used to show the blockage of CD47 by the expressed fusion protein.

For this staining, Vectastain ABC kit was used and the staining was performed according to the standard protocol. HIER was performed using Tris-EDTA Buffer

Primary antibody	Product No.	Lot No.	concentration
Rabbit monoclonal anti CD47	ab218810	GR3216895-1	1:2000

Table 3 Primary antibody for CD47 staining

Isotype	Product No.	Lot No.
Rabbit IgG Isotype monoclonal [EPR25A] control	ab172730	GR3179509-19

Table 4 Isotype for CD47 staining

6.8. Firefly Luciferase staining

Because the human tumor cells were stably transduced to express Luciferase, this staining allows the distinction between human tumor cells and mouse tissue.

For this staining, the VitroView™ 1-Step anti Goat Polymer based IHC/DAB kit was used. This kit uses a polymer-based detection system, which was described in the introduction.

The standard protocol had to be modified accordingly for this staining. HIER was performed with EDTA buffer.

Primary antibody	Product No.	Lot No.	concentration
Goat pAB to Firefly Luciferase	ab181640	GR257345-31	1:1000

Table 5 Primary antibody for Firefly luciferase staining

Isotype	Product No.	Lot No.
Goat IgG Isotype	bs0294P	AE091001

Table 6 Isotype for Firefly luciferase staining

6.9. SIRP α staining

This staining was performed to detect SIRP α positive macrophages in tumor tissue. Vectastain ABC kit was used, HIER was performed with Sodium citrate buffer.

Primary antibody	Product No.	Lot No.	concentration
Rabbit Anti SIRP alpha [EPR16264]	ab191419	GR178545-2	1:400

Table 7 Primary Antibody for SIRP α staining

Isotype	Product No.	Lot No.
Rabbit IgG Isotype monoclonal [EPR25A] control	ab172730	GR3179509-19

Table 8 Isotype for SIRP α staining

6.10. CD 16 staining

With this staining the Fc receptor on macrophages and NK cells should be detected. This staining is performed according to the standard protocol, using the Vectastain ABC kit and Sodium citrate buffer for HIER.

Primary antibody	Product No.	Lot No.	concentration
Rabbit pAb to CD16	ab203883	GR3256555-2	1:100

Table 9 Primary Antibody for CD 16 staining

Isotype	Product No.	Lot No.
Rabbit IgG Isotype monoclonal [EPR25A] control	ab172730	GR3179509-19

Table 10 Isotype for CD 16 staining

6.11. Immunocytochemistry (ICC)

To determine usability and specificity of the NCR1 antibodies, staining of blood cells and their analysis by flow cytometry was performed. For these experiments mouse and pig blood was used.

Because only white blood cells were of interest, the blood was lysed using a red blood cell (RBC) lysis buffer. 50 µL blood were incubated with 1 mL lysis buffer for 10 minutes at room temperature and then centrifuged at 300g for 5 minutes. The liquid was removed with a pipette and the pellet resuspended in 100-200 µL PBS. This solution was spread thinly onto a slide using a pipette.

Cells were fixed onto the slides using 4% Paraformaldehyde in HBS for 5 minutes. Then the cells were permeabilized with 0.5% Triton X in PBS for 10 minutes. After letting the slides dry, they were stained according to the standard protocol for IHC, in this case no HIER was necessary. For training purposes sections were also stained with Haematoxylin for 3-4 minutes to depict the morphology of the different immune cells.

For further training, some blood smears were performed. For this a small drop of blood was put on a slide, a clean spreader slide was brought to the drop at a 45° angle until the blood spread along the entire side of the slide. The slide was pushed forward smoothly, and the smears were left to dry. They were either stained with Haematoxylin for 3-4 minutes, or with Giemsa stain for 1 minute and 30 seconds and then washed in a jar of deionized water for 4 minutes and left to dry.

6.12. Analysis of results

Staining results were analysed using bright field microscopy with an Olympus BX53 light microscope. Pictures were taken with the Olympus DP-73 colour camera at different magnifications using the cellSens Standard software from Olympus.

Objectives		
2x	PLAPON2X/0,08 Plan Apo	Olympus, Shinjuku, Tokyo, Japan
4x	UPLSAPO4X/0,16 U Plan S Apo	Olympus, Shinjuku, Tokyo, Japan
10x	UPLSAPO10X2 U Plan S Apo	Olympus, Shinjuku, Tokyo, Japan
20x	UPLSAPO20X/0.75 U Plan S Apo	Olympus, Shinjuku, Tokyo, Japan
40x	UPLSAPO20X/0.75 U Plan S Apo	Olympus, Shinjuku, Tokyo, Japan

Table 11 Objectives used for microscopy

6.13. Materials, Reagents, Devices

Materials, Reagents and Devices used are listed in the tables below.

	Product No	LOT No	Supplier
Acetic Acid glacial	30721	STBG8626	Sigma-Aldrich, St.Louis, Mo, USA
Ammonium chloride (NH ₄ Cl)	0718	BCBM9152V	Sigma-Aldrich, St.Louis, Mo, USA
Ammonium Solution	221228	SZBD3180V	Sigma-Aldrich, St.Louis, Mo, USA
Biotin/ Avidin blocking kit	BUF016	146543; 147519	BIO-RAD, Hercules, CA, USA
BSA (Bovine Serum Albumin)	A9647	SLBT0167	Sigma-Aldrich, St.Louis, Mo, USA
DAB (3,3'- Diaminobenzidine tetrahydrochloride)	D5905	SLBS4779	Sigma-Aldrich, St.Louis, Mo, USA
DAB (3,3'- Diaminobenzidine tetrahydrochloride)	980681	S2021	MP Biomedicals, Solon, Ohio, USA

Disodium Phosphate Dodecahydrate ($\text{Na}_2\text{HPO}_4 \cdot 12\text{H}_2\text{O}$)	A3906	3P009818	AppliChem, Darmstadt, Germany
Dulbecco's PBS 10x concentrated	D1408	RNBH2012	Sigma-Aldrich, St.Louis, Mo, USA
EDTA	E6758	SLBR6878V	Sigma-Aldrich, St.Louis, Mo, USA
Entellan [®] new	107961	HX72093761	Merck, Darmstadt, Germany
Eosin Y	318906	MKBW8933V	Sigma-Aldrich, St.Louis, Mo, USA
Ethanol denatured 99.8%	K928.2	Ch.: 248272285	Carl Roth, Karlsruhe, Germany
Giemsa stain	GS500	SLBS0364V	Sigma-Aldrich, St.Louis, Mo, USA
Haematoxylin Harris	X903.3	Ch.: 037253899	Carl Roth, Karlsruhe, Germany
HEPES	A3724	7IO15011	AppliChem, Darmstadt, Germany
hydrochloric acid fuming	20104.334	Batch: 14A160513	VWR Chemicals, Radnor, USA
Hydrogen peroxide 35%	9683.1	Ch.: 295231751	Carl Roth, Karlsruhe, Germany
Paraformaldehyde	A3813	R014578	AppliChem, Darmstadt, Germany
Paraplast [®]	P3558	SLBN3818V	Sigma-Aldrich, St. Louis, MO, USA
Paraplast [®] Plus	39602004	-	Leica Biosystems, Buffalo Grove, IL, USA
Potassium bicarbonate (KHCO_3)	60339	BCBP3665V	Sigma-Aldrich, St.Louis, Mo, USA
Potassium chloride (KCl)	A2939	3R007818	AppliChem, Darmstadt,

			Germany
Potassium dihydrogen orthophosphate (KHO ₄)	P5655	SLBJ7258V	Sigma-Aldrich, St.Louis, Mo, USA
Sodium chloride	1.06400.5000	K49776800805	Merck, Darmstadt, Germany
Steriflip	SCGP00525	MPSF184807	Merck, Darmstadt, Germany
Tris Base	T1503	SLBL0891V	Sigma-Aldrich, St.Louis, Mo, USA
Tri-Sodium citrate dihydrate	27833.237	13/170003	VWR chemicals, Radnor, USA
Triton X-100	X-100	SLBM3864V	Sigma-Aldrich, St.Louis, Mo, USA
Tween [®] 20	A4974	4G009367	AppliChem, Darmstadt, Germany
Xylol	9713.4	Ch.: 108268747	Carl Roth, Karlsruhe, Germany

Table 12 Reagents and Materials

Staining kit	Product No.	Lot No.	Supplier	Stainings
Ultra Sensitive ABC Peroxidase Staining kit	35052	TO264647	Thermo Fisher Scientific, Waltham, USA	Luciferase
Vectastain [®] ABC kit	PK-4001	290617; 2E1207	Vector Laboratories, Burlingame, CA, USA	NCR 1 CD16 SIRP α CD47
VitroView [™] IHC/DAB kit anti- goat	VB-6026D	076VB18; 1026VB18	VitroVivo Biotech, Maryland, USA	Luciferase

Table 13 Staining kits used

Materials	Supplier
coverslip 24x50 mm	1831; Carl Roth, Karlsruhe, Germany
Elite PAP pen	CLSG80125; Cederlane Laboratories, Ontario, Canada
HISTOSETTE [®] I Tissue Processing/ embedding cassettes (45 DEGREE ANGLE)	M498; Simport, Beloeil, Canada
microscope slides SUPER-FROST [®]	2101; Carl Roth, Karlsruhe, Germany
microscope slides SUPER-FROST [®]	5088; Thermo Fisher Scientific, Waltham, USA
microscope slides SUPER-FROST [®] PLUS	J1800AMNZ; Thermo scientific, Waltham, MA, USA

Table 14 Materials

Devices	Supplier
cellSens Standart	Olympus, Shinjuku, Tokyo, Japan
Embedding station MPS/P1	Slee medical GmbH, Mainz, Germany
Microtome CUT 40062	Slee medical GmbH, Mainz, Germany
Olympus BX53 light microscope	Olympus, Shinjuku, Tokyo, Japan
Olympus DP-73 color camera	Olympus, Shinjuku, Tokyo, Japan
Para cooler model A	Ralf W. Weinlauf, Hallendorf, Germany
SLEE MTP embedding carousel	Slee medical GmbH, Mainz, Germany

Table 15 Devices

Antibodies	Product No.	Lot No.	Supplier
Goat IgG Isotype	bs0294P	AE091001	Bioss, USA

Goat pAB to Firefly Luciferase	ab181640	GR257345-31	Abcam, Cambridge, UK
Rabbit anti NCR1	ab199128	GR256711-45	Abcam, Cambridge, UK
Rabbit Anti SIRP alpha [EPR16264]	ab191419	GR178545-2	Abcam, Cambridge, UK
Rabbit IgG Isotype monoclonal [EPR25A] control	ab172730	GR3179509-19	Abcam, Cambridge, UK
Rabbit monoclonal anti CD47	ab218810	GR3216895-1	Abcam, Cambridge, UK
Rabbit pAb to NCR1	ab214468	GR3224201-4	Abcam, Cambridge, UK
Rabbit pAb to CD16	ab203883	GR3256555-2	Abcam, Cambridge, UK

Table 16 Antibodies

7. Results

7.1. Haematoxylin & Eosin staining

H&E stainings of different organs were performed as practice for sectioning and staining.

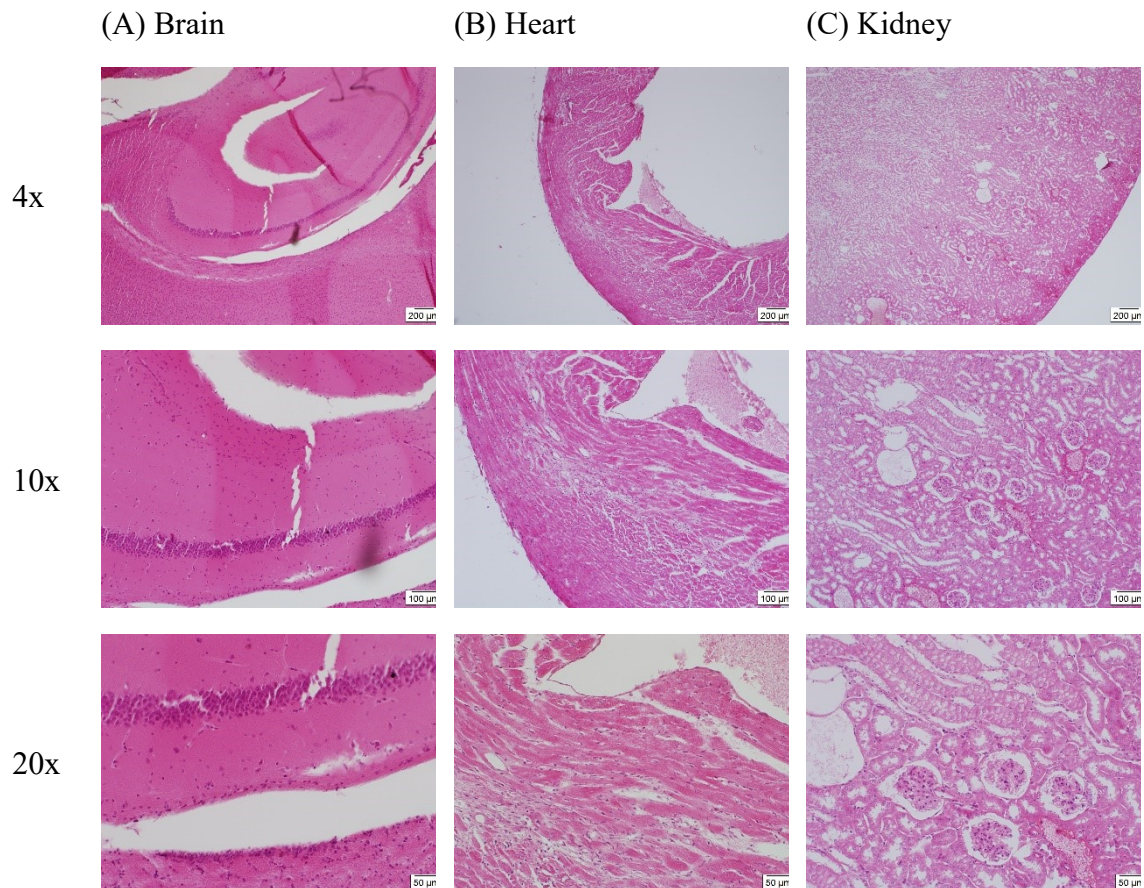
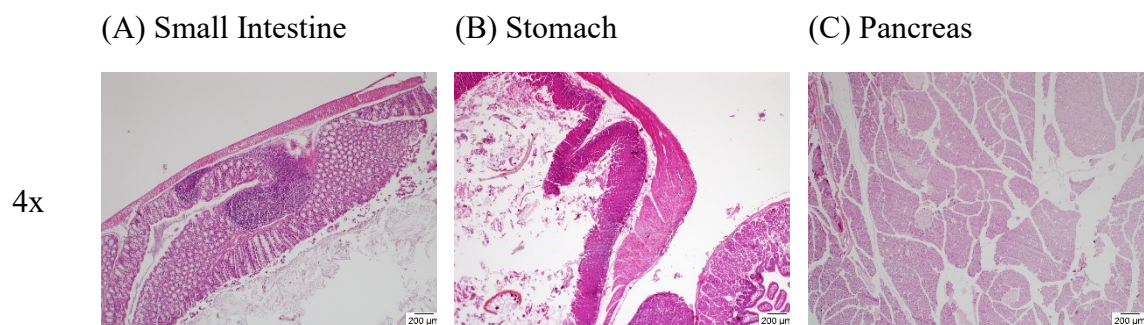


Figure 5 H&E staining (A) Brain, (B) Heart, (C) Kidney. Magnification 4x, 10x, 20x, scale bar 200 μm , 100 μm , 50 μm .



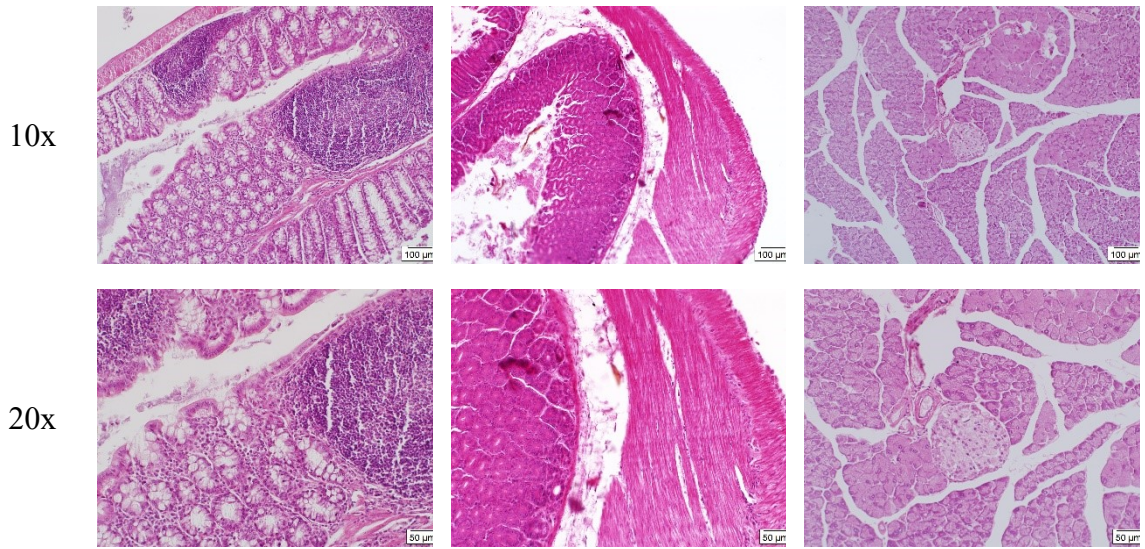
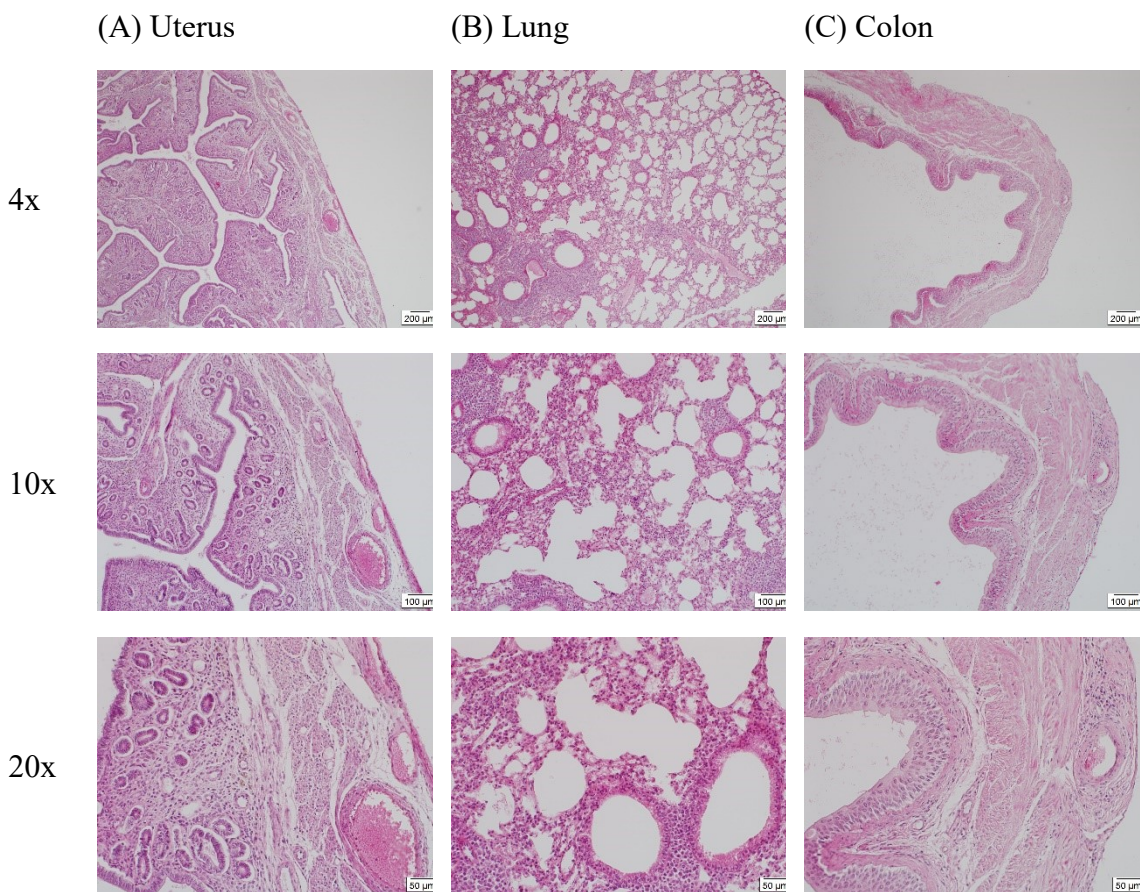


Figure 6H&E staining (A) Small Intestine, (B) Stomach, (C) Pancreas. Magnification 4x, 10x, 20x, scale bar 200 μm , 100 μm , 50 μm



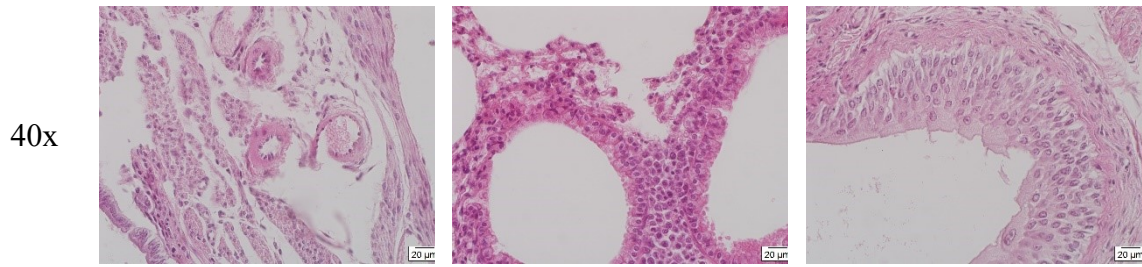
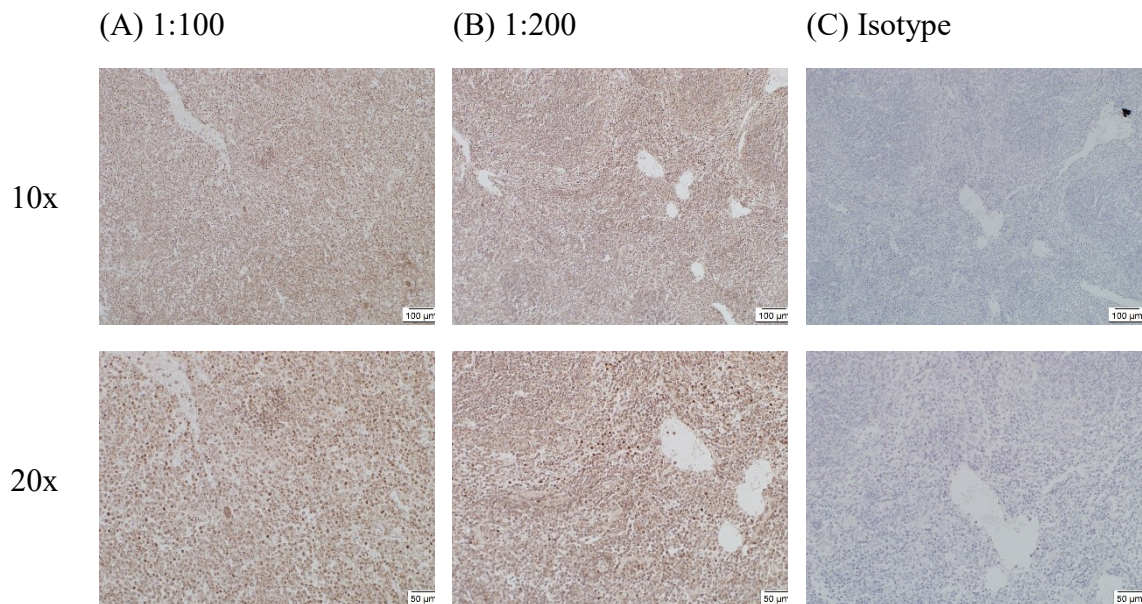


Figure 7 H&E staining (A) Uterus, (B) Lung, (C) Colon. Magnification 4x, 10x, 20x, 40x, scale bar 200 µm, 100 µm, 50 µm, 20 µm.

7.2. Optimization of NCR1 staining

This staining was necessary to detect NK cells in the tumor tissue. For this purpose, two different primary Antibodies were tested at different concentrations.

The first staining was performed using the Anti NCR1 Antibody ab214468 at a dilution of 1:100 using the Vectastain ABC kit. Because of the strong background staining, the same staining was performed at a dilution of 1:200.



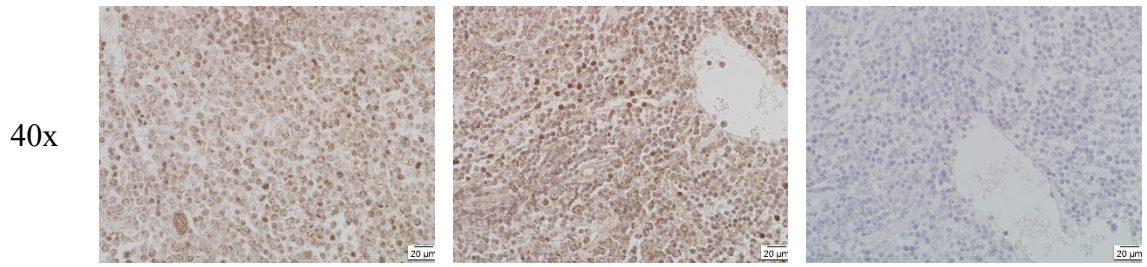
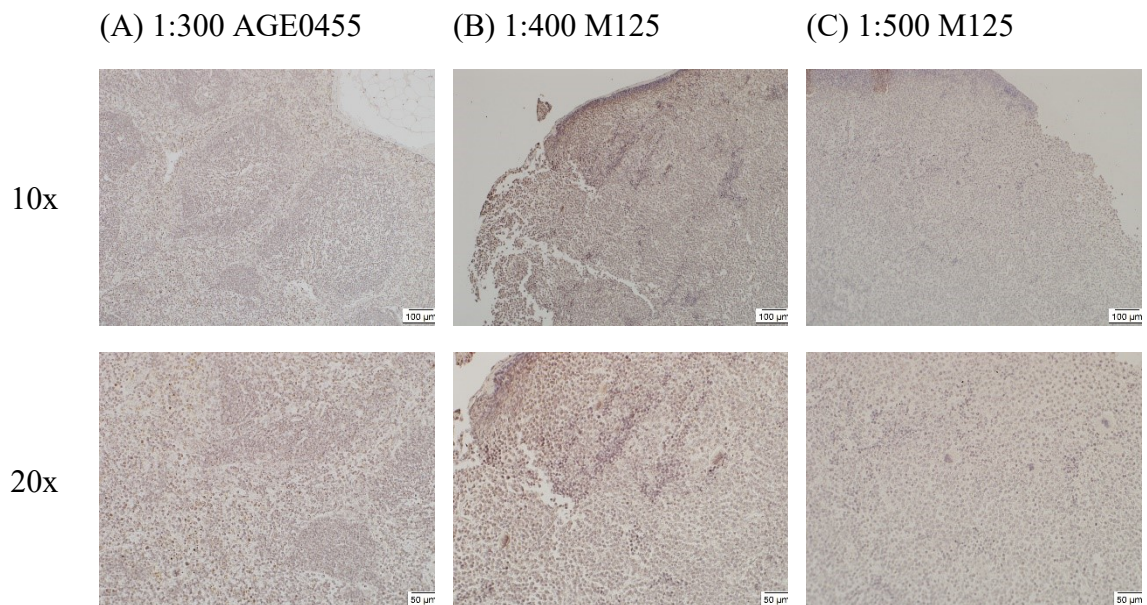


Figure 8 NCR1 staining ab214468 of Spleen M285, dilutions of the primary antibody at (A) 1:100 and (B) 1:200, and (C) isotype control. Magnification: 10x, 20x, 40x, Scale bar: 100 µm, 50 µm, 20 µm.

As can be seen in Figure 8 , the staining showed some darker stained cells in the spleen, but in this organ, it was not possible to determine if the staining was specific or not. It was also not possible to see if the staining occurred in the red pulp, where NK cells should be found, or in the white pulp. The 40x magnification showed that the nuclei seemed to be stained, which was unexpected, because NCR1 should be a cell surface protein. The background staining did not improve at 1:200, so several more dilutions were tested on two different healthy spleens.



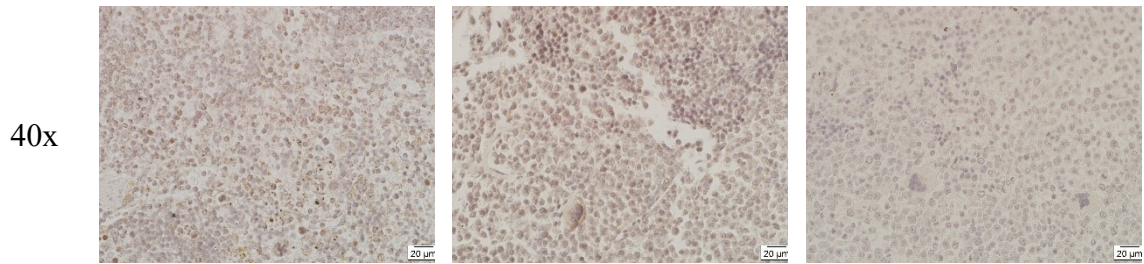


Figure 9 NCR1 staining ab214468 of spleen (A) AGE0455, dilution: 1:300, (B) M125, dilution: 1:400 and (C) M125, dilution: 1:500. Magnification: 10x, 20x, 40x, Scale bar: 100 µm, 50 µm, 20 µm.

As shown in Figure 9 the background staining still occurred at higher dilutions, but at the dilutions 1:400 and 1:500 stained cells could not be clearly seen anymore, so it was decided to proceed with the dilution 1:300 for further experiments.

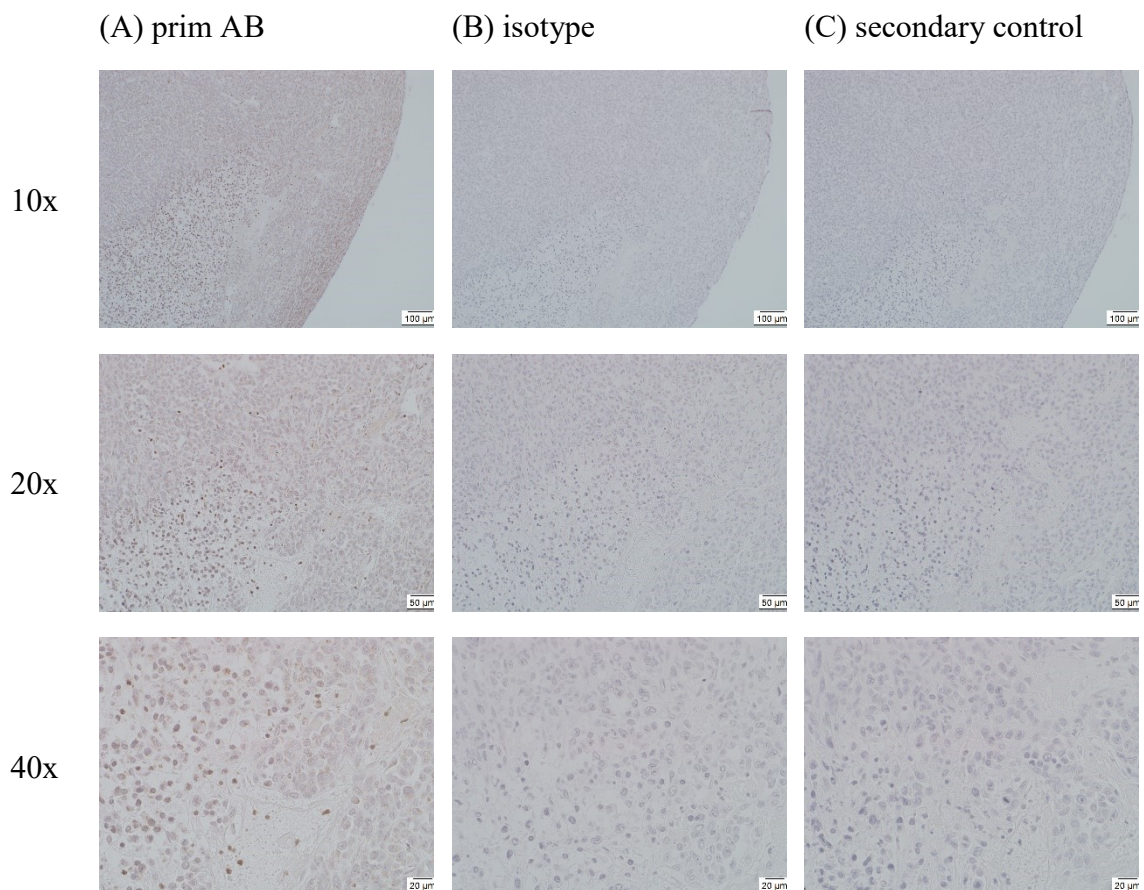


Figure 10 NCR1 staining ab214468 MCT-209 tumor, (A) primary antibody dilution 1:300, (B) isotype control, (C) secondary antibody control. Magnification: 10x, 20x, 40x, Scale bar: 100 µm, 50 µm, 20 µm.

To determine whether the staining was specific or not, other organs that should not contain any lymphocytes were stained with the antibody. For this purpose, liver, lung and a tumor were stained, in which we expect low levels or absence of NK cells. In the tumor tissue (Figure 10) some clusters of positive cells were observed, although the staining pattern appeared ambiguous with whole cells stained. In lung (Figure 11), structures in the bronchial epithelium appeared strongly positive for the stain, whereas in live some single cells were positive, albeit a high background was observed.

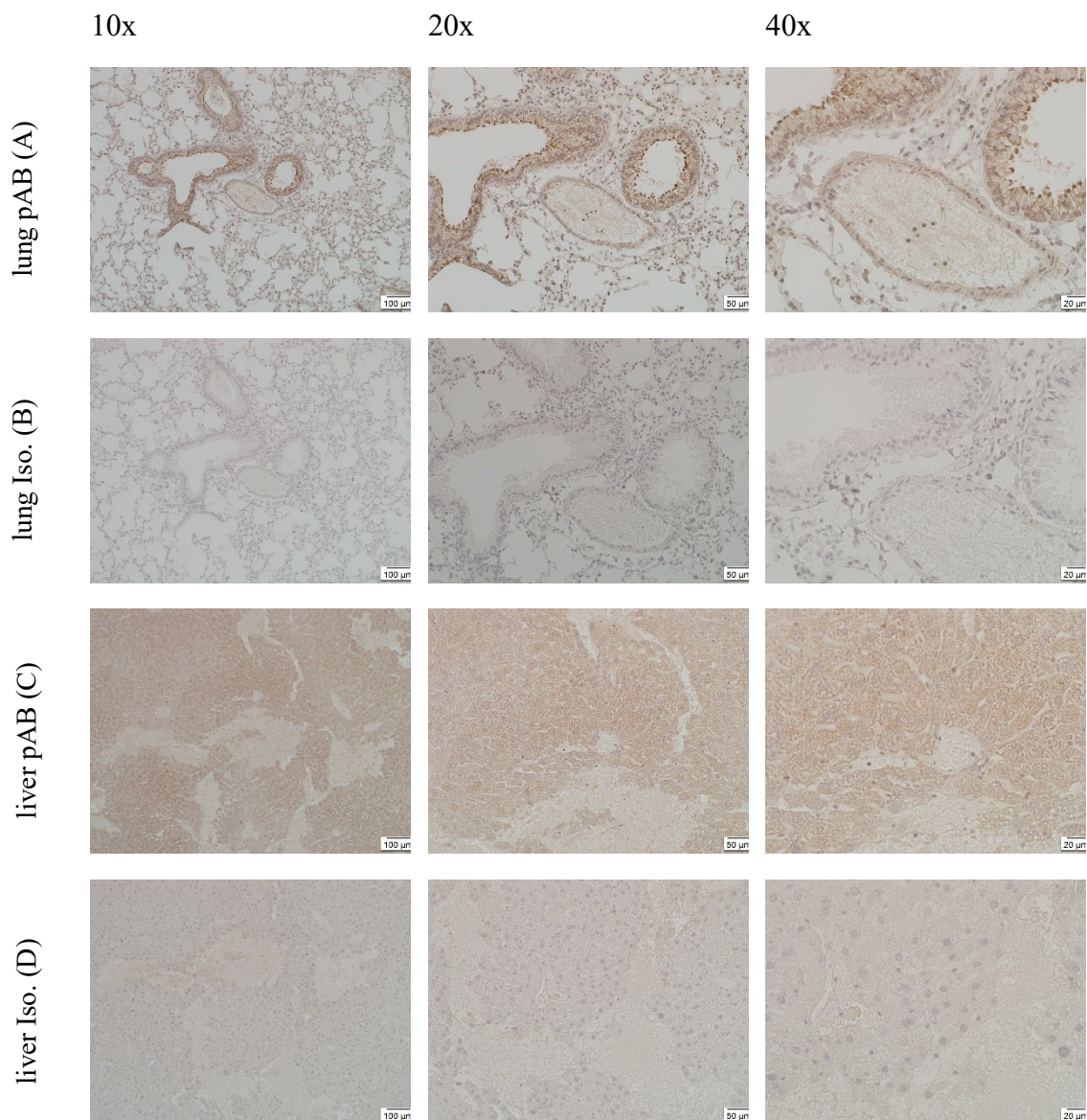


Figure 11 NCR1 staining ab214468 of different organs, (A) AGE0455 lung, dilution of the primary antibody 1:300 and (B) isotype control; (C) AGE0455 liver, dilution of the primary antibody 1:300 and (D) isotype control. Magnification: 10x, 20x, 40x, Scale bar: 100 μ m, 50 μ m, 20 μ m.

As clearly visible in Figure 11, this antibody also stained cells other than NK cells, there was no staining in the controls, so it was concluded that the primary antibody was also recognises antigens others than the target antigen on NK cells.

Because of the issues and due to the strong background staining and unspecific staining, an alternative Anti NCR1 antibody was tested.

Next, the Anti NCR1 Antibody ab199128 was tested. This Antibody was first tested staining spleen at the dilutions 1:50 and 1:100 using the Vectastain ABC kit.

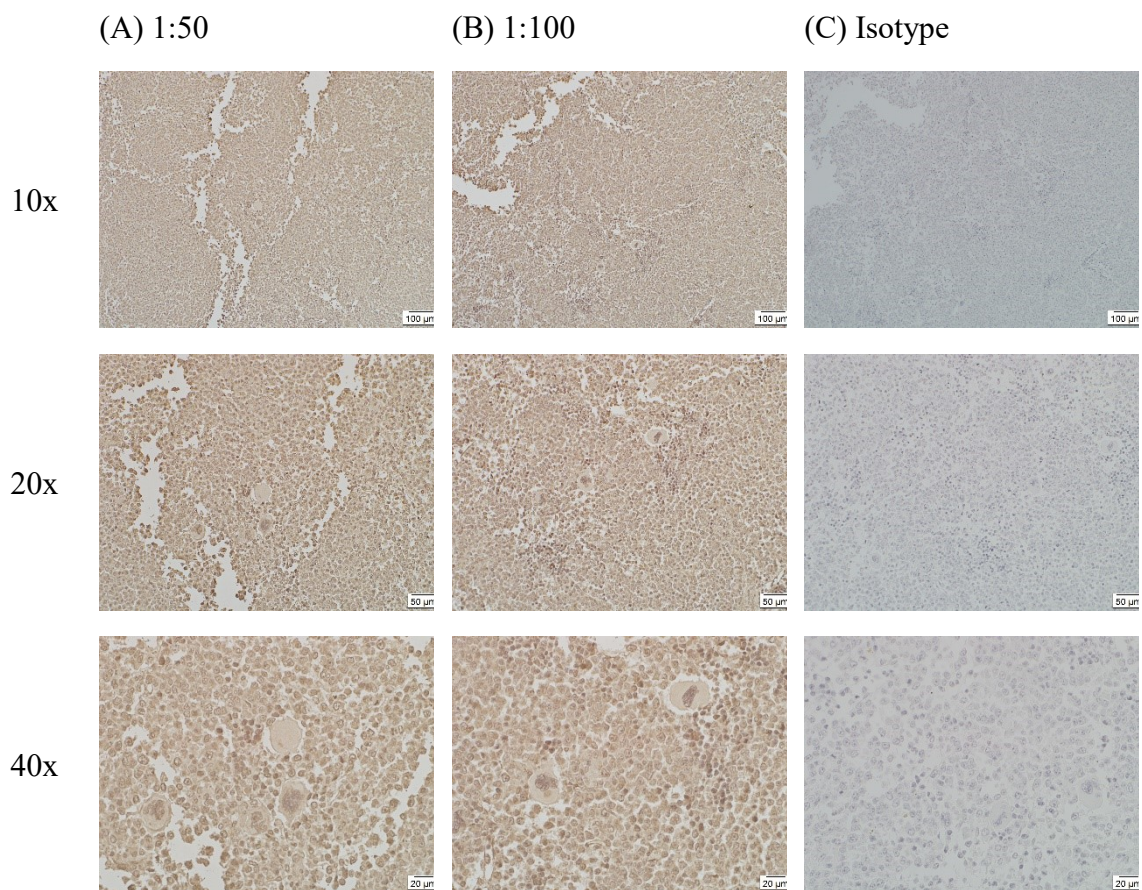


Figure 12 NCR1 staining ab199128, M125 Spleen, primary Antibody dilutions: (A) 1:50, (B) 1:100 and (C) isotype control; Magnification: 10x, 20x, 40x, Scale bar: 100 μm, 50 μm, 20 μm.

As shown in Figure 12, this antibody had the same issues as the first one with a very high background staining. Furthermore, this antibody also seemed to stain the nuclei instead of the cell surface, as it was expected. Because of the high background, the staining was repeated with the dilutions 1:200 and 1:500.

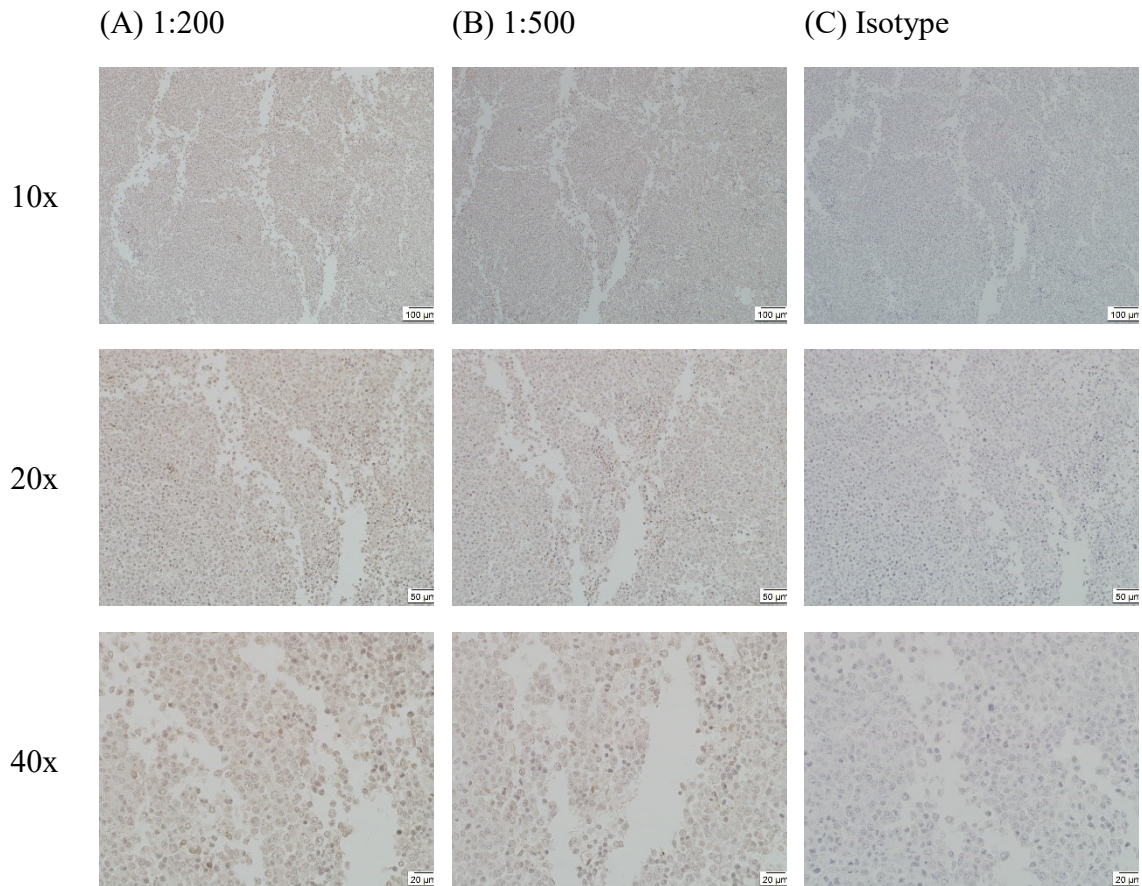


Figure 13 NCR1 staining ab199128, M125 Spleen, primary antibody dilutions: (A) 1:200, (B) 1:500 and (C) isotype control. Magnification: 10x, 20x, 40x, Scale bar: 100 μm , 50 μm , 20 μm .

Figure 13 shows significantly reduced background staining at these dilutions. Because there was almost no difference between 1:500 and 1:200 it was unclear which dilution would be better to use in further experiments. To determine this, another experiment was performed, staining the same tumor with both dilutions.(Figure 14)

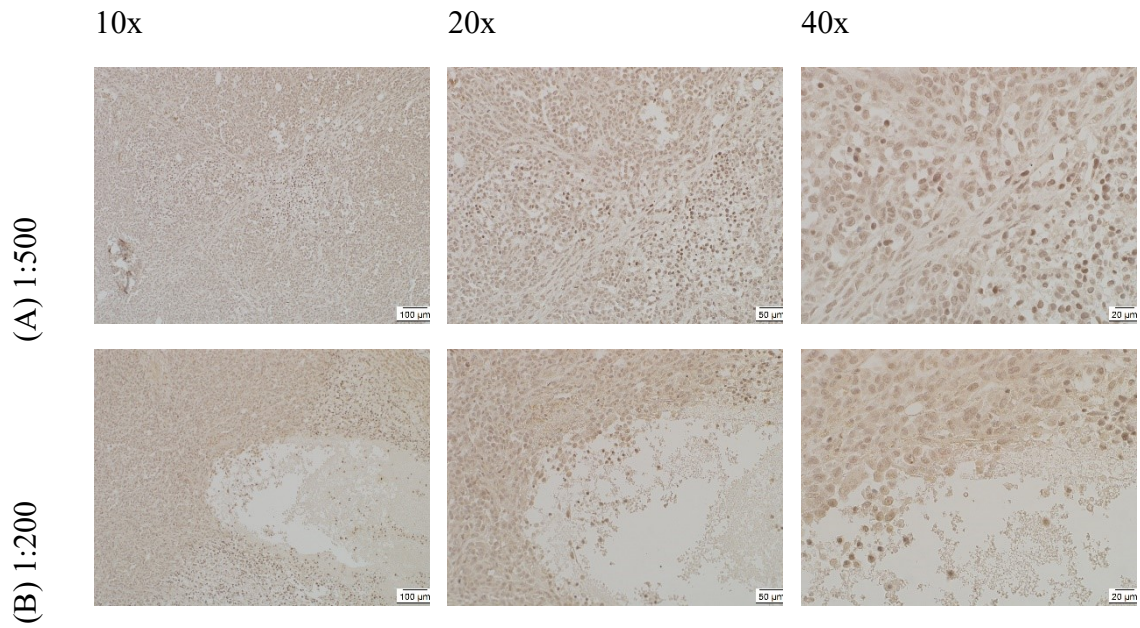
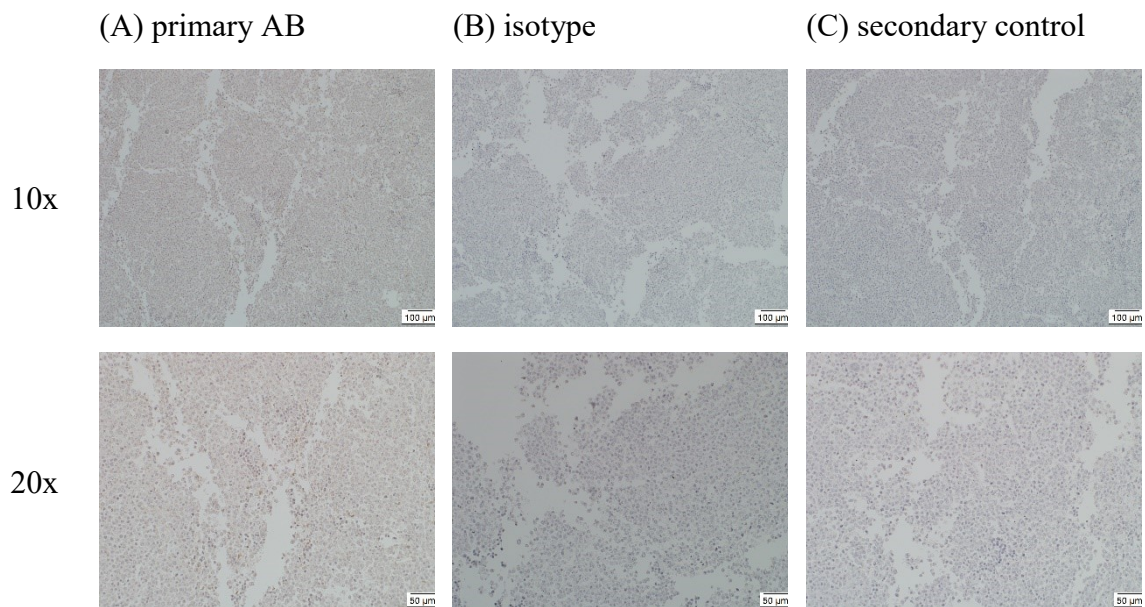


Figure 14 NCR1 staining ab199128 (A) M209, dilution of the primary antibody: 1:500. (B) M209, dilution of the primary Antibody: 1:200. Magnification: 10x, 20x, 40x, Scale bar: 100 μm , 50 μm , 20 μm .

As shown in Figure 14, there was almost no difference between the two dilutions of the primary antibody, so it was decided to use the dilution 1:500 for further experiments.



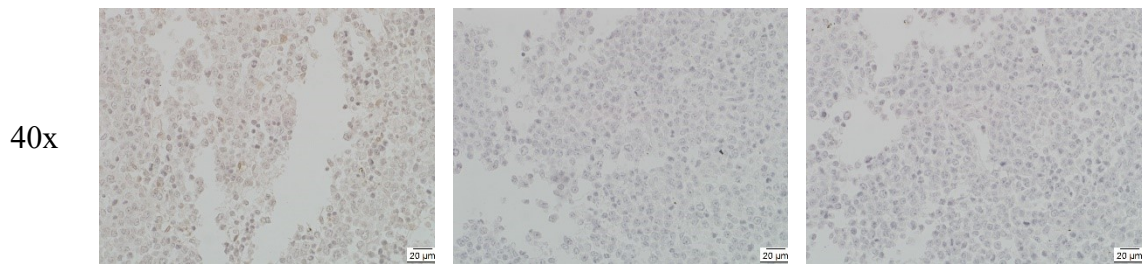


Figure 15 NCR1 staining ab199126 M-125 Spleen (A) primary antibody dilution 1:500, (B) isotype control, (C) secondary control. Magnification: 10x, 20x, 40x, Scale bar: 100 µm, 50 µm, 20 µm.

With the 1:500 dilution, clusters of positive cells could be indeed observed, although with a non-typical staining pattern (Figure 15). Since it was also unclear if the staining was specific, a staining of pig blood was performed. The red blood cells were lysed and only the white blood cells were used for this staining.

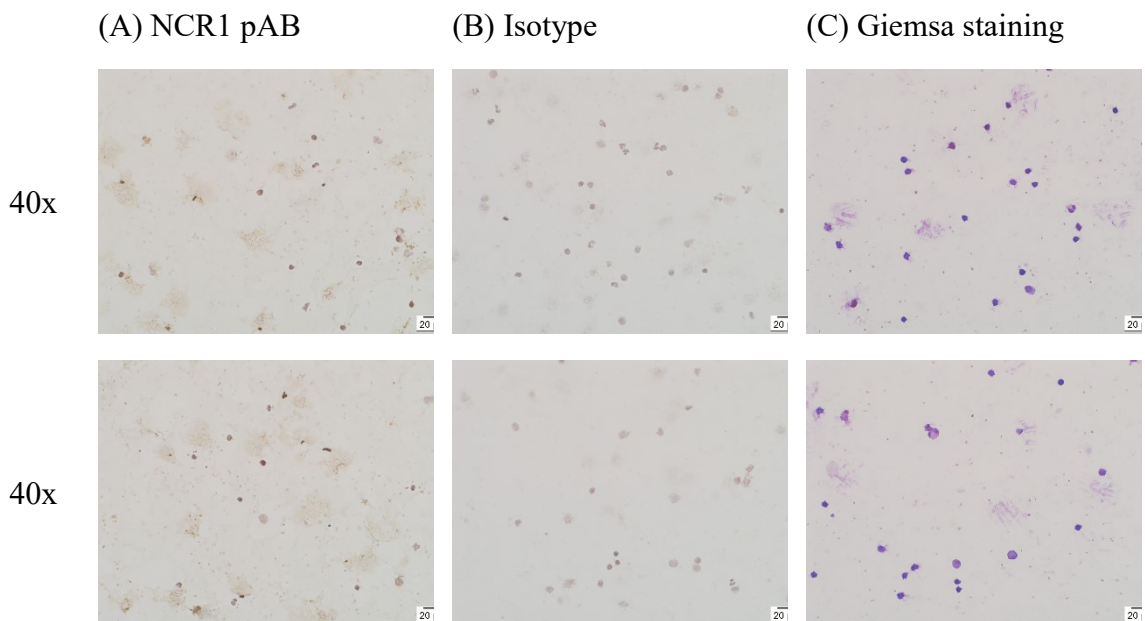


Figure 16 NCR1 staining 199128 of pig blood, (A) primary antibody dilution 1:500 and (B) isotype control, counterstain with Haematoxylin. (C) Giemsa staining. Magnification 40x, scale bar 20 µm.

This staining, shown in Figure 16, provided no further information about the specificity of the primary antibody. It showed positive staining of all cells and darker staining of a few

cells. It seemed that also in this staining the nuclei were dark and not the cell surface, but it was not at all clear if this was because of background staining or a specific staining of these cells. Because of these problems this staining was not performed on mouse blood.

7.3. Optimization of SIRP α staining

This staining was performed to detect SIRP α positive macrophages in the tumor tissue. These macrophages are not activated if there is an interaction with CD47. Because CD47 is blocked by the fusion protein in the in vivo experiments these macrophages can be activated.

The staining was performed with spleen, using the Vectastain detection kit.

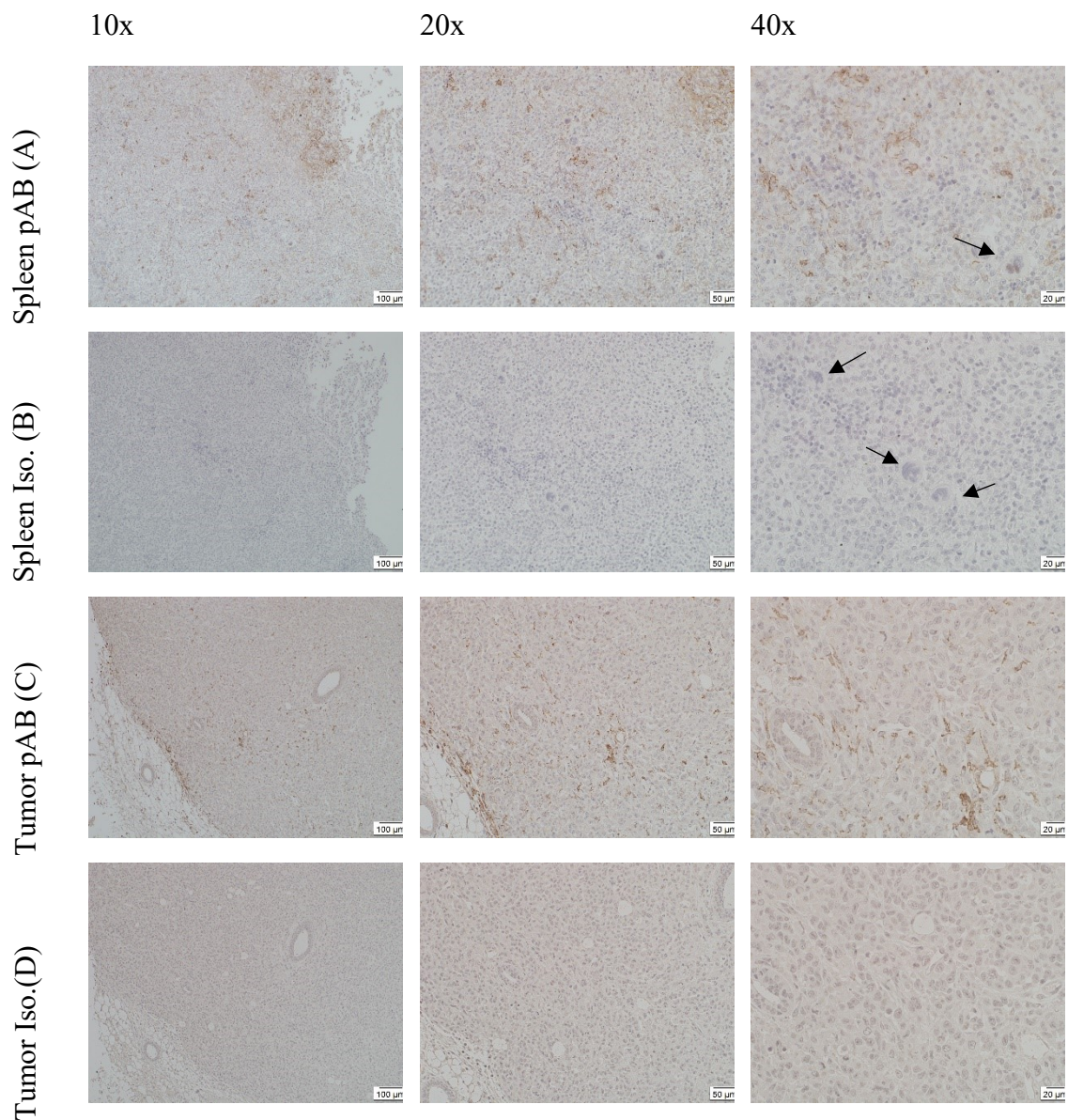


Figure 17 SIRP α staining, (A) M125 spleen and (B) isotype control. (C) MCT-209 tumor (in vivo experiment 3, MDA-MB-231 cells) and (D) isotype control, dilution of the primary antibody: 1:400. Arrows denote morphologically identified macrophages. Magnification 10x, 20x, 40x, scale bar

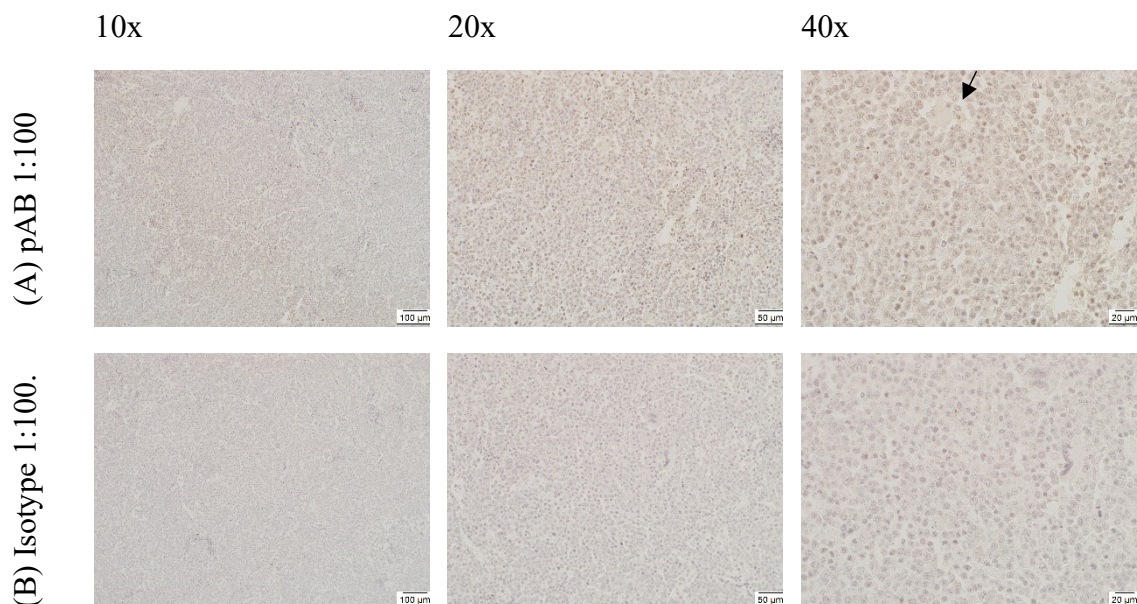
100 μ m, 50 μ m, 20 μ m.

As shown in Figure 17, both in spleen and tumor tissue clusters of positive cells could be observed. Also, a membranous staining pattern could be seen at the highest magnification. Nevertheless, structures identified morphologically as macrophages (marked with arrows) remains unstained. The reason for this is not clear, it is possible that the macrophages in these organs did not express SIRP α , but it is also possible that the primary antibody was already deteriorated and unable to recognise the antigen. It was decided to not use this antibody for any further experiments.

7.4. Optimization of CD16 staining

The blockage of CD47 could promote the accumulation of macrophages in tumor tissues, which should ultimately lead to the phagocytosis of tumor cells with a blocked CD47 surface protein. Because of the Fc part on the fusion protein expressed, both macrophages and NK cells should be affected, since they both express the Fc receptor CD16.

This staining was first performed on spleen, which should contain a large number of macrophages, using the Vectastain ABC kit.



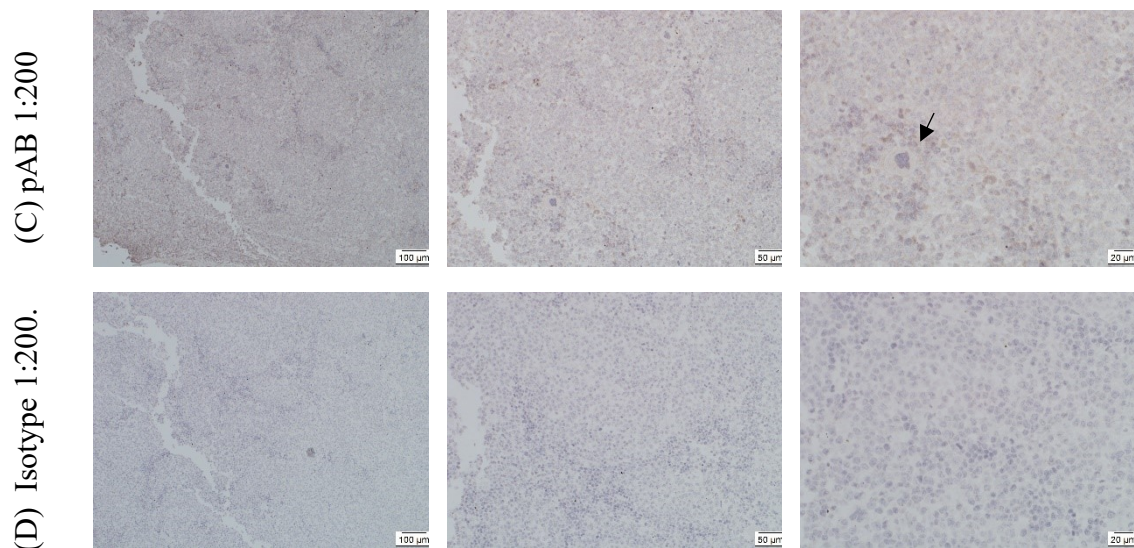


Figure 18 CD16 staining (A) M125 spleen, dilution of the primary antibody: 1:100 and (B) isotype control. (C) M125 spleen, dilution of the primary antibody: 1:200 and (D) isotype control. Arrows denote macrophages. Magnification 10x, 20x, 40x, scale bar 100 μm , 50 μm , 20 μm .

Figure 18 shows that there was no significant staining of any cells, only a slight background staining. Because the recommended dilution of 1:200 did not work, the dilution 1:100 was also evaluated. As NCR1 staining showed a large number of NK cells in this organ (Figure 13-Figure 15), one could also expect the presence of CD16, which is not only expressed on macrophages, but is also the surface protein on NK cells. Because even the higher concentration of 1:100 did not work, it was decided not to use this staining in further experiments. Macrophage staining will be performed by the Krebsforschungsinstitut Wien in further experiments.

7.5. Optimization of ICC

The aim of this staining was to stain lymphocytes with an NCR1 antibody to check the specificity of the antibody. It was tried to establish a method to produce a lymphocyte concentrate and fix this on slides so that it can be stained according to the standard protocol. For the first experiment pig blood was used for blood smears, which were stained with Giemsa stain or Haematoxylin to see the difference between the two stainings. (Figure 19)

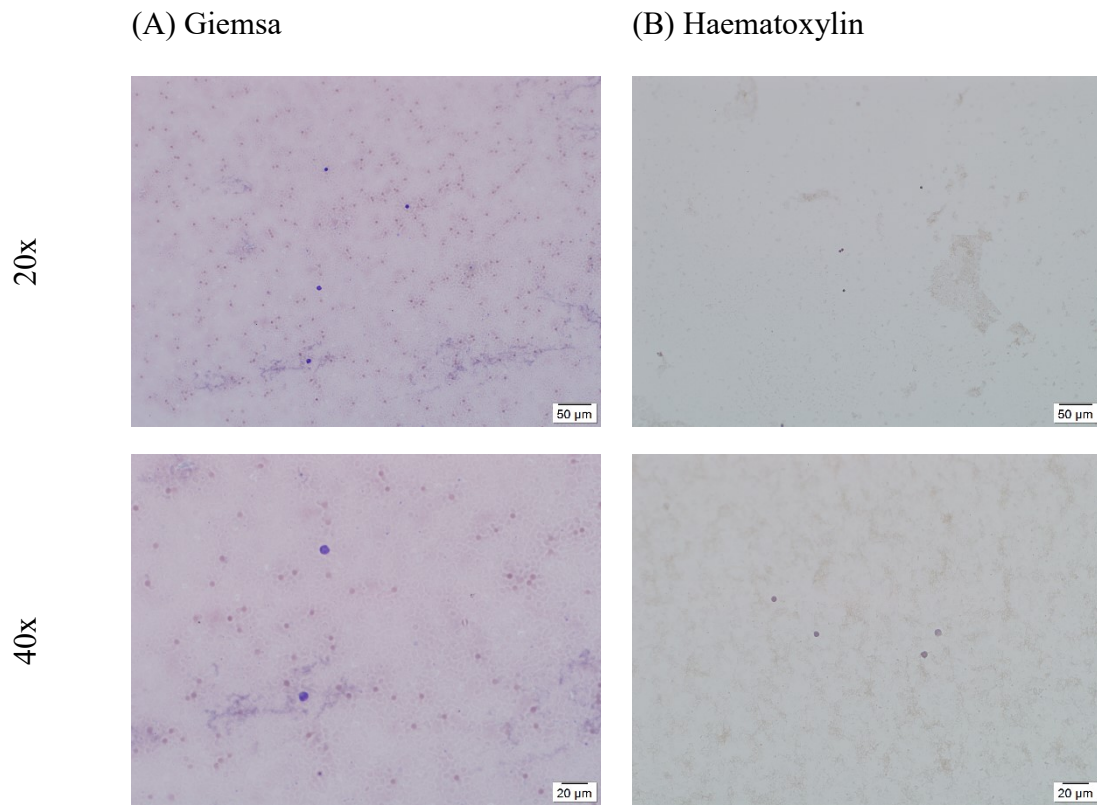


Figure 19 Blood smears of pig blood (A) Giemsa staining, (B) Haematoxylin staining. Magnification 20x, 40x, scale bar 50 µm, 20 µm.

In the next experiment the blood cells were fixed onto the slides using formalin and it was investigated if a permeabilization with Triton X is necessary. Since the staining with Haematoxylin worked better after permeabilization, it was used in further experiments. (Figure 20)

(A) fixation & permeabilization

(B) fixation & no permeabilization

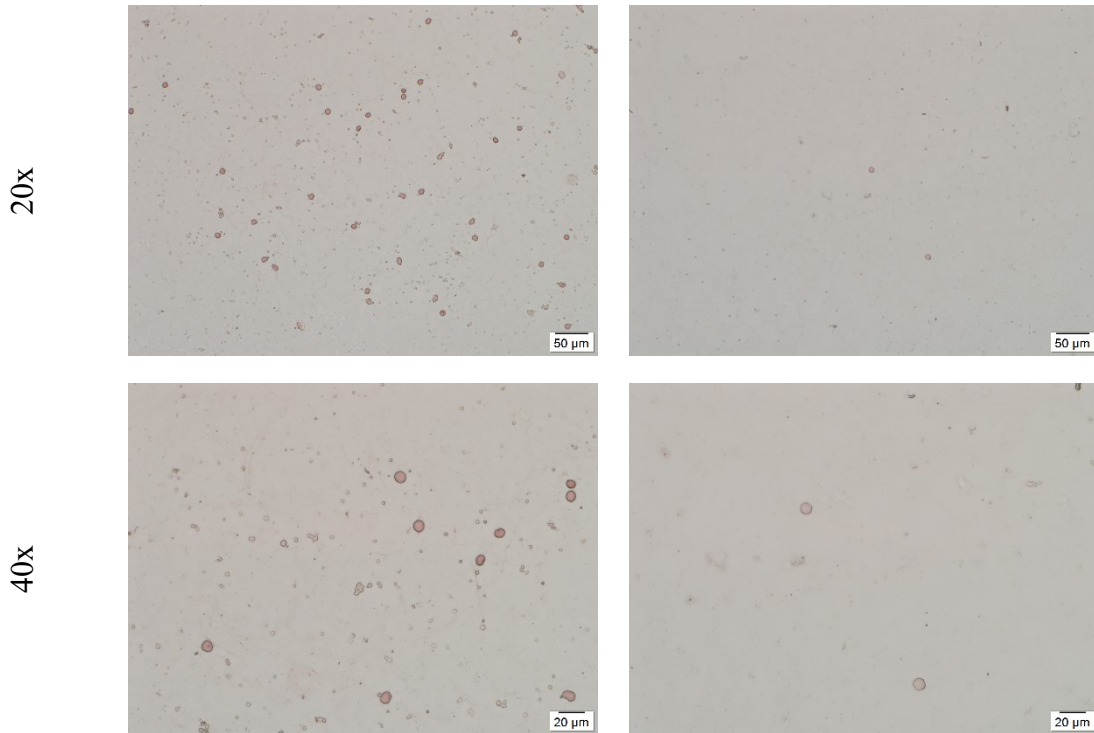
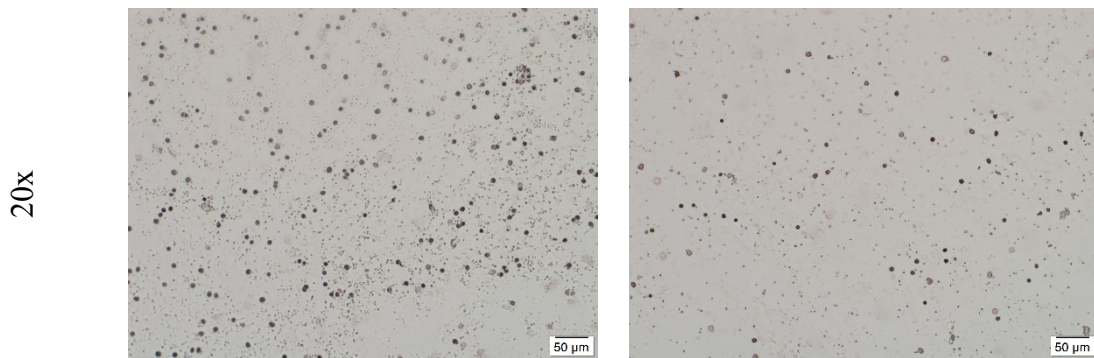


Figure 20 Blood smears of pig blood (A) fixation and permeabilization with Triton X, (B) fixation without permeabilization. Magnification 20x, 40x, scale bar 50 μm, 20 μm.

The blood was lysed and centrifuged in the next experiment to get rid of most of the erythrocytes and the resulting pellet was resuspended in different amounts of PBS. (Figure 21)

(A) pellet in 100 μl PBS

(B) pellet in 200 μl PBS



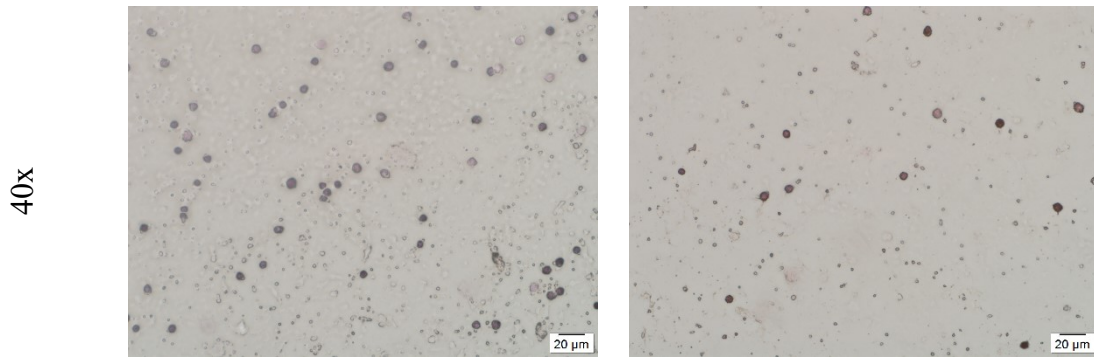


Figure 21 Blood staining of lymphocyte concentrate (A) Pellet suspended in 100 µl of PBS, (B) pellet suspended in 200 µl of PBS. Magnification 20x, 40x, scale bar 50 µm, 20 µm.

Since the method of fixation and the counterstaining with Haematoxylin worked the next step was to stain pig blood with the NCR1 antibody (Figure 22 NCR1 staining 199128 of pig blood, (A) primary antibody dilution 1:500 and (B) isotype control, counterstain with Haematoxylin. (C) Giemsa staining. Magnification 40x, scale bar 20 µm. Figure 22). Because the antibody was unspecific, all cells were slightly stained, and the staining gave no clear result.

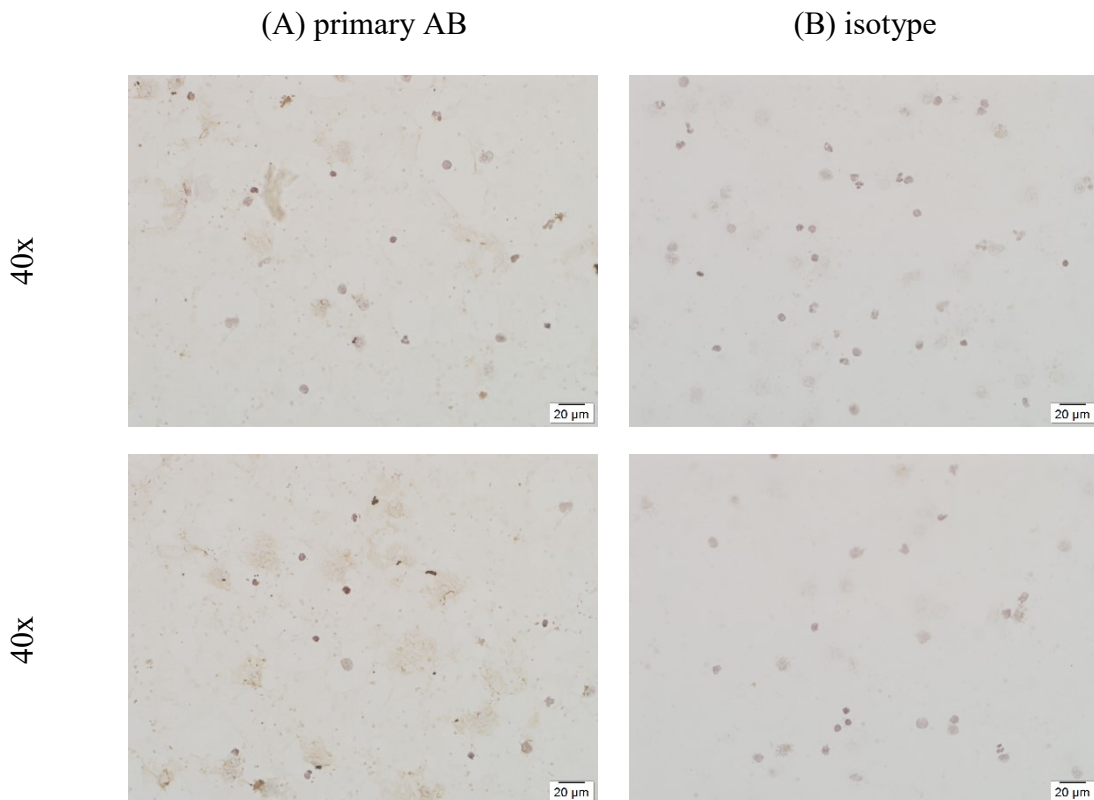


Figure 22 NCR1 staining 199128 of pig blood, (A) primary antibody dilution 1:500 and (B) isotype

control, counterstain with Haematoxylin. (C) Giemsa staining. Magnification 40x, scale bar 20 μm.

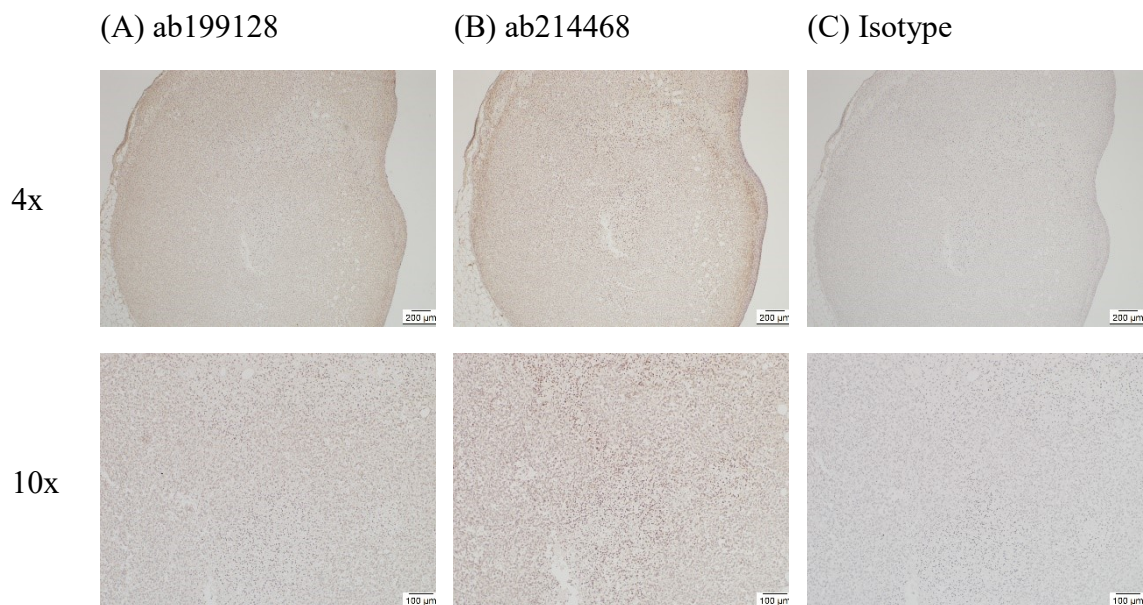
7.6. In vivo experiments

In vivo experiment 2

The NCR1 staining was performed using both available primary Antibodies (ab199128, 1:500 and ab214468, 1:300). The dilution used was selected due to the results in the experiments described above (see Figure 9, Figure 12, Figure 13 NCR1 staining ab199128, M125 Spleen, primary antibody dilutions: (A) 1:200, (B) 1:500 and (C) isotype control. Magnification: 10x, 20x, 40x, Scale bar: 100 μ m, 50 μ m, 20 μ m. Figure 13).

Mouse number	tumor	transfection	group
MCT-115	TU LE	IL2-P-Fc	treated group
MCT-118	TU RI	IL2-P	CD 47 blocked
SGE-0051	TU LE	bb-mCherry	transfection control
Age-0352	TU RI	untransfected	Control group

Table 17 NCR1 stained tumors from in vivo experiment 2, Mouse number and tumors stained.



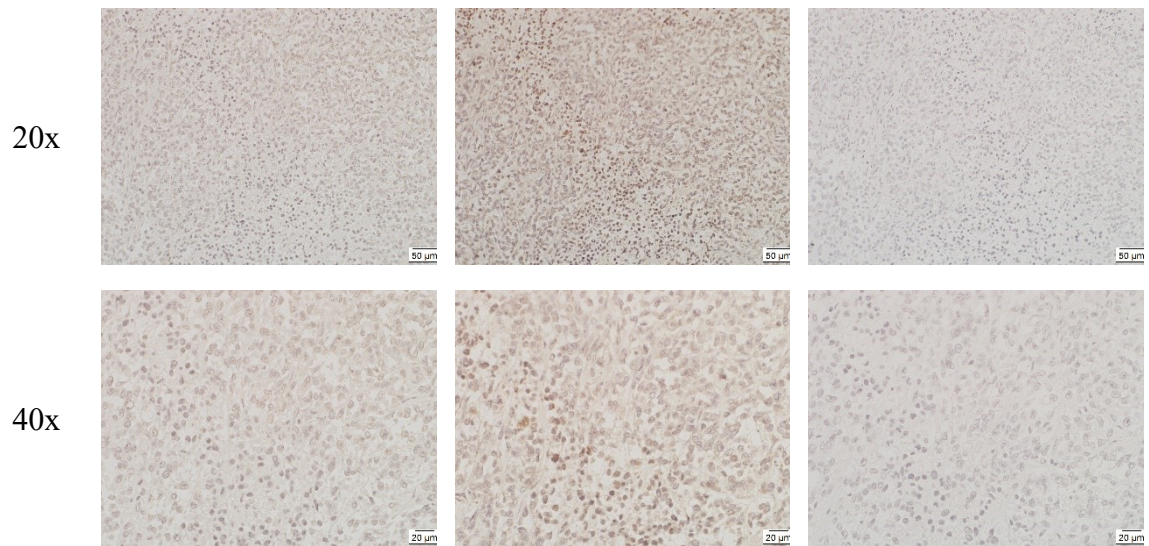
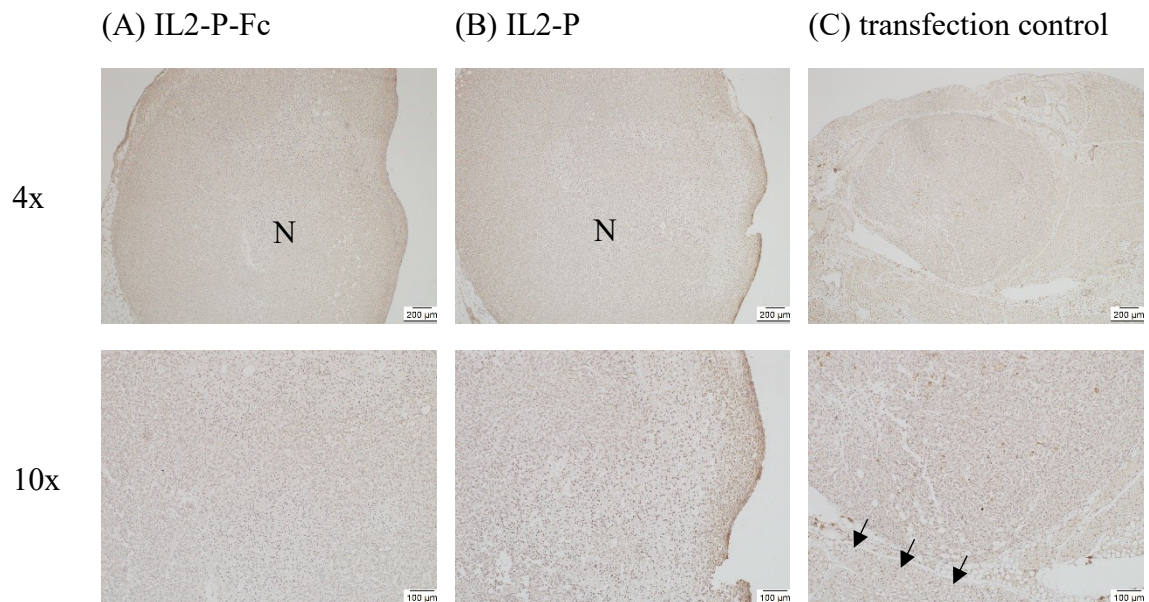


Figure 23 MCT-115, IL2-P-Fc. (A) Anti NCR1 antibody ab199128, dilution: 1:500. (B) Anti NCR1 antibody ab214468, dilution: 1:300. (C) Isotype control. Magnification 4x, 10x, 20x, 40x, scale bar 200 μm , 100 μm , 50 μm , 20 μm .

As both NCR1 Antibody would be in principle suitable for the staining, the tumors of in vivo experiment 2 were stained with antibodies ab199128 and ab214468. As can be seen in Figure 23, they give clearly different results, the antibody ab199128 seems to be more specific, but the staining of NK cells is more intense with the antibody ab214468.



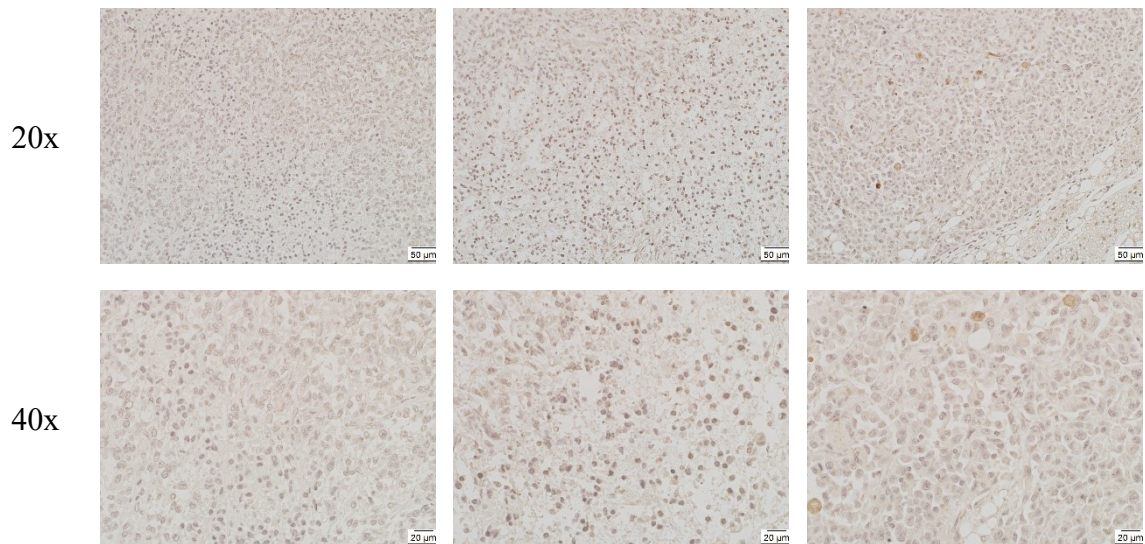


Figure 24 NCR1 staining in vivo experiment 2. Anti NCR1 antibody ab199128, dilution: 1:500. (A) MCT-115, IL²-P-Fc treated group. (B) MCT-115, IL²-P CD47 blocked group. (C) SGE-0051, bb-mCherry transfection control. Arrows denote stained cells outside the tumor tissue. (N) necrotic parts. Magnification 4x, 10x, 20x, 40x, scale bar 200 μm, 100 μm, 50 μm, 20 μm.

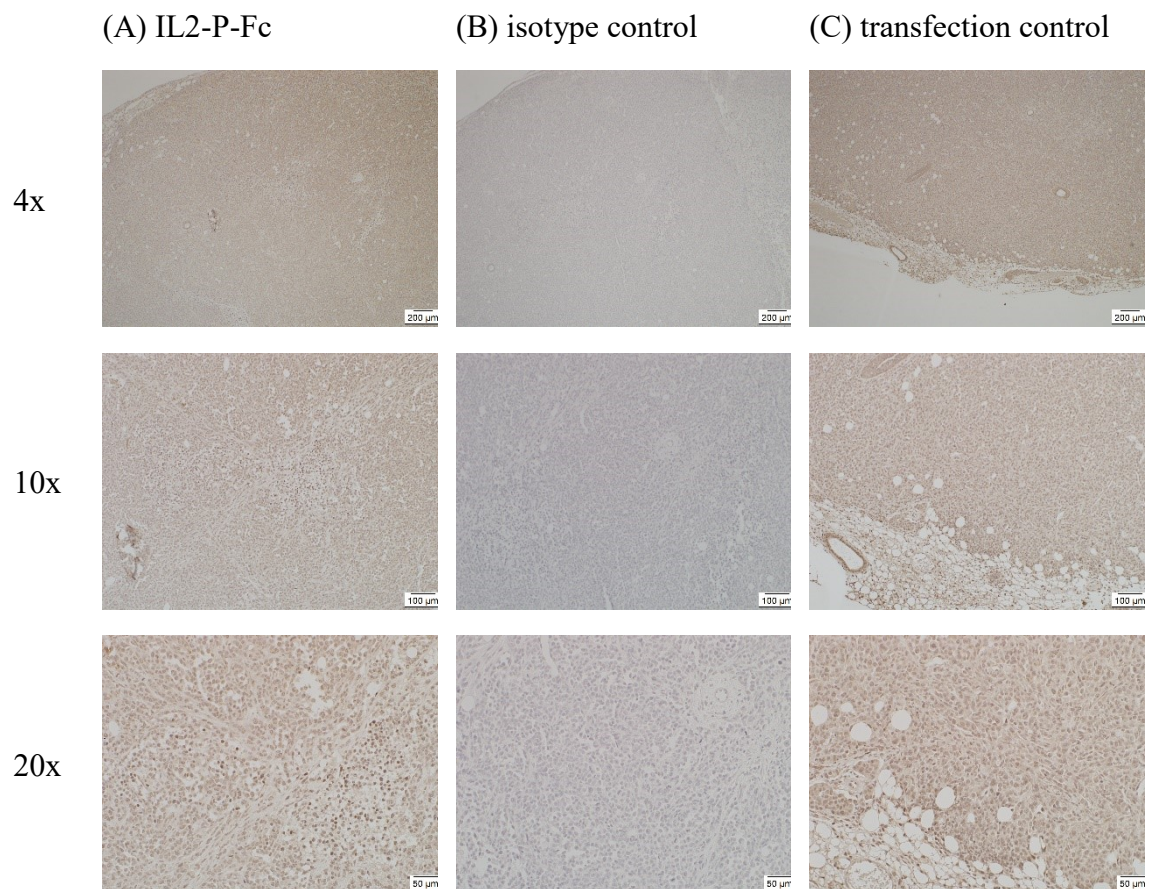
Due to the higher specificity observed in Fig 37, it was decided to use ab199128 to stain tumors from all three groups of the in vivo experiment 2 (Figure 24). It can be seen, that there are more stained cells in the IL2-P and IL2-P-FC treated group than in the transfection control group. In the transfection control group, also some cells are stained. Of note, they do not appear in the tumor area but rather in the tissue surrounding the tumor. The tumor sections of the treated group with the fusion protein IL2-P-Fc and the CD47 blocked group expressing the protein IL2-P without the Fc part show some necrotic parts and stained cells within those. It was expected to find a stronger immune reaction in the IL2-P-Fc transfected group, but the results show more stained cells in the IL2-P transfected group. The reason for this is unclear, since the Fc part should provide a better immune recognition. A possible reason can be the timepoint at which the tumors were harvested. Because of the additional Fc part, the immune reaction in the treated group could be faster than in the CD47 blocked group and the immune cells could no longer be seen in the tumor, but additional experiments would be necessary to confirm this.

In vivo experiment 3

Tumors from in vivo experiment 3 have been transfected in vivo by intratumoral injection of polyplexes with plasmid encoding for either IL2-P-Fc or bb-mCherry. The tumors were harvested 24 hours after intratumoral injection and NCR1 staining with ab199128 as primary antibody was performed to detect NK cells in the tumor tissue. .

Mouse number	tumor	transfection	group
MCT-0209	TU LE	IL2-P-Fc	treated group
MCT-0204	TU LE	bb-mCherry	transfection control

Table 18 NCR1 stained tumors of in vivo experiment 3 mouse number and tumors stained.



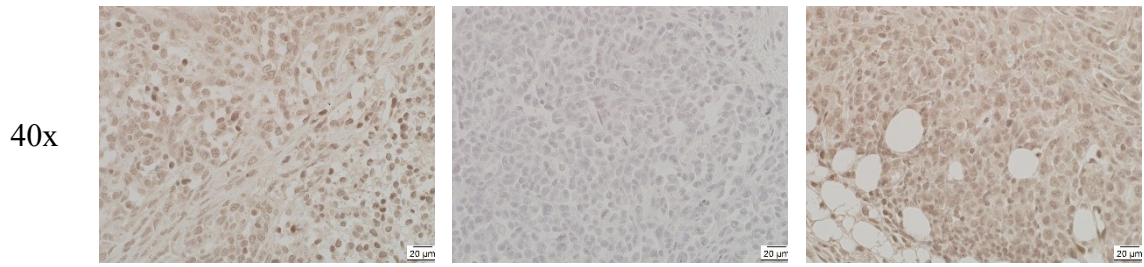
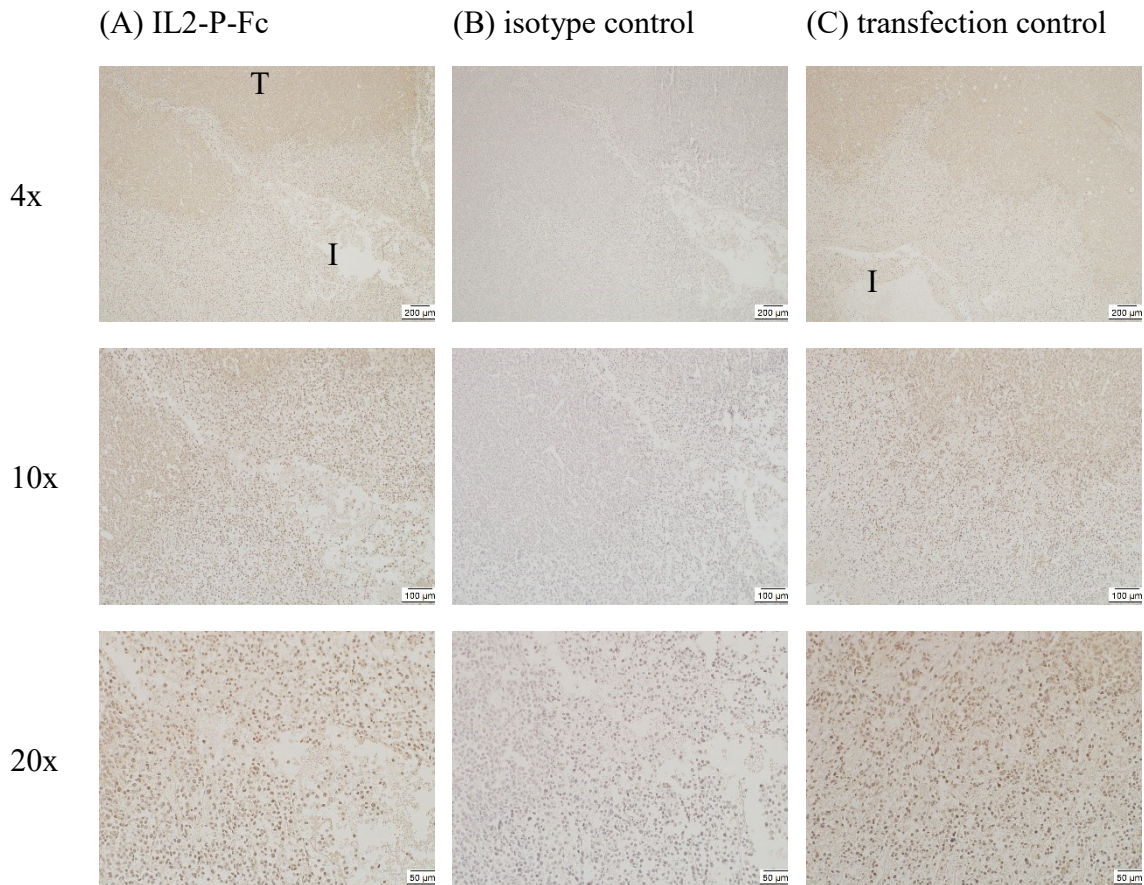


Figure 25: NCR1 staining in vivo experiment 3 dilution of the primary antibody 1:200 (A) MCT-0209 IL2-P-Fc treated group primary antibody, (B) MCT-0209 isotype control. (C) MCT-0204 bb-mCherry transfection control primary antibody, Magnification 4x, 10x, 20x, 40x, scale bar 200 µm, 100 µm, 50 µm, 20 µm.



40x

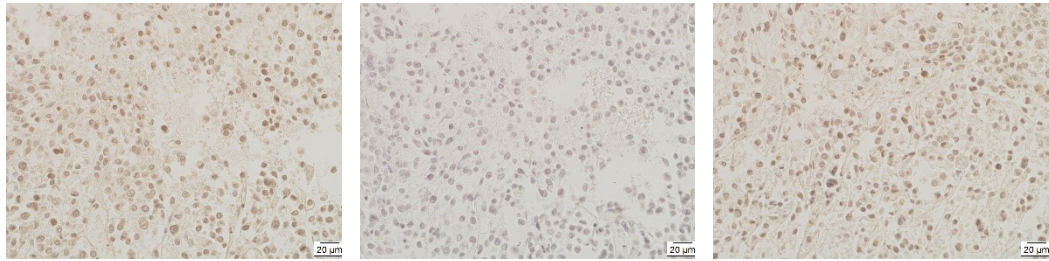


Figure 26: NCR1 staining in vivo experiment 3 dilution of the primary antibody 1:500 (A) MCT-0209 IL2-P-Fc treated group primary antibody (B) MCT-0209 isotype control. (C) MCT-0204 bb-mCherry transfection control primary antibody. (I) injection sites. (T) intact tumor areas. Magnification 4x, 10x, 20x, 40x, scale bar 200 μm, 100 μm, 50 μm, 20 μm.

The NCR1 staining after intratumoral injection of the polyplexes (Figure 26) shows some infiltration of the tumor by NK cells, especially around the injection sites, where also some necrotic areas can be seen and stained cells within them. It is not clear if these stained cells in the necrotic areas are NK cells or if necrotic cells are stained darker than other tumor cells. Some areas further away from the injection sites tissue seems to be completely intact, which could indicate that the polyplexes did not penetrate the whole tumor. These necrotic sites with stained cells could be seen in both the treated group and the control group with the transfection bb-mCherry instead of IL2-P-Fc. It was expected to find a better result in the treated group, but the number of NK cells seems to be similar in both groups. The reason for this can be for example that also the mCherry protein could induce immune cell infiltration, or the polyplex components.

In vivo experiment 4

Here, tumors were similarly transfected with polyplexes, but harvested 12, 17 and 14h after transfection. Both, H&E staining and IHC (for NCR1 and CD47) was conducted.

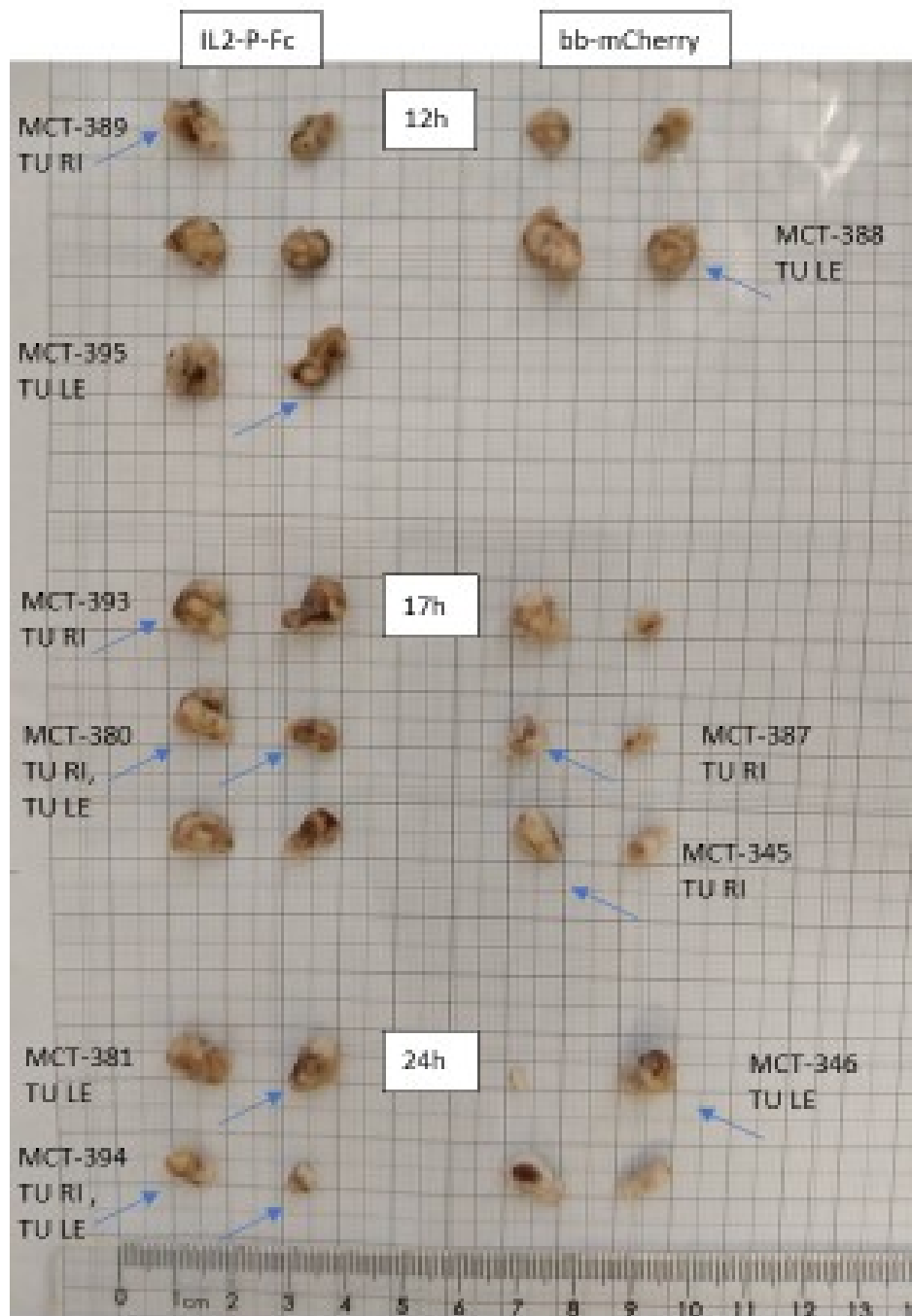


Figure 27 tumors in vivo experiment 4 after fixation in formalin. Arrows show tumors which were used in the histological study.

Mouse number	tumor	timepoint	transfection	group
MCT-389	TU RI	12 h	IL2-P-Fc	treated group
MCT-395	TU LE	12 h	IL2-P-Fc	treated group
MCT-393	TU RI	17 h	IL2-P-Fc	treated group
MCT-380	TU RI	17 h	IL2-P-Fc	treated group
MCT-380	TU LE	17 h	IL2-P-Fc	treated group
MCT-394	TU RI	24 h	IL2-P-Fc	treated group
MCT-394	TU LE	24 h	IL2-P-Fc	treated group
MCT.381	TU LE	24 h	IL2-P-Fc	treated group
MCT-388	TU LE	12 h	bb-mCherry	transfection control
MCT-387	TU RI	17 h	bb-mCherry	transfection control
MCT-345	TU RI	17 h	bb-mCherry	transfection control
MCT-346	TU LE	24 h	bb-mCherry	transfection control

Table 19: IHC Stained tumors in vivo experiment 4. Mouse number, tumors stained and timepoint of obtaining the tumor after intratumoral injection of polyplexes.

H&E staining

IL2-P-Fc

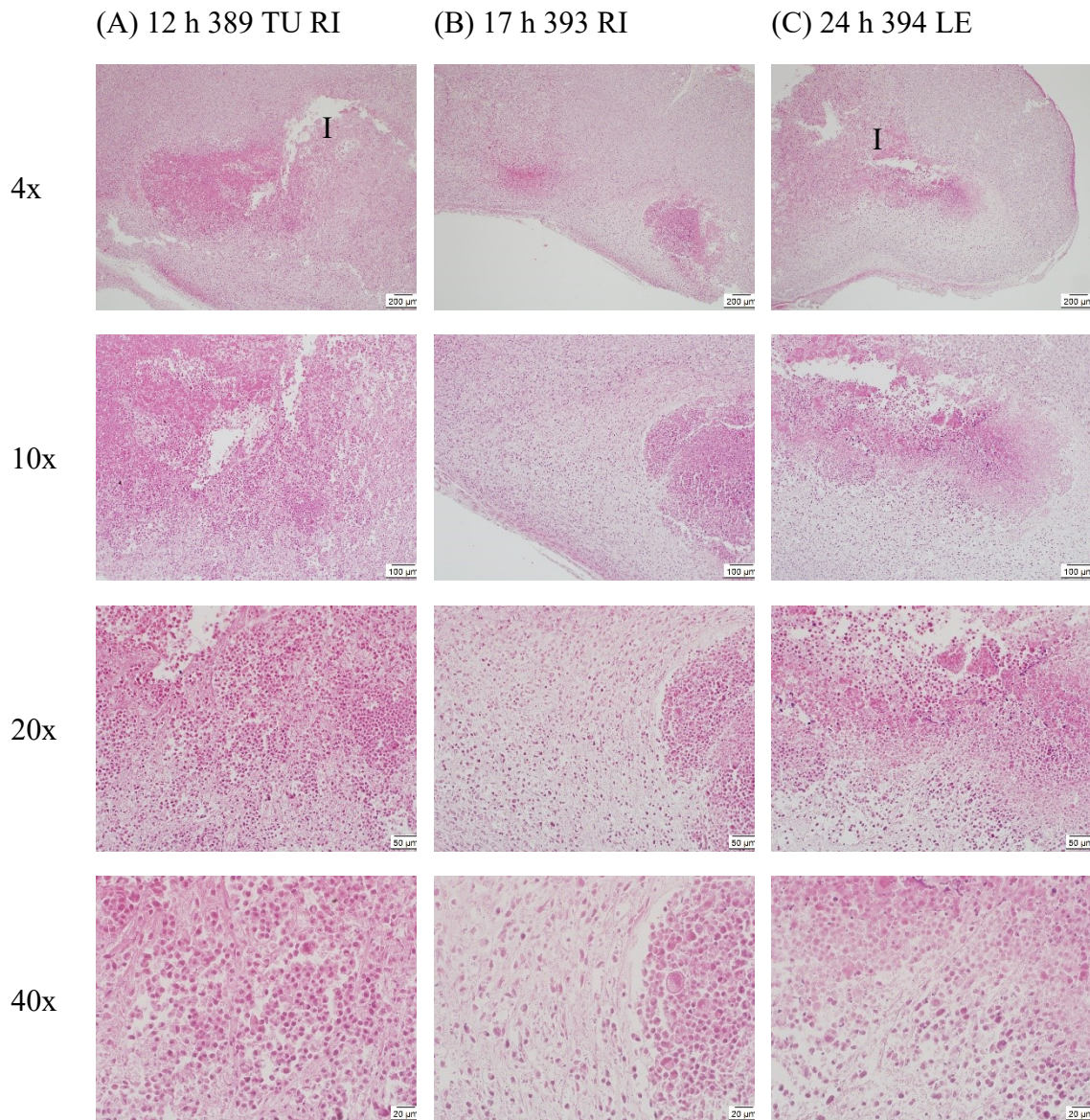


Figure 28 H&E staining in vivo experiment 4 IL2-P-Fc treated group (A) MCT-389 TU RI 12 hours post injection, (B) MCT-393 TU RI 17 hours post injection, (C) MCT-394 TU LE 24 hours post injection. (I) injection sites. Magnification 4x, 10x, 20x, 40x, scale bar 200 μm , 100 μm , 50 μm , 20 μm .

IL2-P-FC

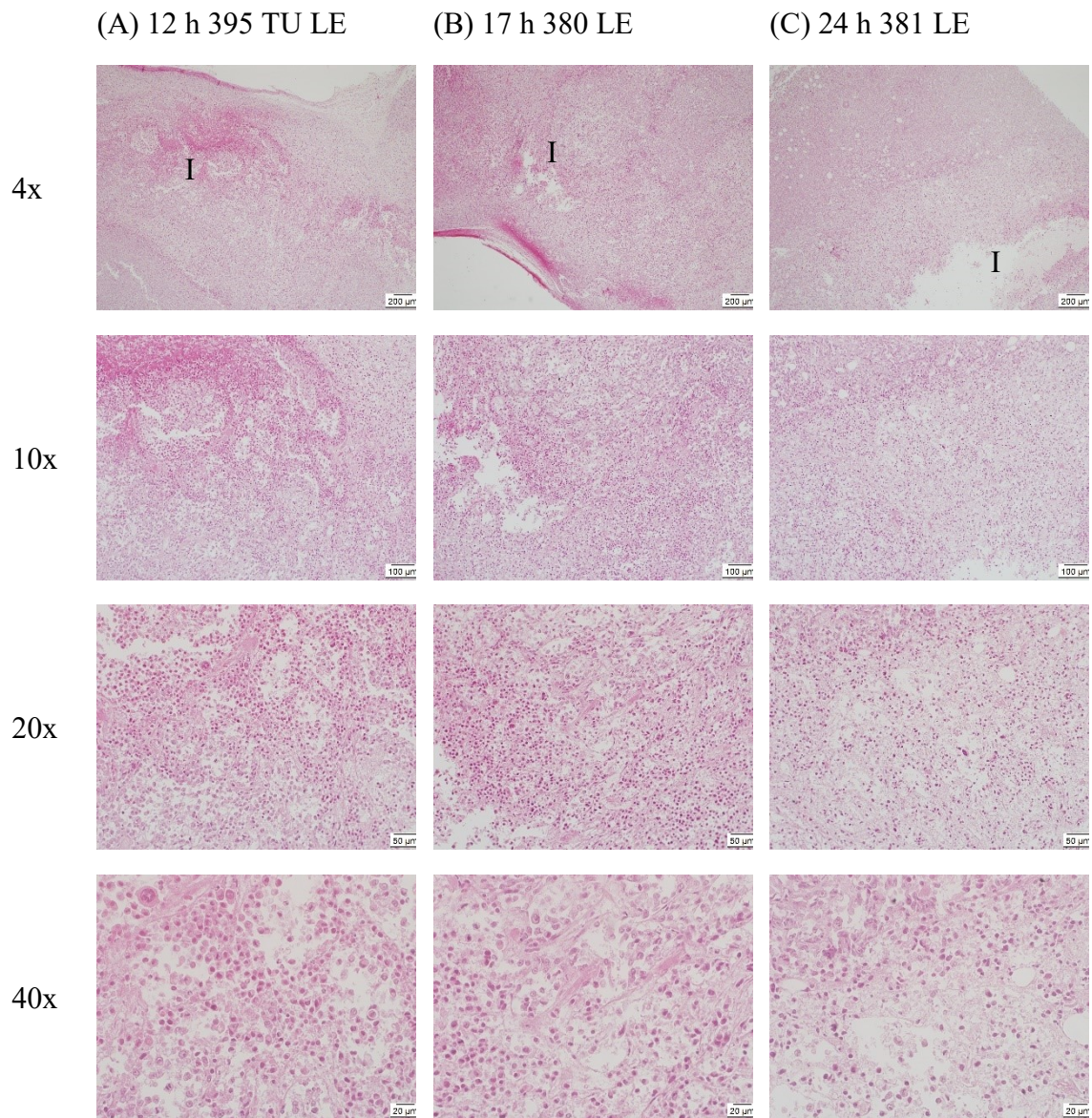


Figure 29 H&E staining in vivo experiment 4 IL2-P-Fc treated group (A) MCT-395 TU LE 12 hours post injection, (B) MCT-380 TU LE 17 hours post injection, (C) MCT-381 TU LE 24 hours post injection. (I) injection sites. Magnification 4x, 10x, 20x, 40x, scale bar 200 μ m, 100 μ m, 50 μ m, 20 μ m.

bb-mCherry transfection control

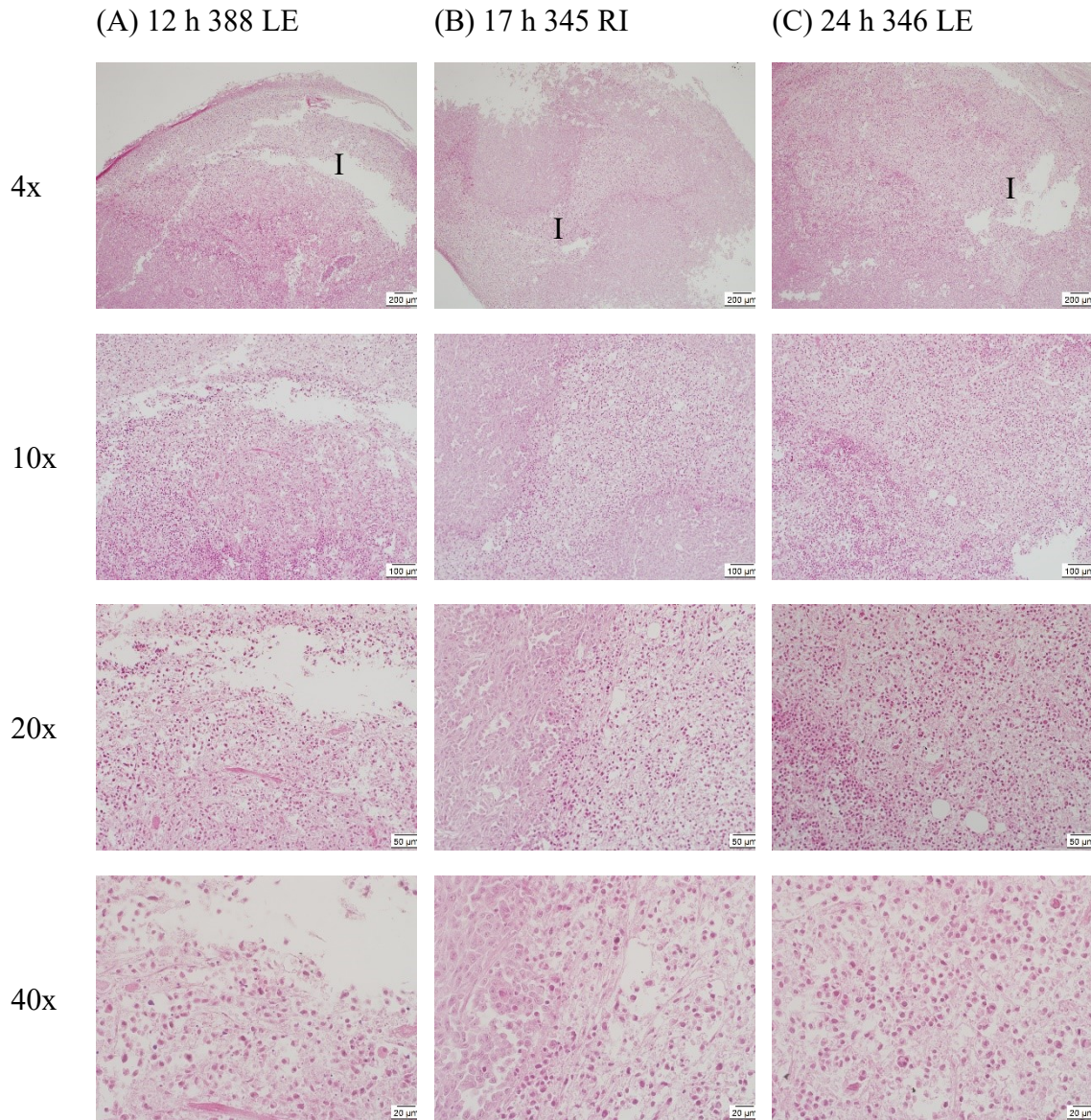


Figure 30 H&E staining in vivo experiment 4 bb-mCherry transfection control group (A) MCT-388 TU LE 12 hours post injection, (B) MCT-345 TU RI 17 hours post injection, (C) MCT-346 TU LE 24 hours post injection. (I) injection sites. Magnification 4x, 10x, 20x, 40x, scale bar 200 μm , 100 μm , 50 μm , 20 μm .

The H&E stainings clearly show the injection site and some necrotic parts in the tumor around it, which is expected after treatment. Also, a small number of immune cells could be seen, but need confirmation by IHC. In some of the tumors haemorrhages were observed,

were erythrocytes and other blood cells appeared at the injection site. In the H&E stainings no clear difference could be observed between the treated and the control group.

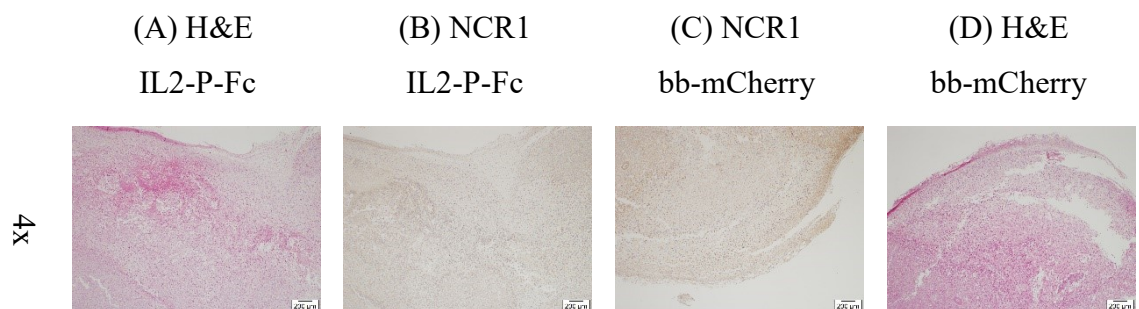
NCR1 staining

The NCR1 staining was performed to detect NK cells infiltrating the tumor tissue. Since the two previously evaluated primary antibodies gave different results in terms of background and staining intensity, both of them were also used here in IHC.

The primary antibody ab214468 shows more stained cells, but it is unclear if any of the staining is specific. In the haemorrhagic tumors, cells that were thought to be NK cells according to the H&E staining were not stained, but there were some unspecific interactions, for example muscle cells were stained and the background staining is generally high, which makes the staining unreliable.

The expected difference between the treated and the control group could not be seen, most stained cells were in the haemorrhagic areas and those occurred in both groups. It is not clear if some NK cells infiltrated the tumor, as there were some stained cells in the tumors of both groups, but since the staining is unspecific the results were not clear. Necrotic parts of the tumors were stained as well, but due to the high background it is unclear if the darker cells are necrotic since especially the nuclei were stained and therefore darker or if NK cells infiltrated the necrotic parts.

Comparison NCR1 staining IL2-P-Fc and bb-mCherry 12 h post injection



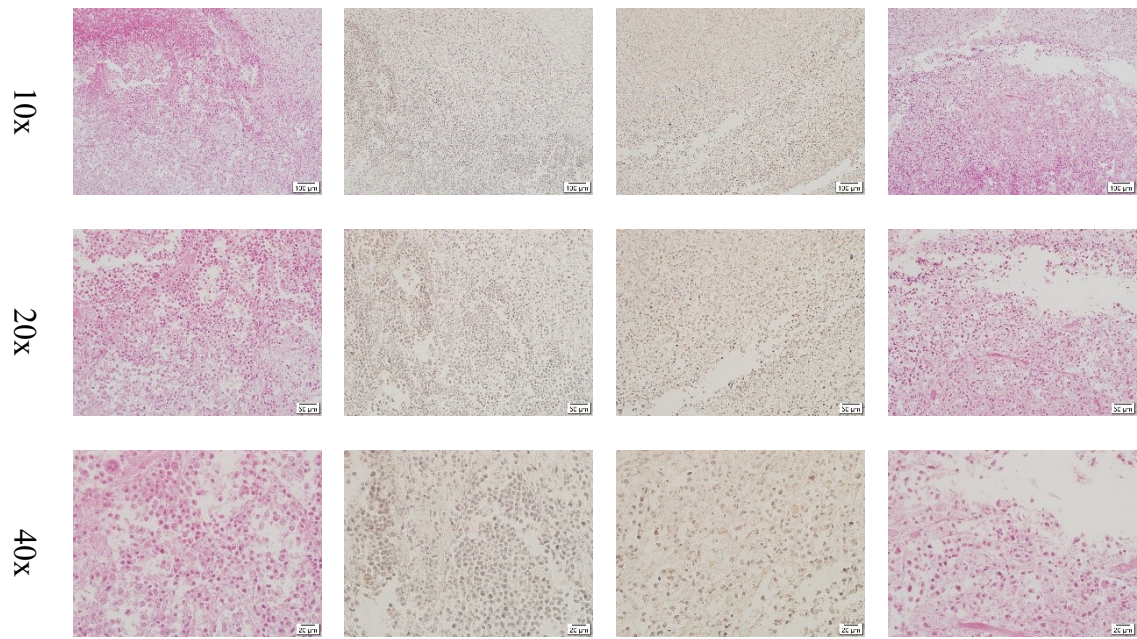
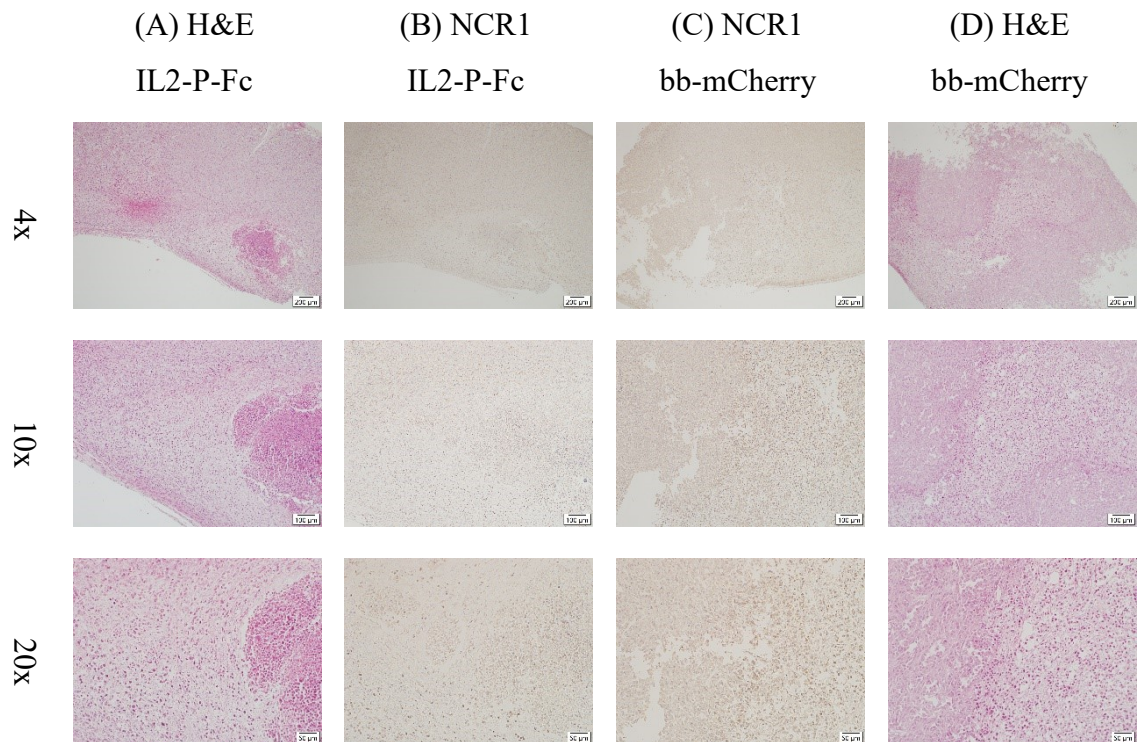


Figure 31 Comparison between NCR1 staining ab214468 IL2-P-Fc and bb-mCherry 12 hours post injection. (A) H&E IL2-P-Fc MCT-395 TU LE, (B) NCR1 ab214468 prim AB IL2-P-Fc MCT-395 TU LE, (C) NCR1 ab214468 prim AB bb-mCherry MCT-388 TU LE, (D) H&E bb-mCherry MCT-388 TU LE. Magnification 4x, 10x, 20x, 40x, scale bar 200 μ m, 100 μ m, 50 μ m, 20 μ m.

Comparison NCR1 staining IL2-P-Fc and bb-mCherry 17 h post injection



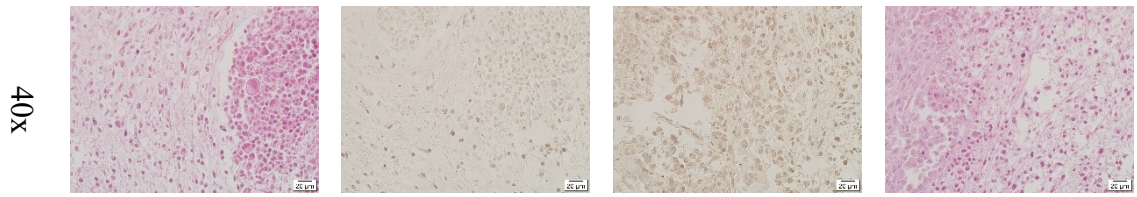


Figure 32 Comparison between NCR1 staining ab214468 IL2-P-Fc and bb-mCherry 17 hours post injection. (A) H&E IL2-P-Fc MCT-393 TU RI, (B) NCR1 ab214468 prim AB IL2-P-Fc MCT-393 TU RI, (C) NCR1 ab214468 prim AB bb-mCherry MCT-345 TU RI, (D) H&E bb-mCherry MCT-345 TU RI. Magnification 4x, 10x, 20x, 40x, scale bar 200µm, 100µm, 50 µm, 20 µm.

Comparison NCR1 staining IL2-P-Fc and bb-mCherry 24 h post injection

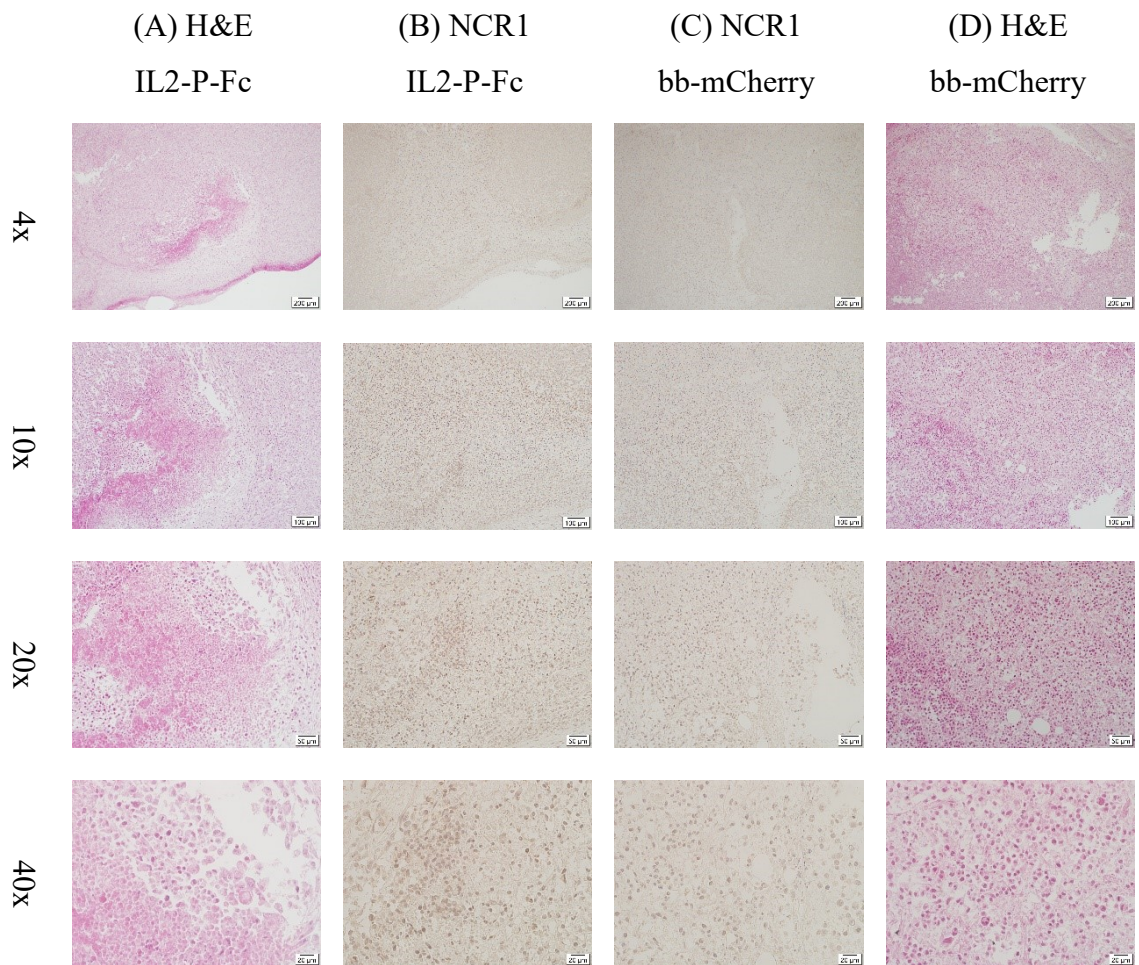


Figure 33 Comparison between NCR1 staining ab214468 IL2-P-Fc and bb-mCherry 17 hours post injection. (A) H&E IL2-P-Fc MCT-394 TU RI, (B) NCR1 ab214468 prim AB IL2-P-Fc MCT-394 TU RI, (C) NCR1 ab214468 prim AB bb-mCherry MCT-346 TU LE, (D) H&E bb-mCherry MCT-346 TU LE. Magnification 4x, 10x, 20x, 40x, scale bar 200µm, 100µm, 50 µm, 20 µm.

IL2-P-FC MCT-395 TU LE, 12 hours

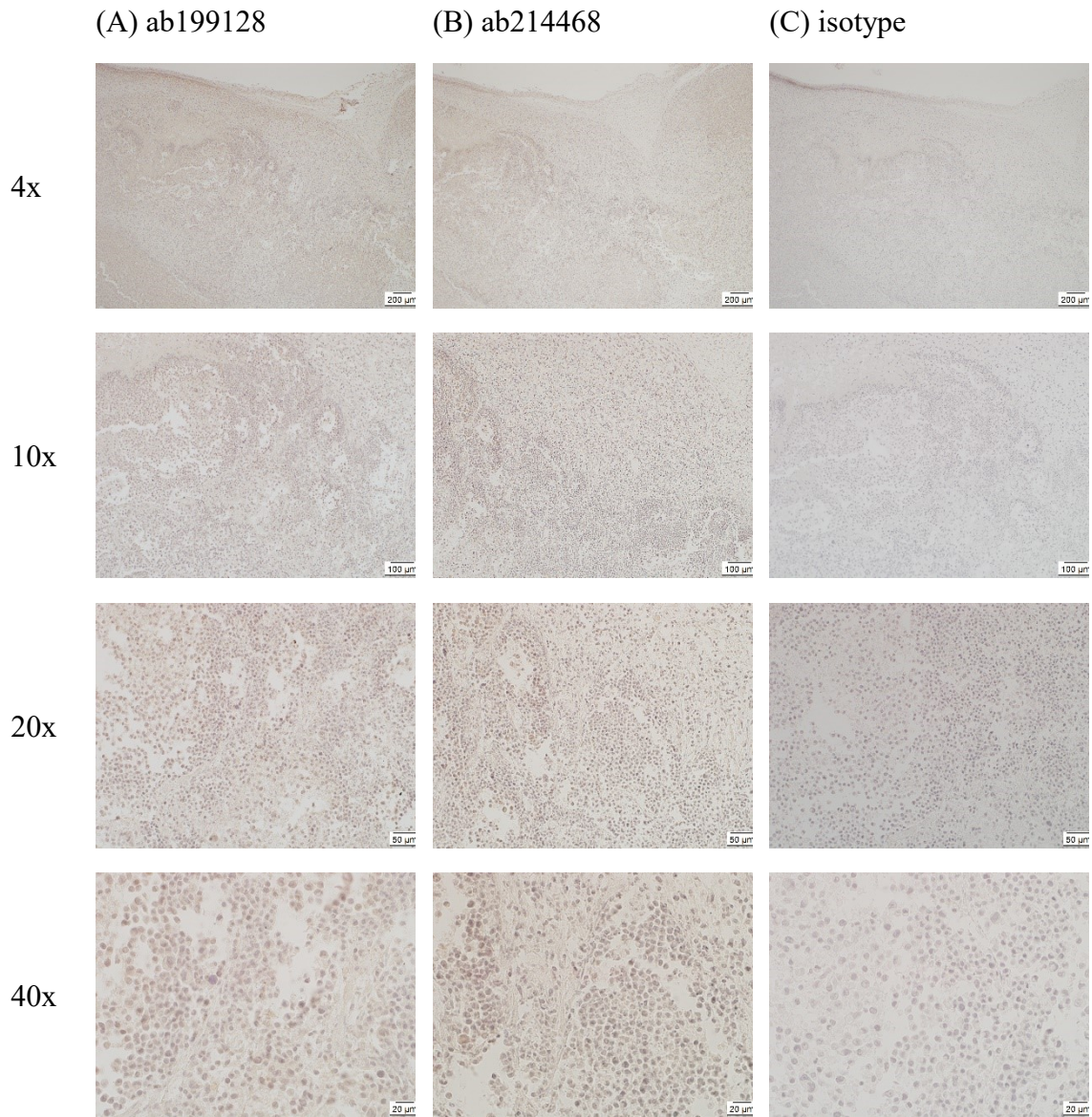


Figure 34 NCR1 staining MCT-395 TU LE, IL2-P-Fc treated group 12 hours post injection. (A) primary antibody ab199128, (B) primary antibody ab214468, (C) isotype control. Magnification 4x, 10x, 20x, 40x, scale bar 200 μm , 100 μm , 50 μm , 20 μm .

IL2-P-Fc MCT-380 TU RI, 17 hours

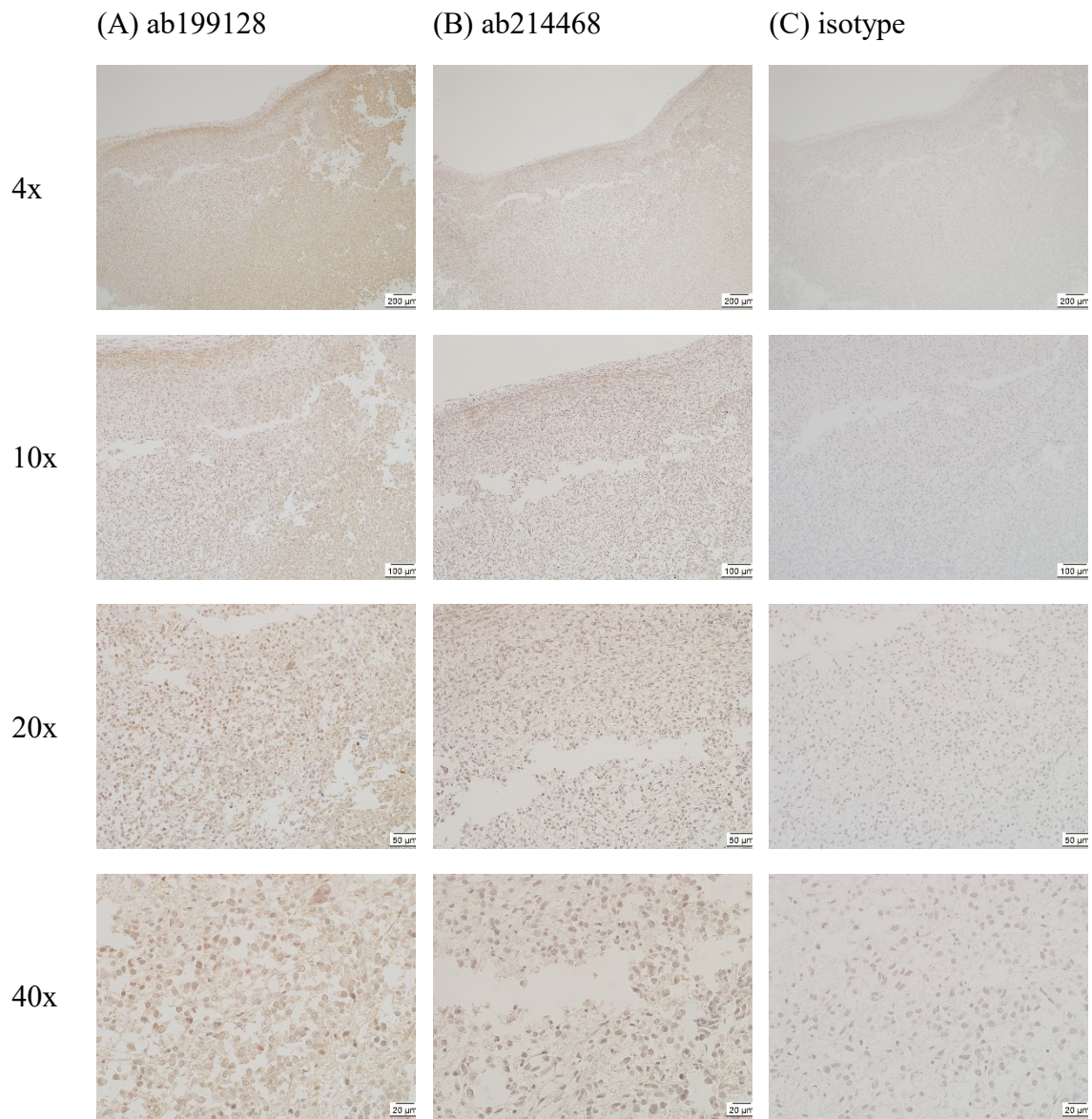


Figure 35 NCR1 staining MCT-380 TU RI, IL2-P-Fc treated group 17 hours post injection. (A) primary antibody ab199128, (B) primary antibody ab214468, (C) isotype control. Magnification 4x, 10x, 20x, 40x, scale bar 200 μm , 100 μm , 50 μm , 20 μm .

IL2-P-Fc MCT-394 TU RI, 24 hours

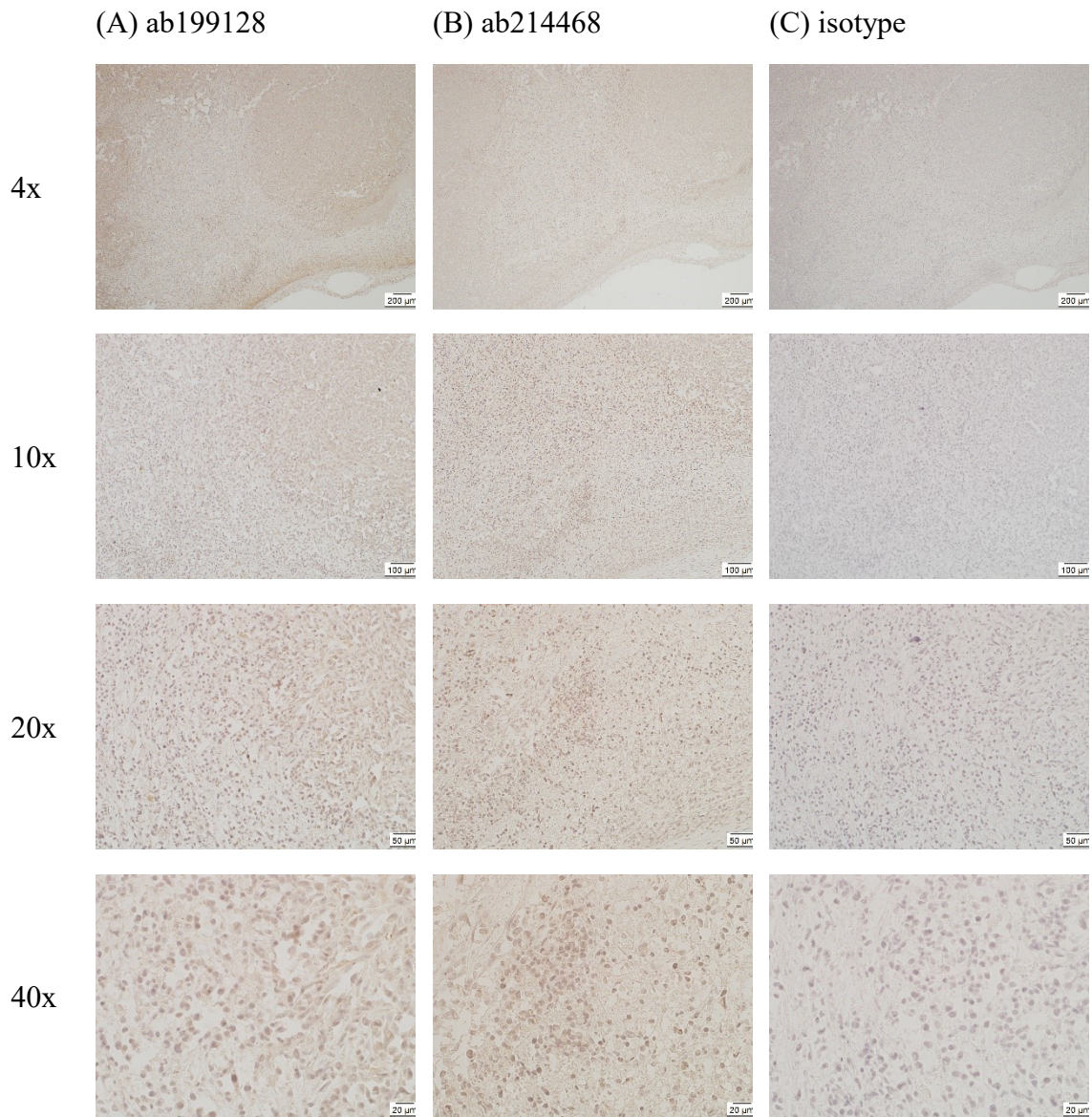


Figure 36 NCR1 staining MCT-394 TU RI, IL2-P-Fc treated group 24 hours post injection. (A) primary antibody ab199128, (B) primary antibody ab214468, (C) isotype control. Magnification 4x, 10x, 20x, 40x, scale bar 200 μm , 100 μm , 50 μm , 20 μm .

bb-mCherry MCT-388 TU LE, 12 hours

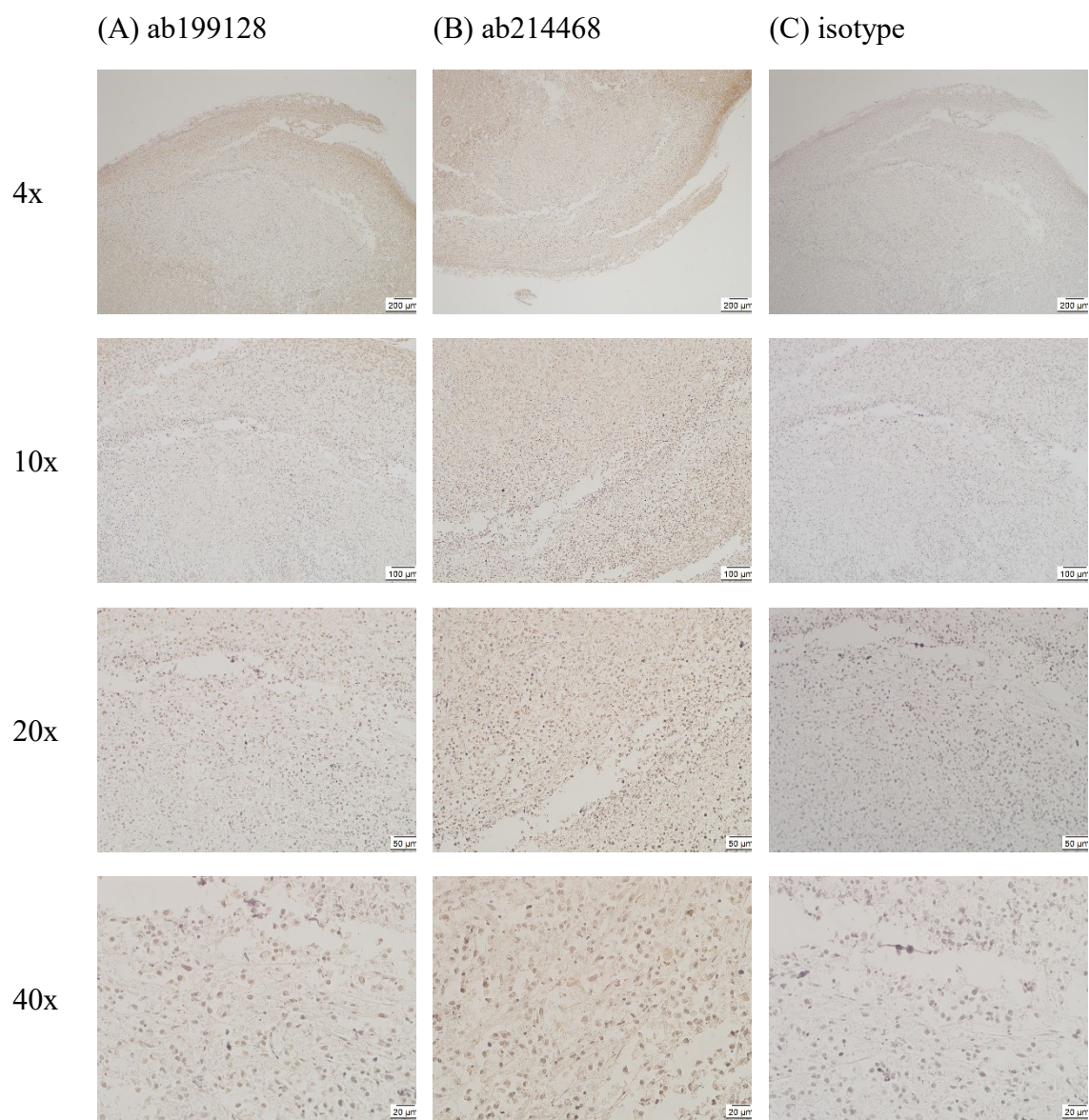


Figure 37 NCR1 staining MCT-388 TU LE, bb-mCherry transfection control group 12 hours post injection. (A) primary antibody ab199128, (B) primary antibody ab214468, (C) isotype control. Magnification 4x, 10x, 20x, 40x, scale bar 200 μm , 100 μm , 50 μm , 20 μm .

IL2-P-FC

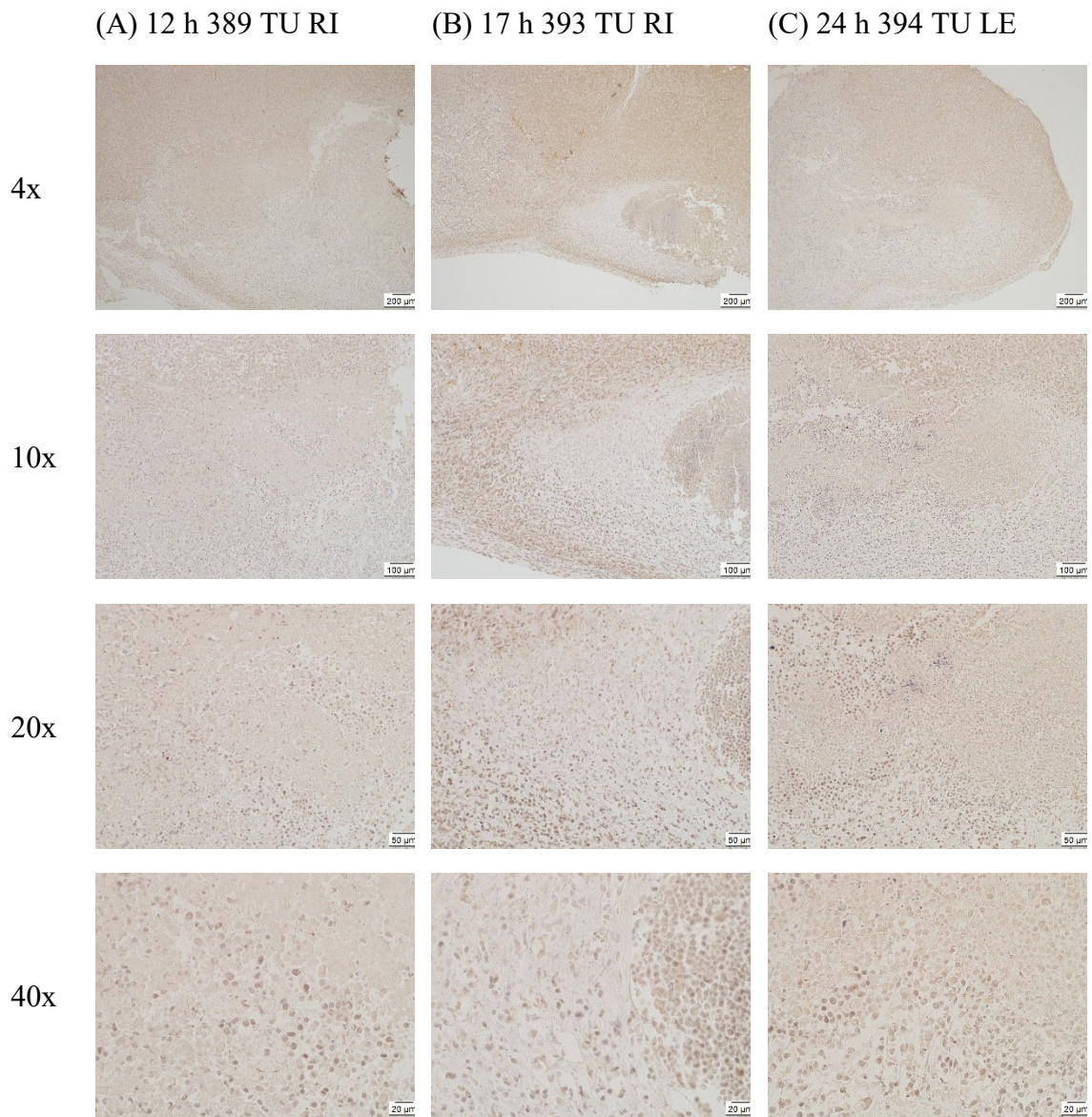


Figure 38 NCR1 ab199128 staining in vivo experiment 4 IL2-P-Fc treated group (A) MCT-389 TU RI 12 hours post injection, (B) MCT-393 TU RI 17 hours post injection, (C) MCT-394 TU LE 24 hours post injection. Magnification 4x, 10x, 20x, 40x, scale bar 200 μm , 100 μm , 50 μm , 20 μm .

IL2-P-FC

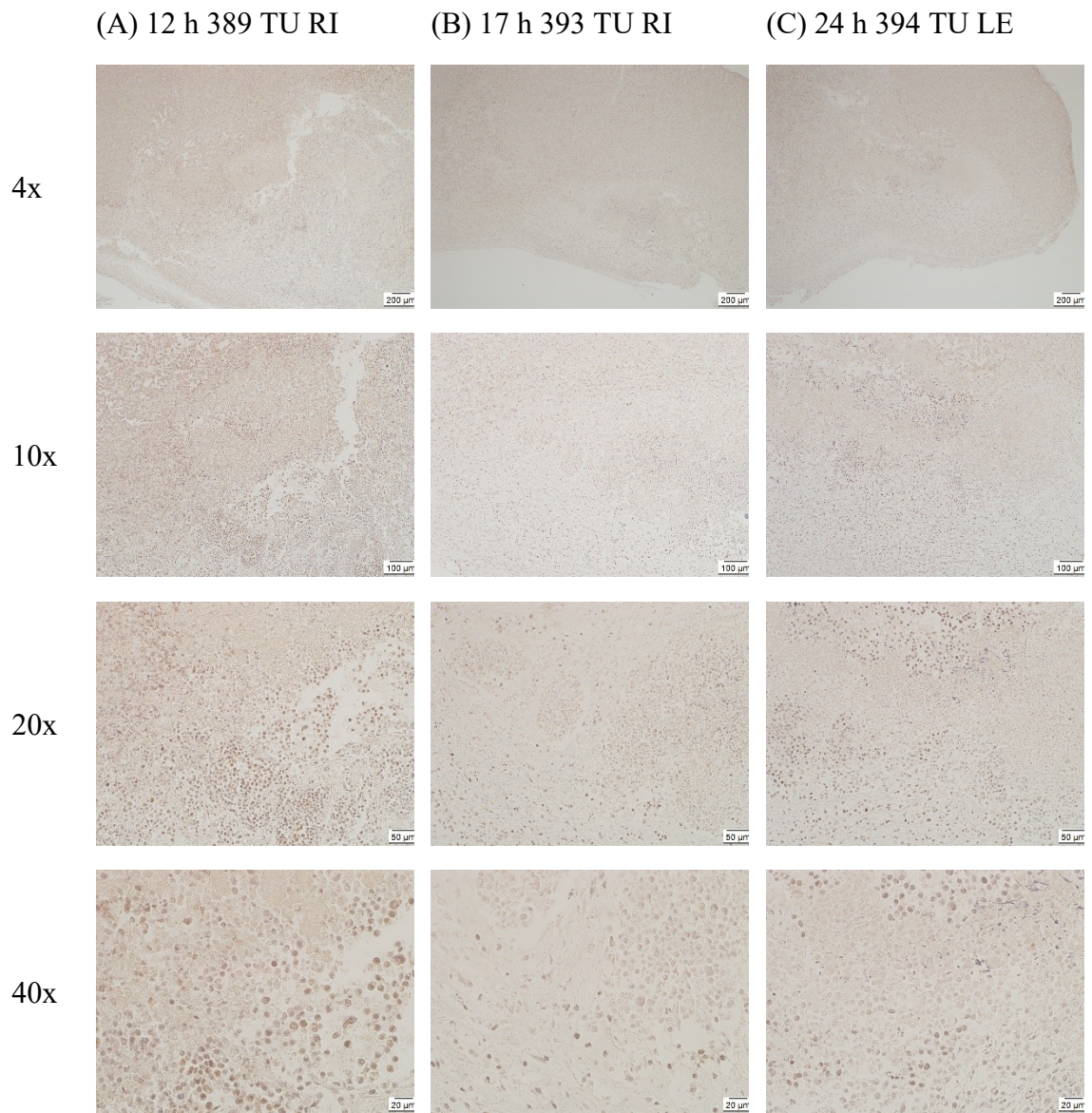


Figure 39 NCR1 ab214468 staining in vivo experiment 4 IL2-P-Fc treated group (A) MCT-389 TU RI 12 hours post injection, (B) MCT-393 TU RI 17 hours post injection, (C) MCT-394 TU LE 24 hours post injection. Magnification 4x, 10x, 20x, 40x, scale bar 200 μm , 100 μm , 50 μm , 20 μm .

IL2-P-FC

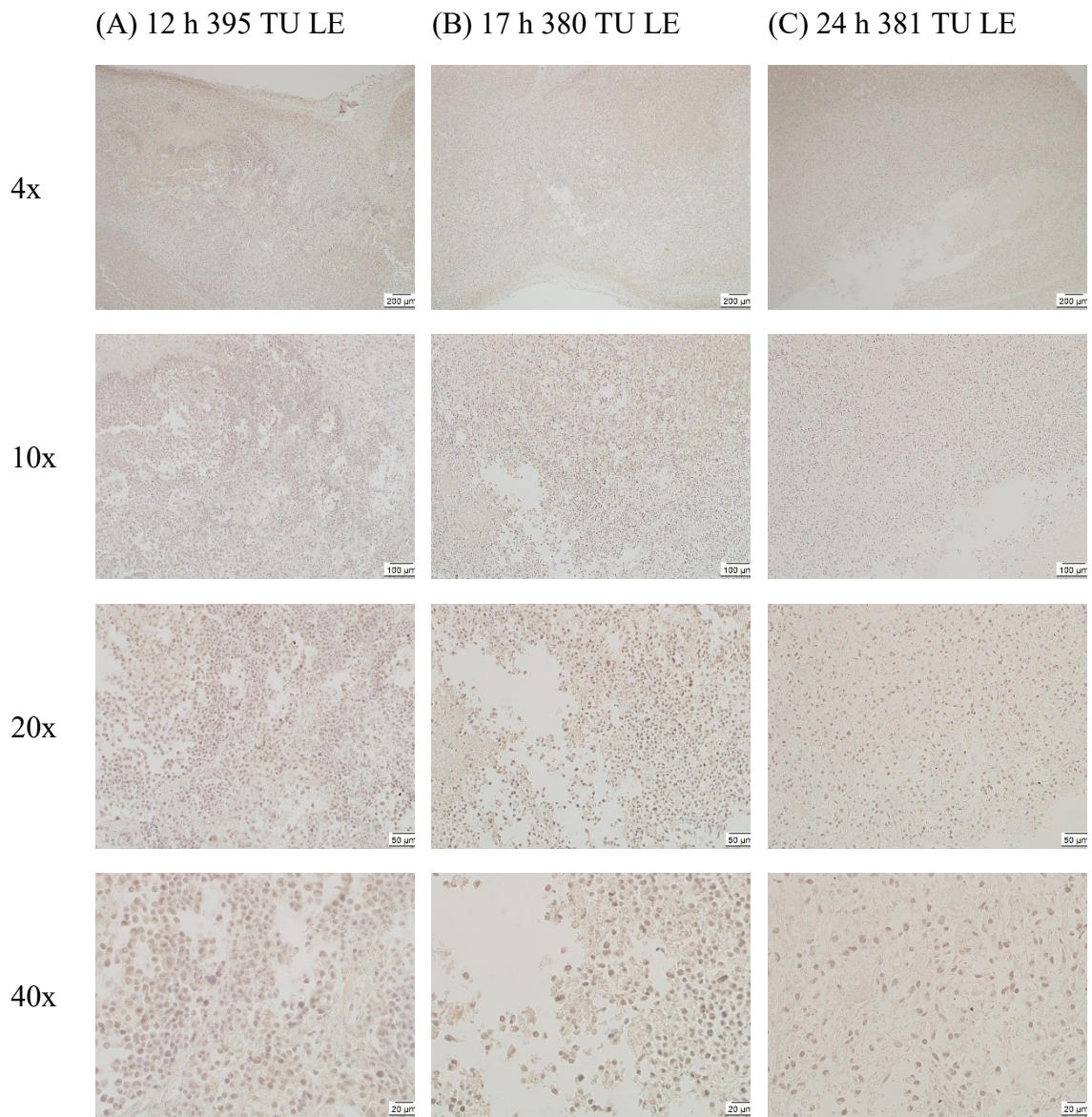


Figure 40 NCR1 ab199128 staining in vivo experiment 4 IL2-P-Fc treated group (A) MCT-395 TU LE 12 hours post injection, (B) MCT-380 TU LE 17 hours post injection, (C) MCT-381 TU LE 24 hours post injection. Magnification 4x, 10x, 20x, 40x, scale bar 200 μm , 100 μm , 50 μm , 20 μm .

IL2-P-FC

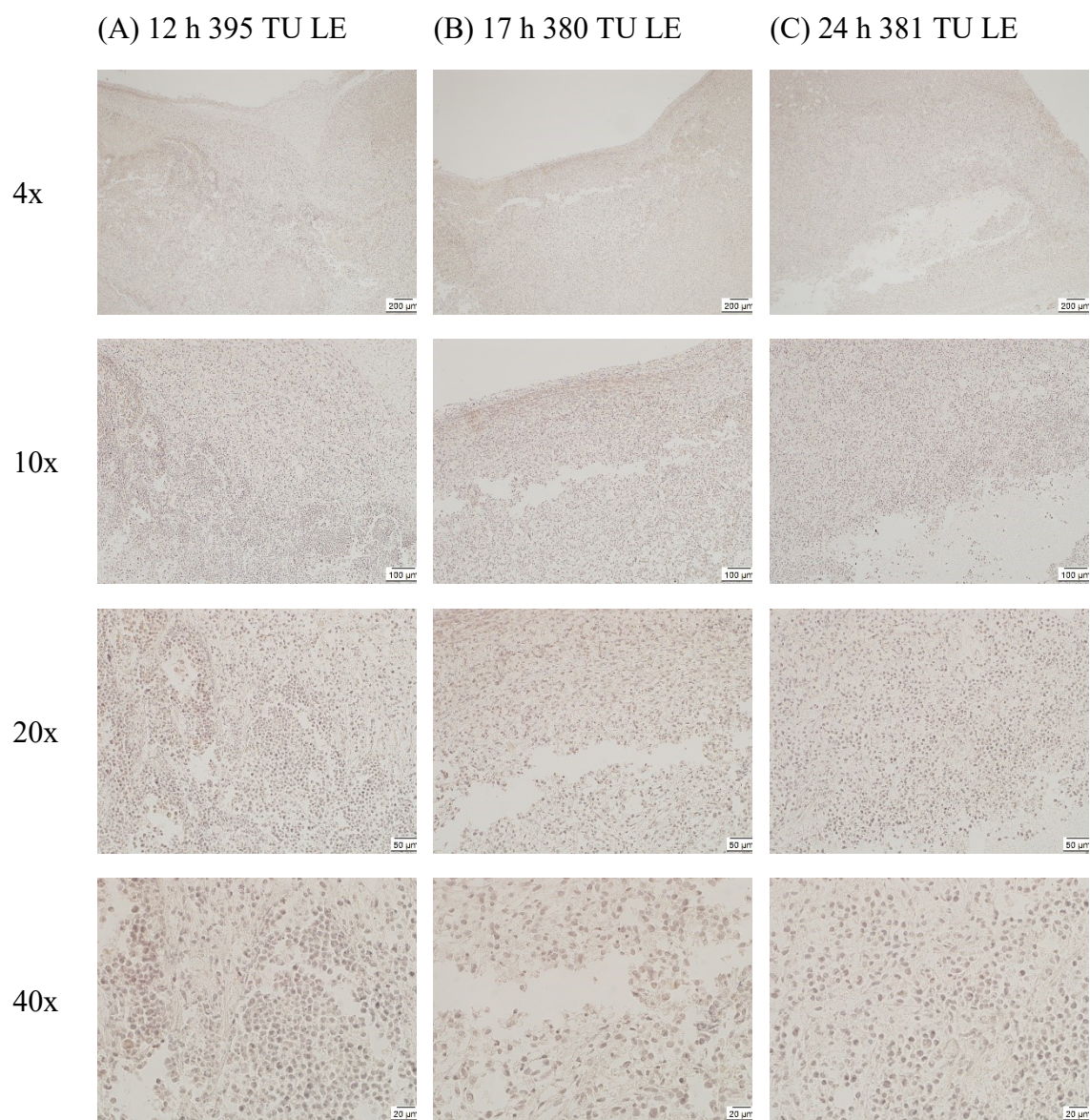


Figure 41 NCR1 ab214468 staining in vivo experiment 4 IL2-P-Fc treated group (A) MCT-395 TU LE 12 hours post injection, (B) MCT-380 TU LE 17 hours post injection, (C) MCT-381 TU LE 24 hours post injection. Magnification 4x, 10x, 20x, 40x, scale bar 200 μm , 100 μm , 50 μm , 20 μm

bb-mCherry transfection control

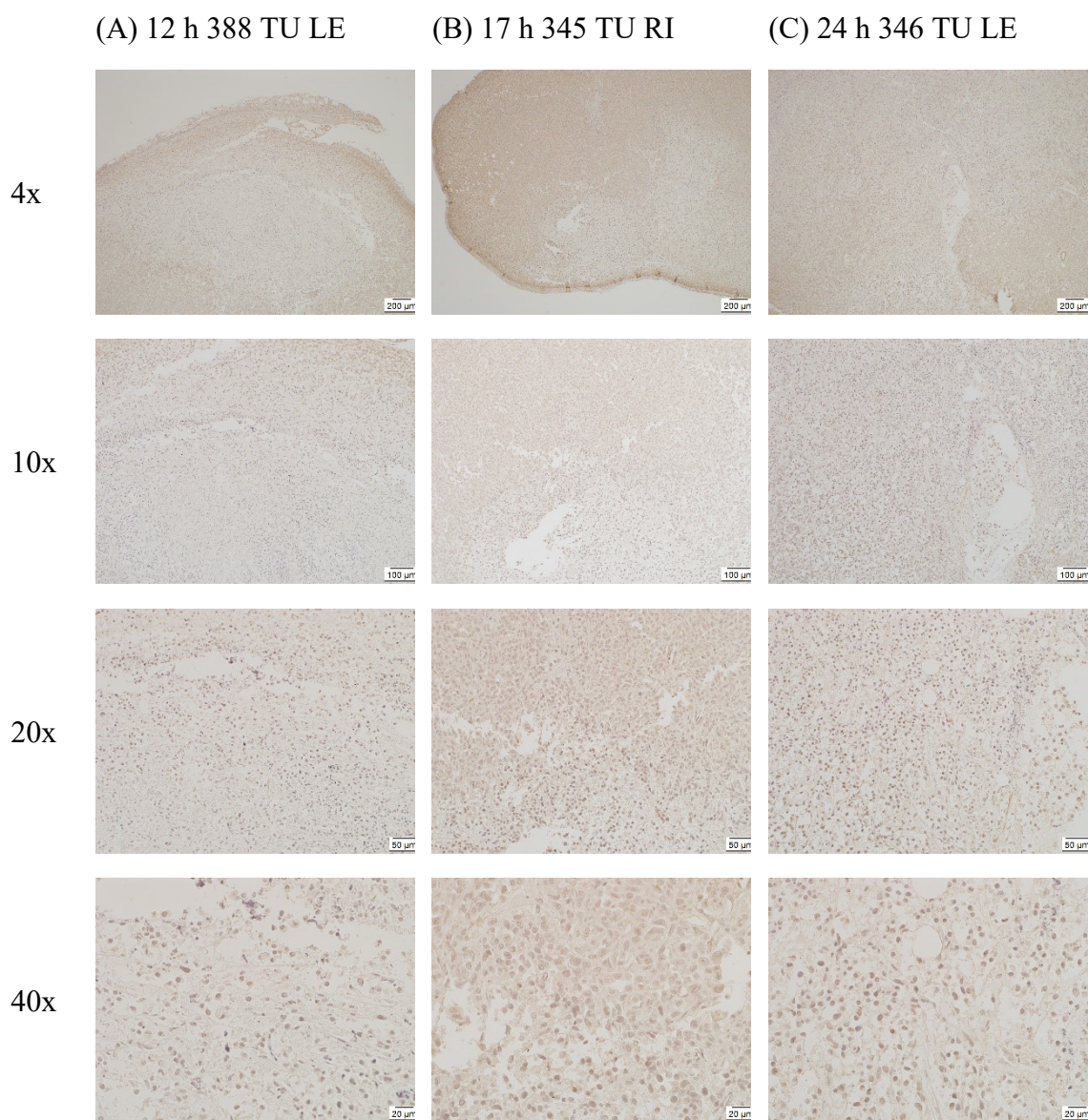


Figure 42 NCR1 ab199128 staining in vivo experiment 4 bb-mCherry transfection control group (A) MCT-388 TU LE 12 hours post injection, (B) MCT-345 TU RI 17 hours post injection, (C) MCT-346 TU LE 24 hours post injection. Magnification 4x, 10x, 20x, 40x, scale bar 200 μm , 100 μm , 50 μm , 20 μm .

bb-mCherry transfection control

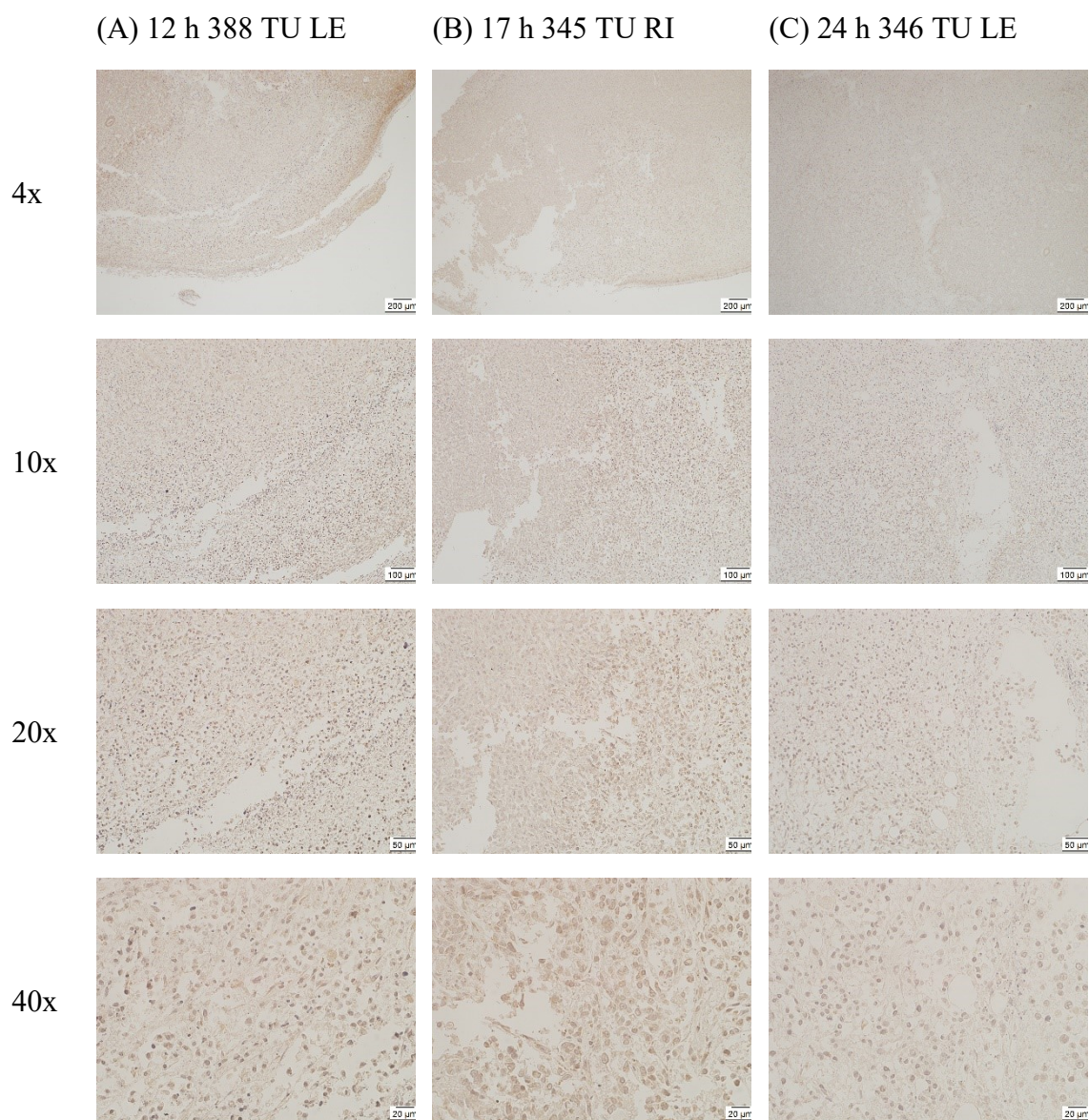


Figure 43 NCRI ab214468 staining in vivo experiment 4 bb-mCherry transfection control group (A) MCT-388 TU LE 12 hours post injection, (B) MCT-345 TU RI 17 hours post injection, (C) MCT-346 TU LE 24 hours post injection. Magnification 4x, 10x, 20x, 40x, scale bar 200 μ m, 100 μ m, 50 μ m, 20 μ m.

CD47 staining

In a separate set of experiments, all tumors were also stained for expression of CD47. This should help identifying human tumor cells, since the primary antibody used (polyclonal rat anti CD47, ab218810) is specifically only recognising human CD47 and does not bind to murine CD47 as evaluated in a xenograft tumor model in SCID mice (Magdalena Billerhart, unpublished observations). With the staining of transfected tumor tissue, a potential blocking of CD47 should be detected.

IL2-P-FC

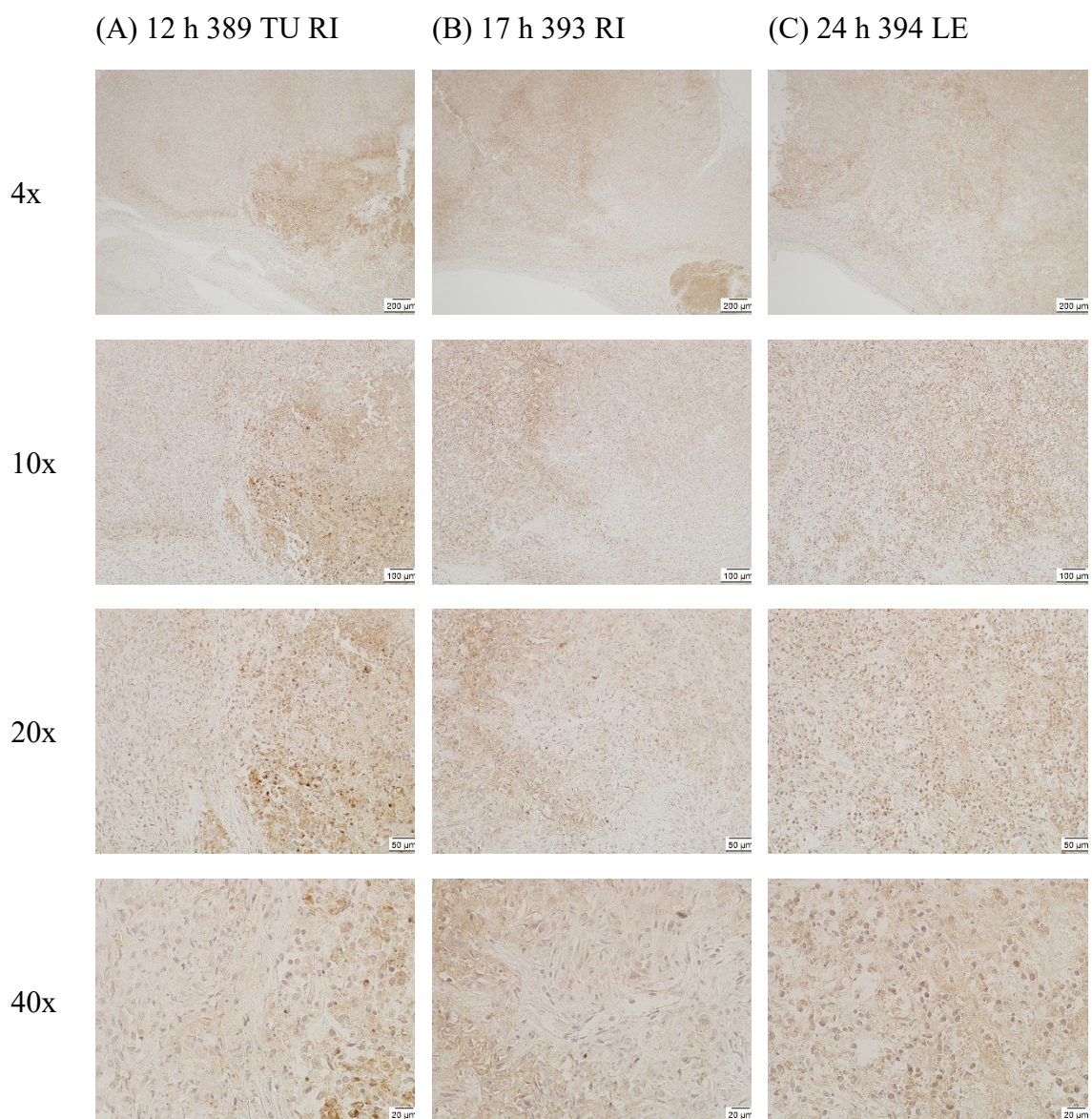


Figure 44 CD47 staining in vivo experiment 4 IL2-P-Fc treated group (A) MCT-389 TU RI 12 hours post injection, (B) MCT-393 TU RI 17 hours post injection, (C) MCT-394 TU LE 24 hours post injection. Magnification 4x, 10x, 20x, 40x, scale bar 200 μ m, 100 μ m, 50 μ m, 20 μ m.

IL2-P-Fc

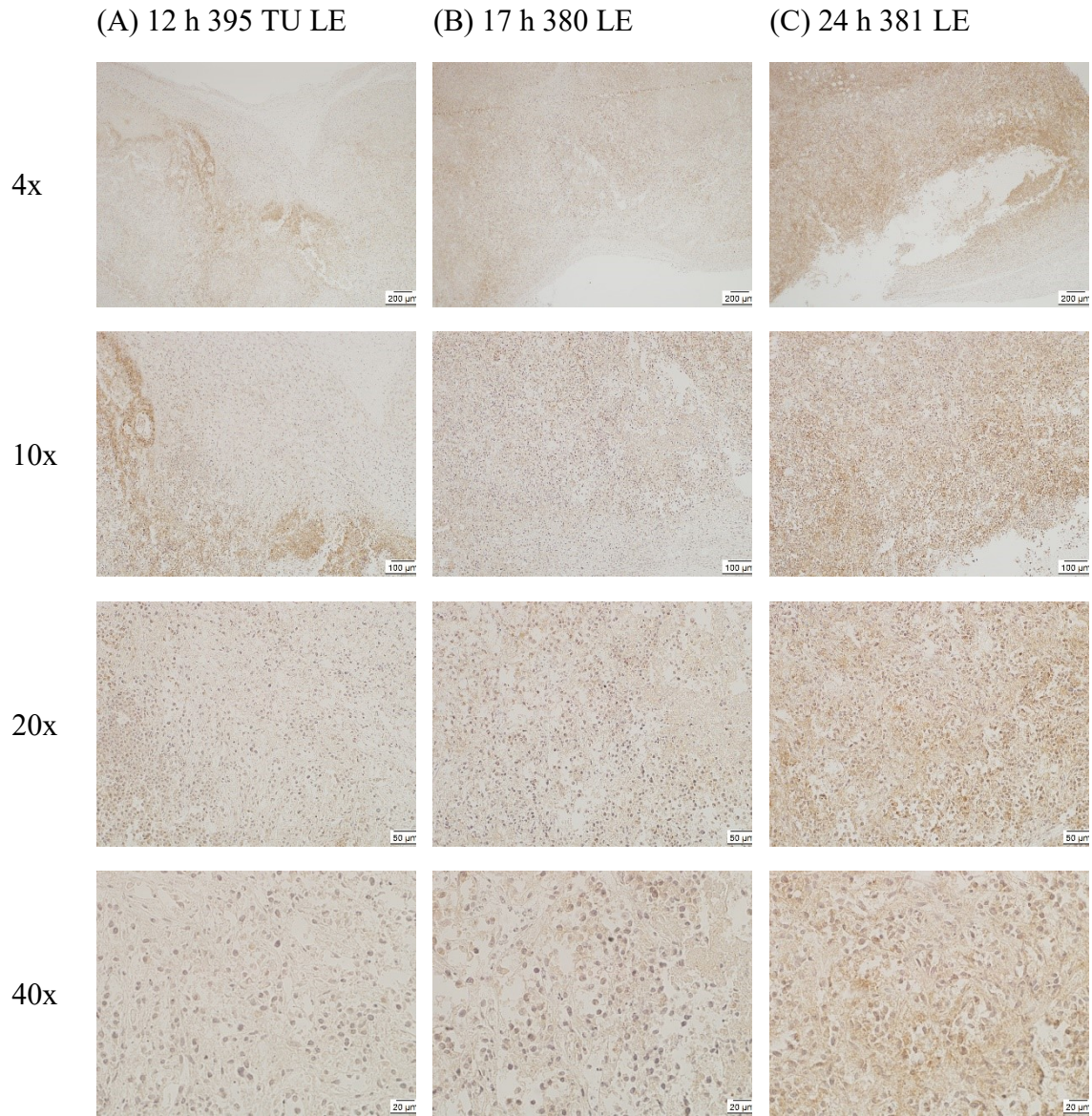


Figure 45 CD47 staining in vivo experiment 4 IL2-P-Fc treated group (A) MCT-395 TU LE 12 hours post injection, (B) MCT-380 TU LE 17 hours post injection, (C) MCT-381 TU LE 24 hours post injection. Magnification 4x, 10x, 20x, 40x, scale bar 200 μm , 100 μm , 50 μm , 20 μm .

bb-mCherry transfection control

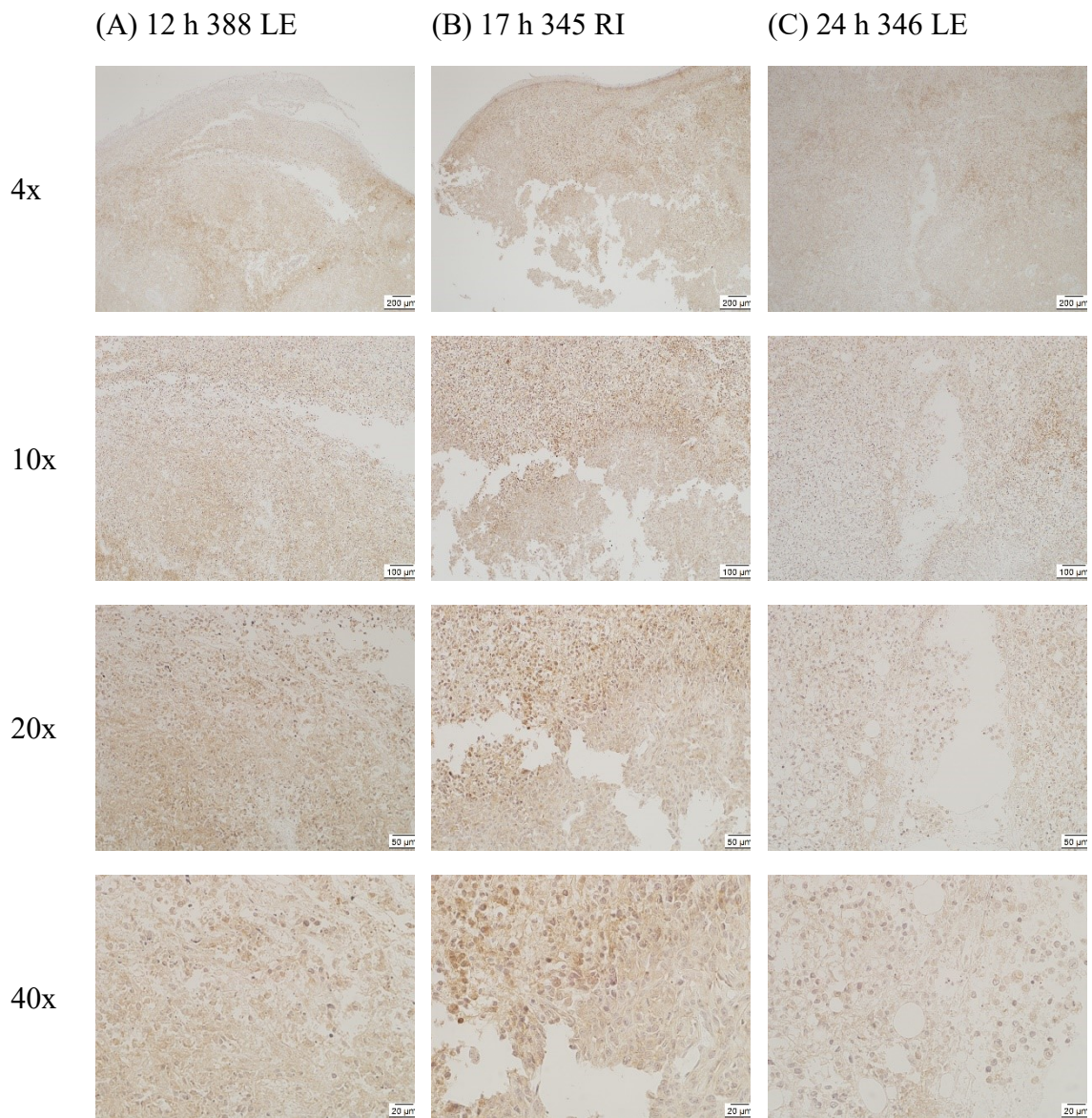


Figure 46 CD47 staining in vivo experiment 4 bb-mCherry transfection control group (A) MCT-388 TU LE 12 hours post injection, (B) MCT-345 TU RI 17 hours post injection, (C) MCT-346 TU LE 24 hours post injection. Magnification 4x, 10x, 20x, 40x, scale bar 200 μm , 100 μm , 50 μm , 20 μm .

IL2-P-Fc, 24 hours, MCT-394, TU LE

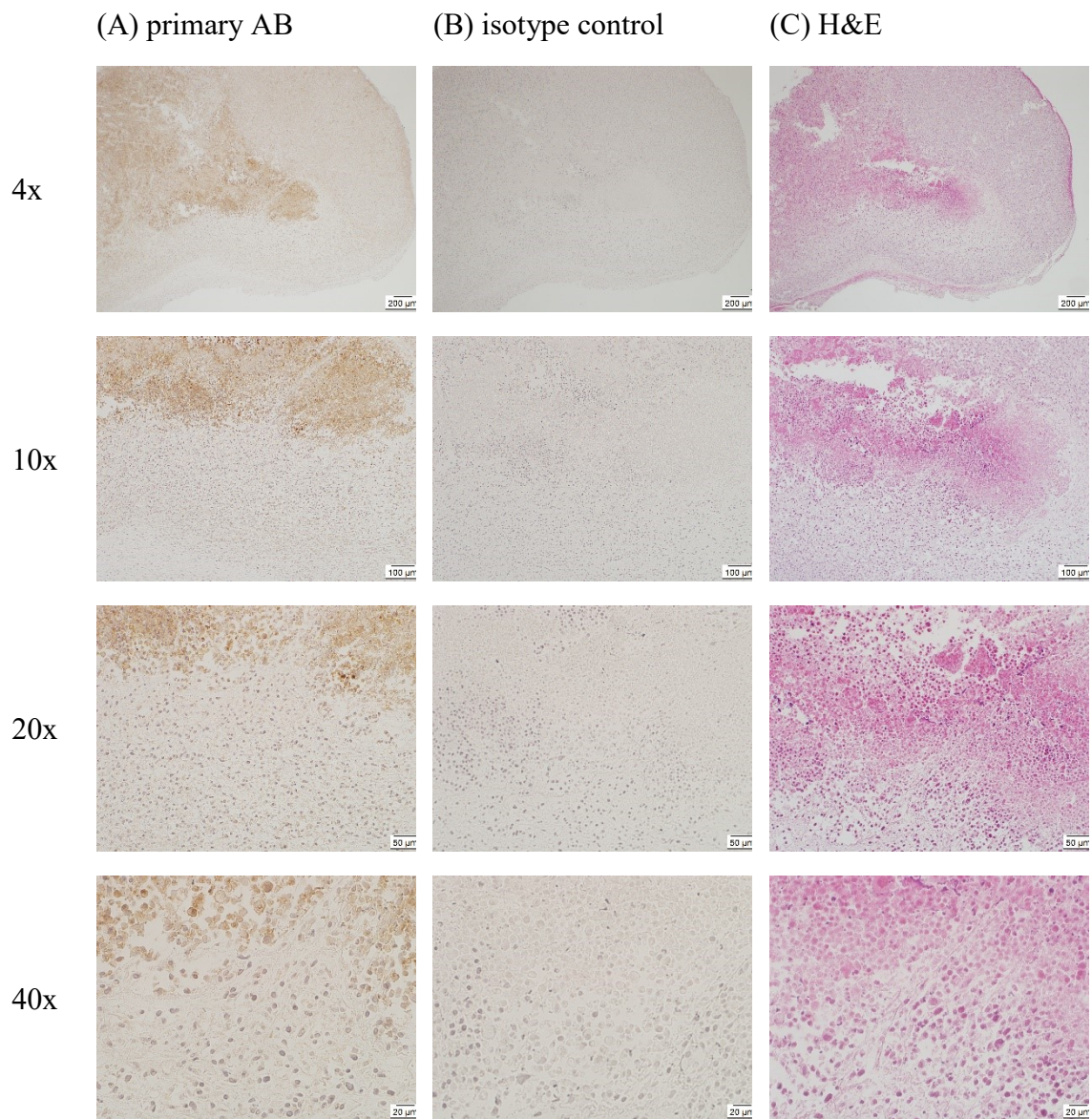


Figure 47 CD47 staining MCT-394 left tumor, IL2-P-Fc group 24 hours post intratumoral injection. (A) primary antibody, dilution 1:2000, (B) isotype control, (C) H&E staining. Magnification 4x, 10x, 20x, 40x, scale bar 200 μ m, 100 μ m, 50 μ m, 20 μ m.

bb-mCherry transfection control, 24 hours, MCT-346, TU LE

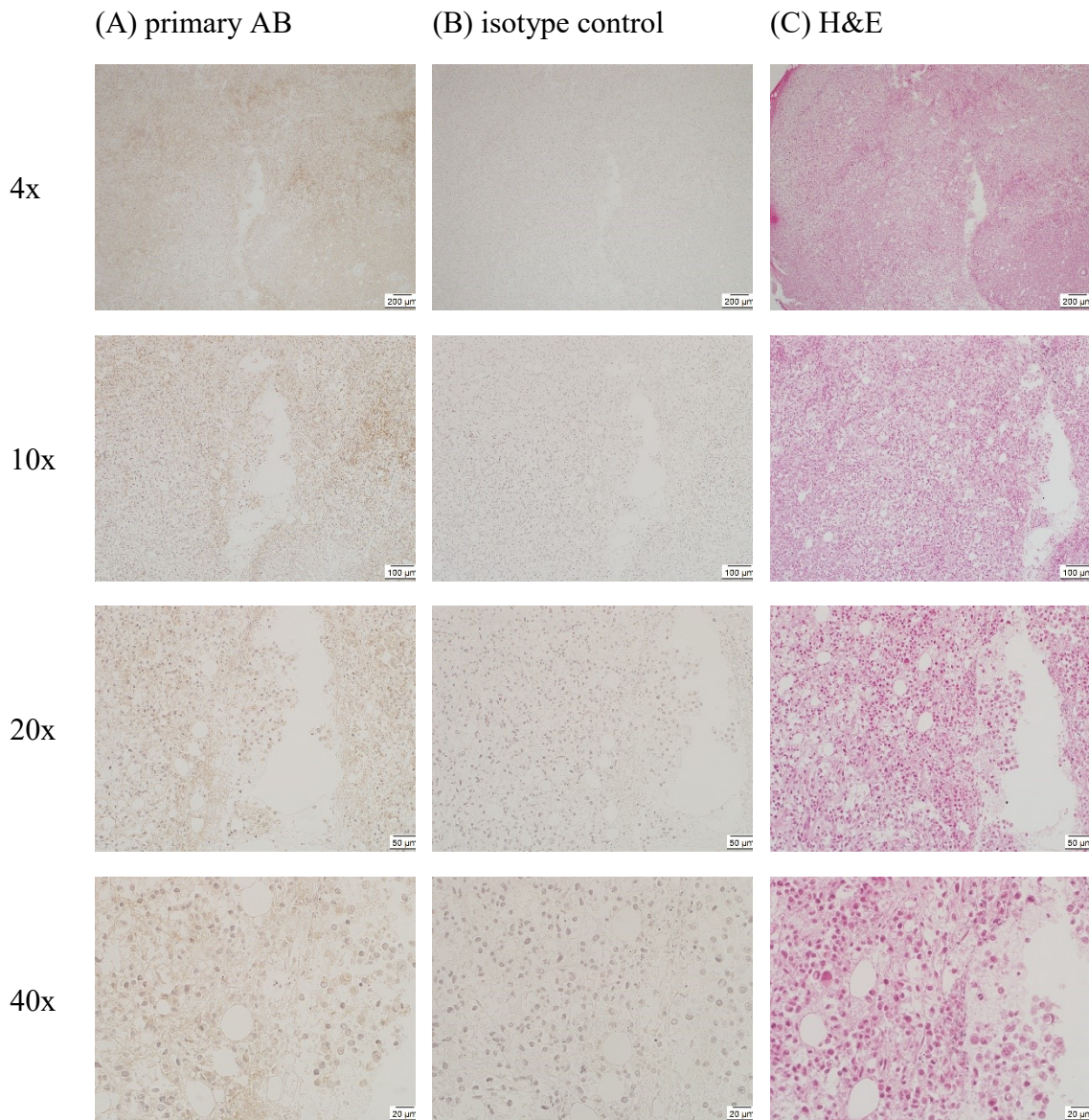


Figure 48 CD47 staining MCT-346 left tumor, bb-mCherry transfection control group 24 hours post intratumoral injection. (A) primary antibody, dilution 1:2000, (B) isotype control, (C) H&E staining. Magnification 4x, 10x, 20x, 40x, scale bar 200 μm , 100 μm , 50 μm , 20 μm .

The CD47 staining seems to be unspecific, the primary antibody should only bind to human CD47, but the murine blood cells are also stained, furthermore a more intense staining of the tumors was expected, especially the cell surface should be stained, but no intense staining could be detected in any of the tumors. Not even the control group where CD47 should not be blocked and should give a strong signal was stained in the expected way.

CD47 positive tumors should be stained quite dark brown, especially the cell surface and no since an anti-human primary antibody was used murine muscle cells, connective tissue

or blood cells should not be stained, as can be seen in Figure 49. These slides were stained simultaneously to the samples of the in vivo experiment. As can be seen, only the tumor tissue is stained and the cells are mostly stained on the surface, which is expected, since CD47 is a surface protein. For this staining an untransfected sample from a former in vivo experiment was used.

CD47 MCT-0041

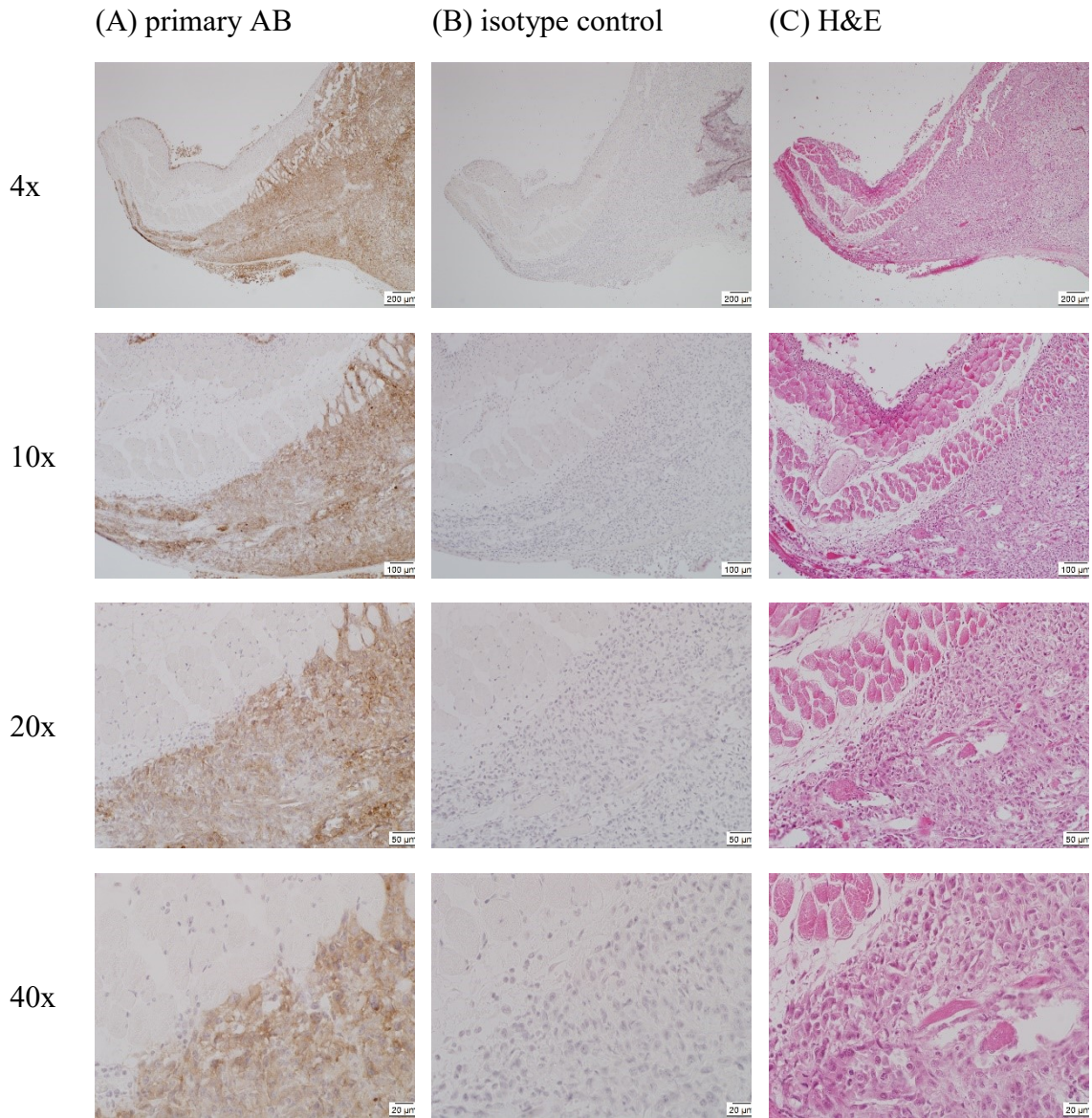


Figure 49 CD47 staining of MCT-0041, (A) primary antibody, dilution 1:200, (B) isotype control, (C) H&E. Magnification 4x, 10x, 20x, 40x, scale bar 200 μm , 100 μm , 50 μm , 20 μm .

Luciferase staining

The staining was performed to identify the tumor cells, since an EGFP-luc transduced cell line was used and implanted in the mice and this antigen is absent in murine tissue. Flow Cytometry showed that about 70% of the cells should be positive for Luciferase (Magdalena Billerhart, unpublished). The staining did not work out, as the secondary antibody binding was unspecific. Therefore, most of the tissue was stained, not only the tumor cells, but also some murine tissue like muscle or connective tissue surrounding the tumors.

Luciferase staining MCT-389 TU RI

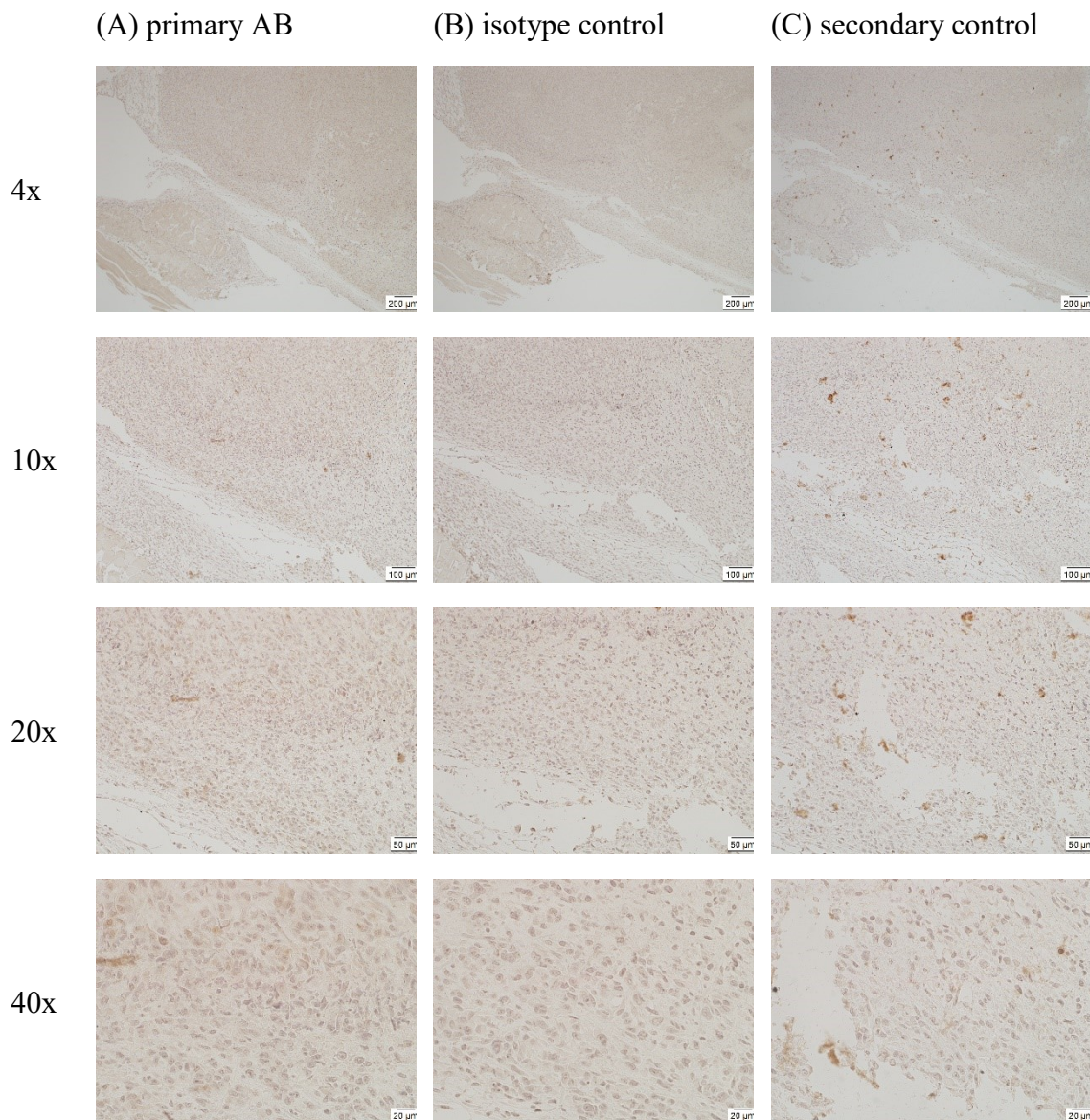


Figure 50 Luciferase staining MCT-389 TU RI, IL2-P-Fc group 12 hours post intratumoral injection, (A) primary antibody, dilution 1:1000, (B) isotype control, (C) secondary antibody control; 90

buffer control was negative. Magnification 4x, 10x, 20x, 40x, scale bar 200 μm , 100 μm , 50 μm , 20 μm .

Luciferase staining MCT-346 TU RI

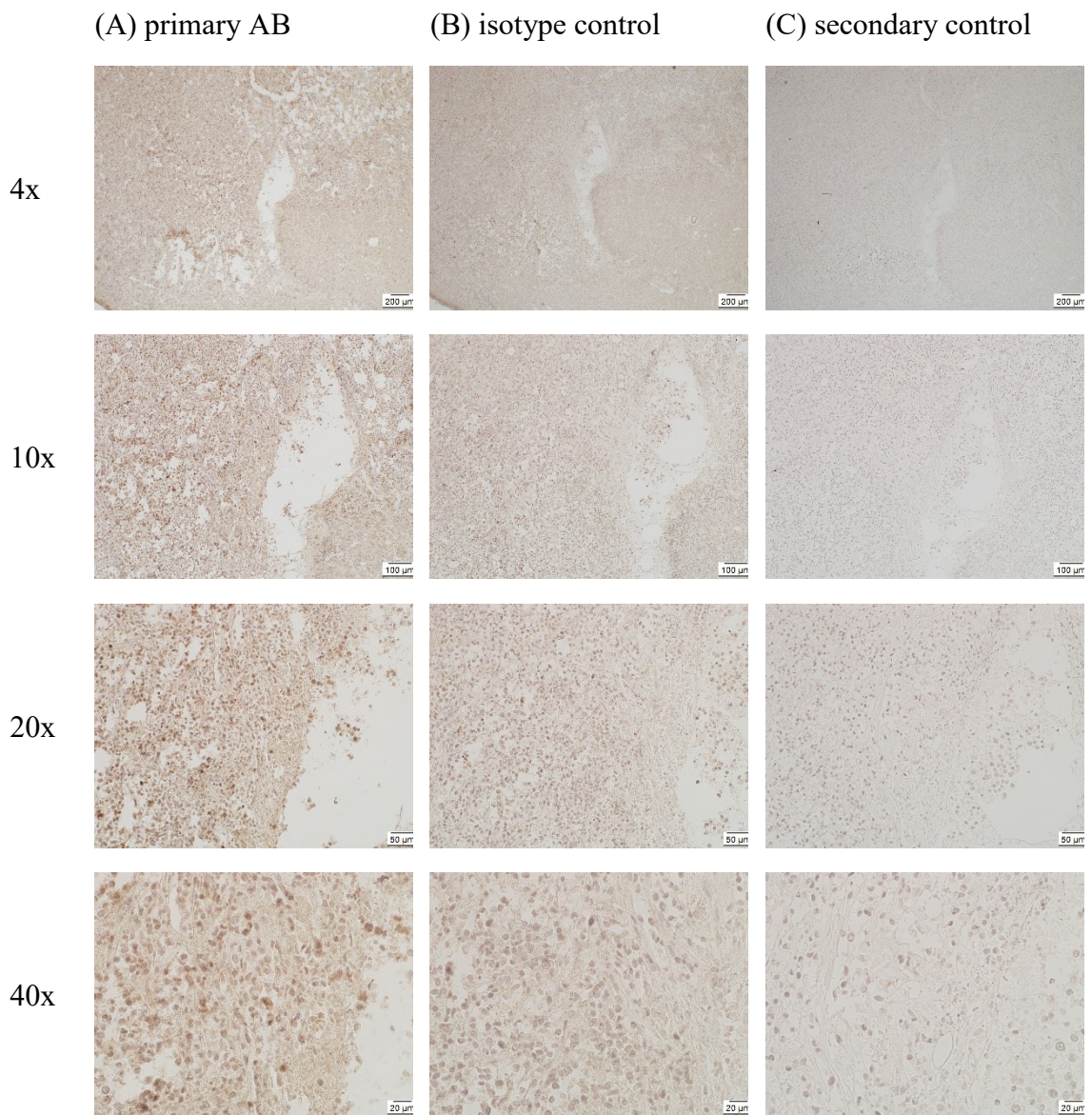
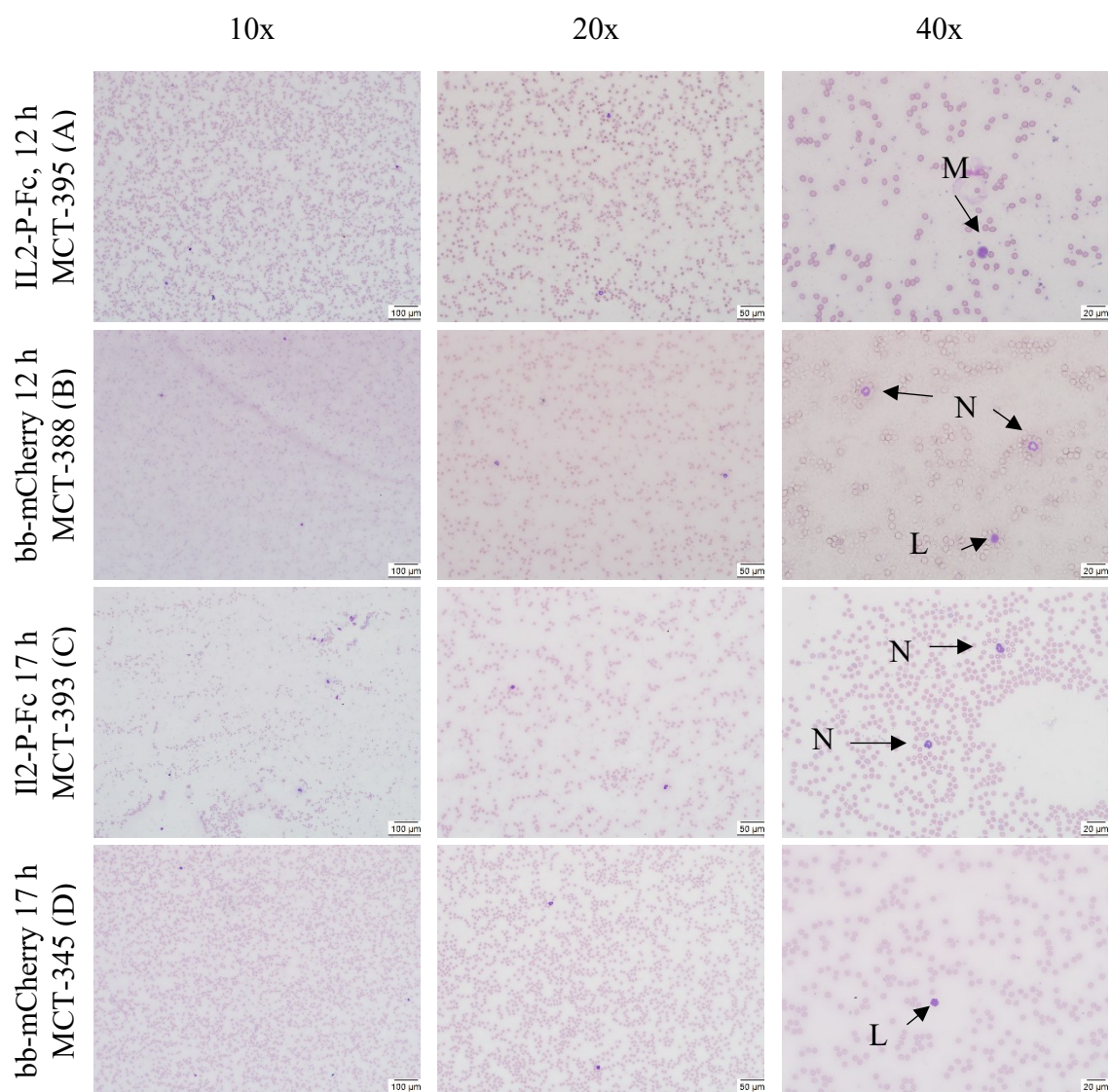


Figure 51 Luciferase staining MCT-346 TU RI, bb-mCherry transfection control group 24 hours post intratumoral injection, (A) primary antibody, dilution 1:1000, (B) isotype control, (C) secondary antibody control; buffer control was negative. Magnification 4x, 10x, 20x, 40x, scale bar 200 μm , 100 μm , 50 μm , 20 μm .

Blood smears

For every mouse in the in vivo experiment, a Giemsa staining of a blood smear was performed in order to see which white blood cells the SCID mice have and it was hoped that a difference in the number of lymphocytes between the treated and the untreated control group could be observed, since this might correlate with the infiltration of lymphocytes into the treated tumors.

Due to some difficulties while obtaining the blood, different amounts of blood could be harvested for each smear. Due to this fact and big individual differences in the amount of white blood cells between the mice, no clear observation was possible.



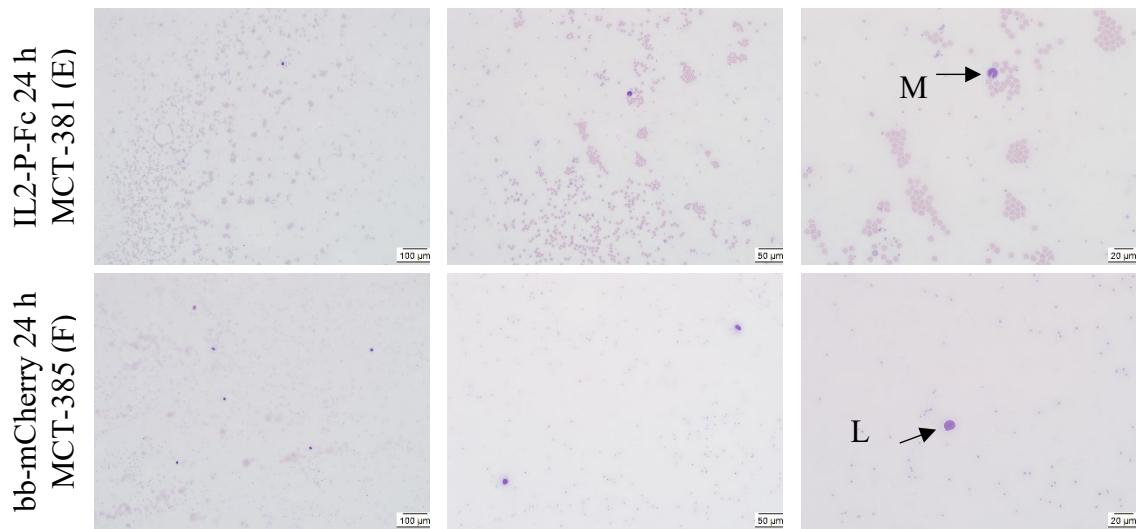


Figure 52 Giemsa staining of blood smears in vivo experiment 4 (A) MCT-395 IL2-P-Fc treated group after 12 hours, (B) MCT-388 bb-mCherry transfection control group after 12 hours, (C) MCT-393 IL2-P-Fc treated group after 17 hours, (D) MCT-345 bb-mCherry transfection control group after 17 hours, (E) MCT-381 IL2-P-Fc treated group after 24 hours, (F) MCT-385 bb-mCherry transfection control group after 24 hours. (L) mark lymphocytes, (M) mark monocytes, (N) mark neutrophils. Magnification 10x, 20x, 40x, scale bar 100 μm , 50 μm , 20 μm .

Figure 52 shows Giemsa staining of blood smears. Giemsa stain consists of Eosin and Methylene blue, therefore the cytoplasm is stained red and the nuclei are stained blue. Since they do not possess a nucleus, erythrocytes are stained red, while nucleated cells are stained blue. Nucleated cells can be identified morphologically. Neutrophils are marked by nuclei consisting of several lobes while monocytes, the precursor cells of macrophages, oftentimes possess C-shaped nuclei. Lymphocytes on the other hand possess very little cytoplasm and round nuclei. (Mescher & Junqueira, 2013)

8. Discussion

The aim of this thesis was to establish protocols for NK cell and macrophage IHC staining for the evaluation of tumors transfected with a plasmid for a fusion protein, which should block CD47. The fusion protein consists of an IL2 part for secretion, the SIRP α domain which blocks CD47 and an Fc part, which leads to ADCC via NK cells and also macrophages due to the interaction with the Fc receptor CD16 on these cells.

The first aim was to establish a staining for NK cells. For this purpose, antibodies against NCR1 were used. The first Antibody ab214468 (Figure 8-Figure 11) showed some staining of NK cells but also a strong background staining. Since both the isotype control and the secondary control were negative it was clear that the primary antibody was unspecific, not the detection system. But in some samples stained cells could be seen in blood vessels, and because of the location and the morphology of these cells it is clear, that these are NK cells. Non-lymphatic organs like liver and lung were also stained, were even the hepatocytes were intensely stained. Especially strong staining was observed in the bronchial epithelium in the lung, which have been described to bear high levels of endogenous biotin. (Kuhn, 1988). This would suggest some problem with the Avidin/Biotin blocking, but since the isotype control showed no staining, this is very unlikely. It seems like the primary antibody bound to some structures in these areas.

Because of this the second NCR1 antibody, ab199128, was tested. (Figure 12-Figure 16) This one recognises an intracellular epitope. Nevertheless, the results were still unreliable because of the very high background staining. It was tried to decrease the background stain with higher dilutions of the primary antibody, but the background staining was still visible. It was also tried to use different kinds of blocking serum, such as horse serum instead of goat serum or 5% BSA/PBS, but there was no improvement of the background stain. NK cells were clearly stained with this antibody and less unspecific staining could be observed, but because of the very high background staining the results are not completely reliable. One big problem was that the nuclei of the cells seemed to be stained, although NCR1 is a surface protein, which should mean that only the surface of the cells are stained, but it was not the case. It was planned to perform a positive control staining of an NK cell line to see if the NK cells would be stained on the surface or not, but the cells did not arrive on time. Another explanation that surface expression pattern on the cells was not seen lies within

the morphology of NK cells: they possess very little cytoplasm, so it could be possible that the surface was actually stained, and it only seems like the nuclei is stained. A positive control would be necessary to conform this theory. The provider of the Anti-NCR1 antibody (ab214468), Abcam, is presenting IHC results on the web pages, which would be in line with our results (Figure 53). (Abcam, 2019e)

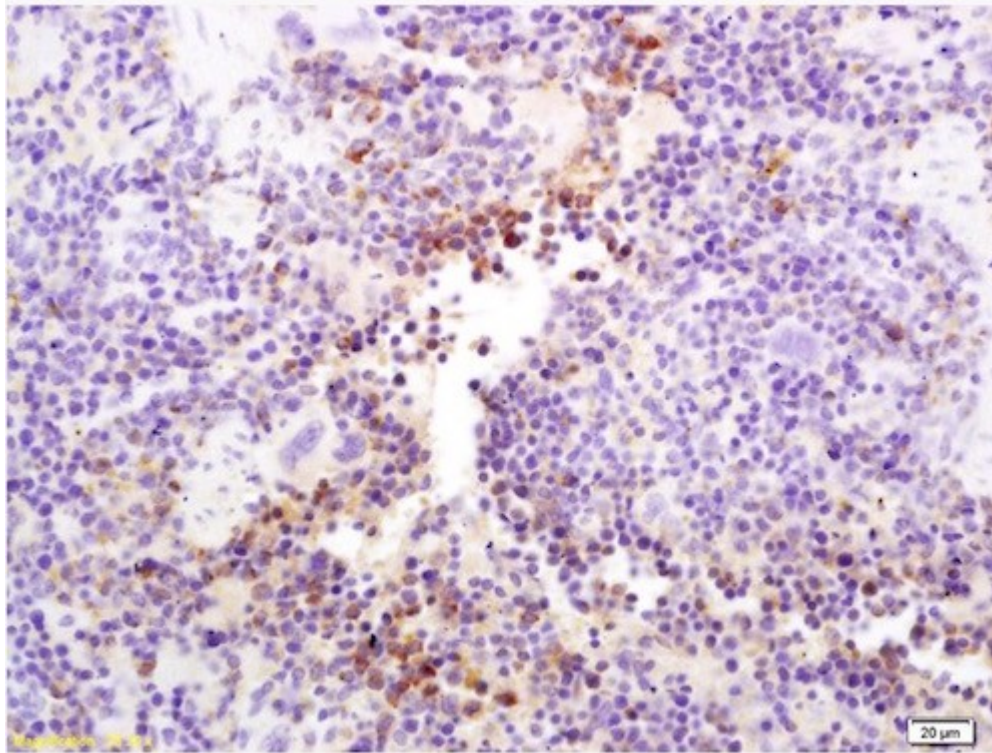


Figure 53 Staining of NK cells ab214468 (Abcam, 2019e)

Similar data are shown in Russel et al as using the same antibody. Also, here, no membranous stain can be seen, rather the whole cell appears positive. Also, the rather high background level should be noted.

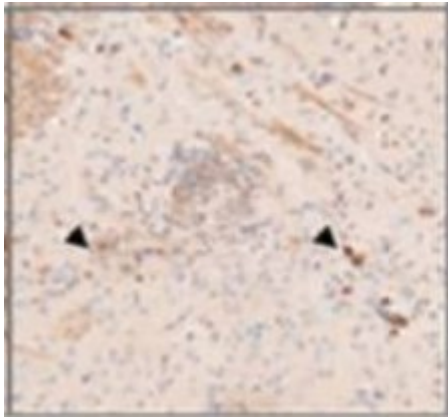


Figure 54 NK cells stained with ab214468. Arrowheads denote NK cells. (Russell et al., 2018)

The second aim was to establish a staining for macrophages. The first antibody evaluated was directed against CD16 (Figure 18). This approach did not result in any positive staining, although some macrophages were clearly visible and the antibody should also stain NK cells, since the receptor is also expressed on those. Several dilutions of the primary antibody were used, but all with the same results. CD16 is also expressed on NK cells (Watzl, 2014) and therefore cells in the spleen should be stained, but only a slight background stain could be observed, there was no specific staining.

Thereafter the anti SIRP α antibody (Figure 17) was evaluated, although also with negative results: there was some staining, but it was not clear which kind of structure was stained, the macrophages were clearly not stained. SIRP α is expressed on the macrophages and the spleen does harbour macrophages (Lin et al., 2018), which could also be seen in the sample, but they remained unstained. It is possible that this antibody was already expired and there was no specific staining due to that fact. Another possibility lies within the antibody, since this primary antibody was not designed for IHC and therefore does not work with the procedure used.

The third aim was the immunohistological evaluation of the *in vivo* experiments performed. In these experiments, tumors were treated with polyplexes containing plasmids for the fusion protein IL2-P-Fc, which should block CD47 and therefore inhibit the interaction between CD47 and SIRP α . Tumor cells were either transfected *ex vivo* prior to implantation (in vivo exp No 1 and 2) or by direct *in vivo* transfection after intratumoral injection (in vivo exp 3 and 4). A control group was treated with the plasmid bb-mCherry. Tumors were

evaluated for CD47, Firefly luciferase and NCR1.

It was expected that CD47 should be blocked in the treated group, former experiments showed that it was blocked after 24 hours (in vivo experiment 3), and a significant reduction in the staining intensity could be observed. (Pichler, 2019) The staining for CD47 did not work as expected, as the tumor cells were only slightly stained (Figure 44-Figure 48), not intensely on the cell surface as it was observed on slides which were obtained from the experiment described in Pichler et al (Figure 49). Instead, the murine blood cells in the tumors were stained intensely, which should not be the case since the primary antibody should only bind to human CD47 and not to murine CD47. Stainings using samples from former in vivo experiments were performed simultaneously and showed the expected results: the cell surface of tumor cells were stained and murine cells remained unstained. This rules out problems with the primary antibody or the staining kit. It is not clear why this staining did not work, but since other stainings with the same procedure did work it is most likely that there were some problems with the tissue processing. There were several problems during the embedding, which could possibly lead to this. A potential problem was the ambient temperature during the time of the embedding, which was continuously over 30°C, at some days up to 35°C. Therefore, the samples could not be embedded immediately after obtaining the tumors and were left in 70% Ethanol for several days. Because they could not be stored any longer the embedding was still done at high ambient temperatures. There, another problem occurred, because during the embedding one jar with paraffin did not heat up properly, the paraffin inside was still partly solid, and the right temperature was not reached. Also, different qualities of paraffin were mixed since there was not enough of the one usually used, and one of those contained DMSO. This should in principle not negatively influence the embedding procedure, but it is not clear if and how this affected the tissues used in this study. However, the H&E stainings worked with the same samples and the morphology looked normal.

Generally, tissue should always be fixed immediately after obtaining and it should be stored at room temperature (>25°C). Both was not the case for these samples. Higher temperature could increase the penetration of the fixative and it accelerates the tissue degradation via enzymes. (Novusbio.com, 2019b)

The temperature also has influences during the staining, higher incubation temperatures could lead to overstaining. (IHC World, 2015d) Another source of the staining problems could be the HIER. It is very important to perform it at a certain pH, which was checked

before the experiments, but also the duration of heating can have huge impact on the staining, which may indicate that a higher room temperature and the resulting longer cool down period could lead to some difference in the staining. (IHC World, 2015a)

However, the fact that stainings on samples from former in vivo experiments performed at the exact same time worked as expected, indicates that the problem lies within the fixation of the tissue and not the staining procedure.

The staining for Firefly luciferase was also not reliable, because the secondary antibody was unspecific and therefore most of the tissue was stained, even murine tissue. Only tumor tissue should be stained, since the cells were Lentiviral transduced with luciferase gene before being implanted in the mice. Why this staining did not work is unclear, since the exact same staining has worked before. (Pichler, 2019) It is possible that there was a problem with the staining kit, no stainings performed on samples from former in vivo experiments worked, there was either no staining at all or an unspecific staining of the secondary antibody.

The major part of this work was the evaluation of NK cell staining procedures. Two different primary antibodies were used, one recognising an extracellular epitope (ab214468), and the other one an epitope on the cytoplasmatic side (ab199128). Some stained cells could be seen in the tumors, especially in haemorrhagic areas, but since the stainings were not specific due to the high background and some unspecific staining in lung and liver, the results are not reliable.

When performing H&E stainings (Figure 28-Figure 30) of the samples, clear and reliable results were obtained: necrotic areas around the injection sites could be observed, and the haemorrhagic areas contained a large number of cells, which might be lymphocytes, and some macrophages could also be seen. Most of the immune cells are located in the haemorrhagic areas, but in some samples it appeared that immune cells also infiltrated the tumor tissue.(Figure 28 tumor number 389 TU RI, Figure 29 tumor number 395 TU LE, Figure 30 tumor number 388 TU LE)

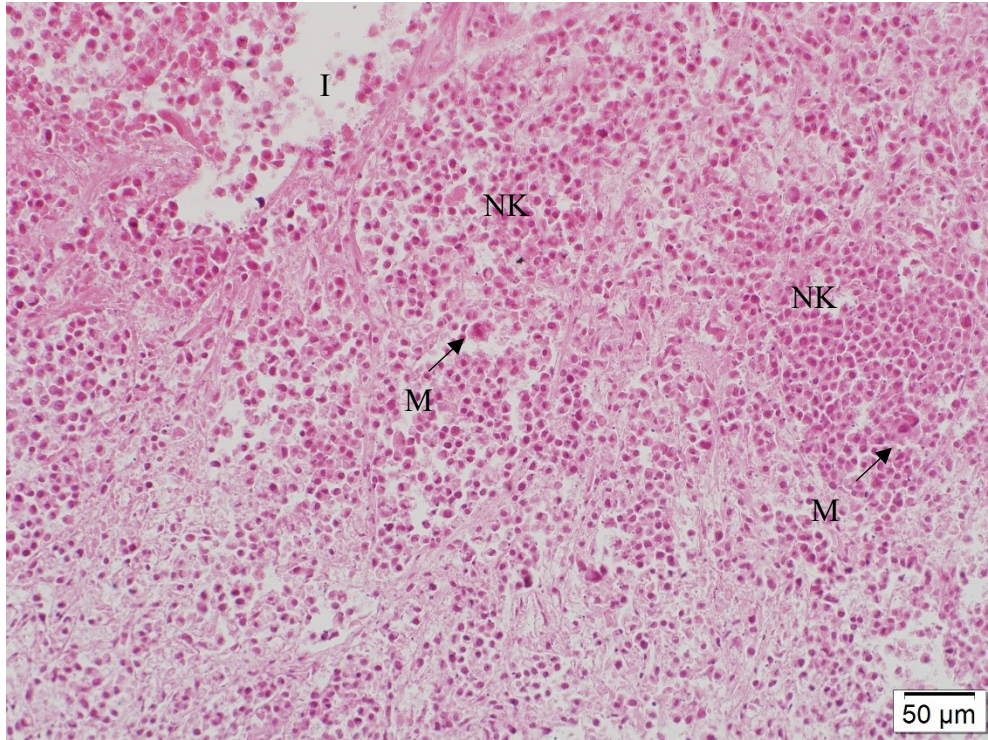


Figure 55 IL2-P-Fc after 12 hours, MCT 389 TU RI: (M) arrows denote infiltrated macrophages. (NK) denote areas with infiltrated NK cells. (I) denotes injection site. Magnification 20x. Scale bar 50 μ m.

This could be observed in both the treated and the control group. Since the plasmid in the control group only contains bb-mCherry this suggests that bb-mCherry or the polyplex components could also be immunogenic and/or induce an inflammatory reaction.

These results could not be confirmed with the IHC stainings.

In conclusion, the H&E stainings of the tumor samples gave reliable results, some NK cells and macrophages and their infiltration into the tumor tissue could be clearly observed. However, these results could not be confirmed with the immunohistochemical stainings, since the primary antibodies were not reliable.

References

- Abcam. (2019a). Blocking for IHC | Abcam. Retrieved from <https://www.abcam.com/kits/blocking-for-ihc>
- Abcam. (2019b). IHC controls | Abcam. Retrieved from <https://www.abcam.com/kits/controls-for-ihc>
- Abcam. (2019c). Anti-NCR1 antibody (ab214468) | Abcam. Retrieved from <https://www.abcam.com/ncr1-antibody-ab214468.html>
- Abcam. (2019d). Anti-NCR1 antibody (ab199128) | Abcam. Retrieved from <https://www.abcam.com/ncr1-antibody-ab199128.html>
- Abcam. (2019e). Anti-NCR1 antibody (ab214468) | Abcam. Retrieved from <https://www.abcam.com/ncr1-antibody-ab214468.html>
- Arnon, T. I., Achdout, H., Lieberman, N., Gazit, R., Gonen-Gross, T., Katz, G., . . . Mandelboim, O. (2004). The mechanisms controlling the recognition of tumor- and virus-infected cells by NKp46. *Blood*, *103*(2), 664–672. <https://doi.org/10.1182/blood-2003-05-1716>
- Bray, F., Ferlay, J., Soerjomataram, I., Siegel, R. L., Torre, L. A., & Jemal, A. (2018). Global cancer statistics 2018: Globocan estimates of incidence and mortality worldwide for 36 cancers in 185 countries. *CA: a Cancer Journal for Clinicians*, *68*(6), 394–424. <https://doi.org/10.3322/caac.21492>
- Breastcancer.org. Triple-Negative Breast Cancer: Overview, Treatment, and More. Retrieved from https://www.breastcancer.org/symptoms/diagnosis/trip_neg
- Brown, E. (2001). Integrin-associated protein (CD47) and its ligands. *Trends in Cell Biology*, *11*(3), 130–135. [https://doi.org/10.1016/S0962-8924\(00\)01906-1](https://doi.org/10.1016/S0962-8924(00)01906-1)
- Buchwalow, I., Samoilo, V., Boecker, W., & Tiemann, M. (2011). Non-specific binding of antibodies in immunohistochemistry: Fallacies and facts. *Scientific Reports*, *1*, 28. <https://doi.org/10.1038/srep00028>
- Cattoretti, G., Pileri, S., Parravicini, C., Becker, M. H., Poggi, S., Bifulco, C., . . . Feudale, E. (1993). Antigen unmasking on formalin-fixed, paraffin-embedded tissue sections. *The Journal of Pathology*, *171*(2), 83–98. <https://doi.org/10.1002/path.1711710205>
- Dako. (2013). *IHC Guidebook: Immunohistochemical Staining Methods*.
- Edris, B., Weiskopf, K., Volkmer, A. K., Volkmer, J.-P., Willingham, S. B., Contreras-Trujillo, H., . . . van de Rijn, M. (2012). Antibody therapy targeting the CD47 protein

- is effective in a model of aggressive metastatic leiomyosarcoma. *Proceedings of the National Academy of Sciences of the United States of America*, 109(17), 6656–6661. <https://doi.org/10.1073/pnas.1121629109>
- Grégoire, C., Cognet, C., Chasson, L., Coupet, C.-A., Dalod, M., Reboldi, A., . . . Walzer, T. (2008). Intrasplenic trafficking of natural killer cells is redirected by chemokines upon inflammation. *European Journal of Immunology*, 38(8), 2076–2084. <https://doi.org/10.1002/eji.200838550>
- Holliday, D. L., & Speirs, V. (2011). Choosing the right cell line for breast cancer research. *Breast Cancer Research : BCR*, 13(4), 215. <https://doi.org/10.1186/bcr2889>
- Huang, Y., Ma, Y., Gao, P., & Yao, Z. (2017). Targeting CD47: The achievements and concerns of current studies on cancer immunotherapy. *Journal of Thoracic Disease*, 9(2), E168-E174. <https://doi.org/10.21037/jtd.2017.02.30>
- The Human Protein Atlas. (2019). Tissue expression of CD47 - Summary - The Human Protein Atlas. Retrieved from <https://www.proteinatlas.org/ENSG00000196776-CD47/tissue>
- IHC World. (2015a). Antigen Retrieval Technical Tips. Retrieved from http://www.ihcworld.com/_technical_tips/antigen_retrieval_tips.htm
- IHC World. (2015b). Citrate Buffer Antigen Retrieval Protocol. Retrieved from http://www.ihcworld.com/_protocols/epitope_retrieval/citrate_buffer.htm
- IHC World. (2015c). EDTA Buffer Antigen Retrieval Protocol. Retrieved from http://www.ihcworld.com/_protocols/epitope_retrieval/edta.htm
- IHC World. (2015d). Immunohistochemistry Troubleshooting. Retrieved from <http://www.ihcworld.com/troubleshooting.htm>
- IHC World. (2015e). Tris-EDTA Buffer Antigen Retrieval Protocol. Retrieved from http://www.ihcworld.com/_protocols/epitope_retrieval/tris_edta.htm
- Kang, Y., Siegel, P. M., Shu, W., Drobnjak, M., Kakonen, S. M., Cordon-Cardo, C., . . . Massagué, J. (2003). A multigenic program mediating breast cancer metastasis to bone. *Cancer Cell*, 3(6), 537–549.
- Kassem, A. (2017). *Evaluation of mCherry tagged SIRPa fusion protein in vitro* (Diloma Thesis). University Vienna, Vienna.
- Kuhn, C. (1988). Biotin stores in rodent lungs: Localization to Clara and type II alveolar cells. *Experimental Lung Research*, 14(4), 527–536. <https://doi.org/10.3109/01902148809087825>

- Ley, K., Pramod, A. B., Croft, M., Ravichandran, K. S., & Ting, J. P. (2016). How Mouse Macrophages Sense What Is Going On. *Frontiers in Immunology*, 7, 204.
<https://doi.org/10.3389/fimmu.2016.00204>
- Li, Y., & Sun, R. (2018). Tumor immunotherapy: New aspects of natural killer cells. *Chinese Journal of Cancer Research = Chung-Kuo Yen Cheng Yen Chiu*, 30(2), 173–196.
<https://doi.org/10.21147/j.issn.1000-9604.2018.02.02>
- Lin, Y., Zhao, J.-L., Zheng, Q.-J., Jiang, X., Tian, J., Liang, S.-Q., . . . Han, H. (2018). Notch Signaling Modulates Macrophage Polarization and Phagocytosis Through Direct Suppression of Signal Regulatory Protein α Expression. *Frontiers in Immunology*, 9, 1744. <https://doi.org/10.3389/fimmu.2018.01744>
- Liu, X., Kwon, H., Li, Z., & Fu, Y.-X. (2017). Is CD47 an innate immune checkpoint for tumor evasion? *Journal of Hematology & Oncology*, 10(1), 12.
<https://doi.org/10.1186/s13045-016-0381-z>
- Marques, S. M., & Esteves da Silva, J. C. G. (2009). Firefly bioluminescence: A mechanistic approach of luciferase catalyzed reactions. *IUBMB Life*, 61(1), 6–17.
<https://doi.org/10.1002/iub.134>
- Martín-Antonio, B., Suñe, G., Perez-Amill, L., Castella, M., & Urbano-Ispizua, A. (2017). Natural Killer Cells: Angels and Devils for Immunotherapy. *International Journal of Molecular Sciences*, 18(9). <https://doi.org/10.3390/ijms18091868>
- Mescher, A. L., & Junqueira, L. C. U. (2013). *Junqueira's basic histology: Text and atlas* (Thirteenth edition). Lange medical book. New York: McGraw-Hill Medical.
- Morton, C. L., & Houghton, P. J. (2007). Establishment of human tumor xenografts in immunodeficient mice. *Nature Protocols*, 2(2), 247–250.
<https://doi.org/10.1038/nprot.2007.25>
- Murray, P. J., & Wynn, T. A. (2011). Protective and pathogenic functions of macrophage subsets. *Nature Reviews. Immunology*, 11(11), 723–737.
<https://doi.org/10.1038/nri3073>
- Novus Biologicals. Immunohistochemistry (IHC) Handbook. Retrieved from <https://www.novusbio.com/support/immunohistochemistry-ihc-handbook>
- Novusbio.com. (2019a). IHC detection systems: Advantages and Disadvantages: Novus Biologicals. Retrieved from <https://www.novusbio.com/ihc-detection>
- Novusbio.com. (2019b). IHC/ICC Sample Fixation (Formalin vs. Alcohol). Retrieved from <https://www.novusbio.com/sample-fixation-for-ihc-icc>

- Okabe, Y., & Medzhitov, R. (2016). Tissue biology perspective on macrophages. *Nature Immunology*, *17*(1), 9–17. <https://doi.org/10.1038/ni.3320>
- Oldenborg, P.-A. (2013). Cd47: A Cell Surface Glycoprotein Which Regulates Multiple Functions of Hematopoietic Cells in Health and Disease. *ISRN Hematology*, *2013*, 614619. <https://doi.org/10.1155/2013/614619>
- Pichler, J. (2019). *Immunohistochemical evaluation of CD47 surface protein in a xenograft triple-negative breast cancer (TNBC) mouse model* (Diploma Thesis). University Vienna, Vienna.
- R&D Systems. (2019). Protocol for Making a 4% Formaldehyde Solution in PBS. Retrieved from <https://www.rndsystems.com/resources/protocols/protocol-making-4-formaldehyde-solution-pbs>
- Richmond, A., & Su, Y. (2008). Mouse xenograft models vs GEM models for human cancer therapeutics. *Disease Models & Mechanisms*, *1*(2-3), 78–82. <https://doi.org/10.1242/dmm.000976>
- Russell, L., Swanner, J., Jaime-Ramirez, A. C., Wang, Y., Sprague, A., Banasavadi-Siddegowda, Y., . . . Kaur, B. (2018). Pten expression by an oncolytic herpesvirus directs T-cell mediated tumor clearance. *Nature Communications*, *9*(1), 5006. <https://doi.org/10.1038/s41467-018-07344-1>
- Shi, S. R., Cote, R. J., & Taylor, C. R. (1997). Antigen retrieval immunohistochemistry: Past, present, and future. *The Journal of Histochemistry and Cytochemistry : Official Journal of the Histochemistry Society*, *45*(3), 327–343. <https://doi.org/10.1177/002215549704500301>
- Shields, R. L., Namenuk, A. K., Hong, K., Meng, Y. G., Rae, J., Briggs, J., . . . Presta, L. G. (2001). High resolution mapping of the binding site on human IgG1 for Fc gamma RI, Fc gamma RII, Fc gamma RIII, and FcRn and design of IgG1 variants with improved binding to the Fc gamma R. *The Journal of Biological Chemistry*, *276*(9), 6591–6604. <https://doi.org/10.1074/jbc.M009483200>
- Thavarajah, R., Mudimbaimannar, V. K., Elizabeth, J., Rao, U. K., & Ranganathan, K. (2012). Chemical and physical basics of routine formaldehyde fixation. *Journal of Oral and Maxillofacial Pathology : JOMFP*, *16*(3), 400–405. <https://doi.org/10.4103/0973-029X.102496>
- Watzl, C. (2014). Chapter Five - How to Trigger a Killer: Modulation of Natural Killer Cell Reactivity on Many Levels. In F. W. Alt (Ed.), *Advances in Immunology* (Vol.

124, pp. 137–170). Academic Press. <https://doi.org/10.1016/B978-0-12-800147-9.00005-4>

Weiskopf, K., Ring, A. M., Ho, C. C. M., Volkmer, J.-P., Levin, A. M., Volkmer, A. K., . . . Garcia, K. C. (2013). Engineered SIRP α variants as immunotherapeutic adjuvants to anti-cancer antibodies. *Science (New York, N.Y.)*, *341*(6141).

<https://doi.org/10.1126/science.1238856>

Yang, L., & Zhang, Y. (2017). Tumor-associated macrophages: From basic research to clinical application. *Journal of Hematology & Oncology*, *10*(1), 58.

<https://doi.org/10.1186/s13045-017-0430-2>

Yeap, W. H., Wong, K. L., Shimasaki, N., Teo, E. C. Y., Quek, J. K. S., Yong, H. X., . . . Wong, S. C. (2016). Cd16 is indispensable for antibody-dependent cellular cytotoxicity by human monocytes. *Scientific Reports*, *6*, 34310.

<https://doi.org/10.1038/srep34310>

Zhao, H., Wang, J., Kong, X., Li, E., Liu, Y., Du, X., . . . Wang, Q. (2016). Cd47 Promotes Tumor Invasion and Metastasis in Non-small Cell Lung Cancer. *Scientific Reports*, *6*, 29719. <https://doi.org/10.1038/srep29719>